Phenotypic response and adaptation of *Candida* species to boric acid

by

Ola E. Salama

B.Sc. Biomedical Science (Honours), York University, 2019

A Thesis submitted to the Faculty of Graduate Studies of The University of Manitoba in partial fulfilment of the requirements of the degree of

MASTER OF SCIENCE

Department of Microbiology

University of Manitoba

Winnipeg, Manitoba, Canada

Copyright © 2021

ABSTRACT

C. albicans is the primary isolated species that causes vulvovaginal candidiasis, an infection that affects ~75% of females at least once in their life. Typically females get prescribed fluconazole, an azole drug, and are able to clear the infection. However, a small but significant number of females will experience recurrence. Boric acid is a broad-spectrum antimicrobial that is given as a second-line treatment for complicated vulvovaginal candidiasis, caused by recurrence or when infection is caused by other *Candida* species that have intrinsic resistance to fluconazole. Compared to fluconazole, far less is known about how boric acid inhibits *Candida* species.

C. albicans is polymorphic, meaning it can grow as yeast, pseudohyphae, and hyphae. It can live as planktonic (free-floating) or in a biofilm. This morphological plasticity of *C. albicans* contributes to its pathogenicity, and is directly involved in evasion of the human immune system and influences resistance to antifungal drugs. One way to examine the morphological plasticity of *C. albicans* is time-lapse microscopy, which generates a large data set which has typically been analyzed qualitatively. In Chapter 2, I describe a computational method I developed to extract parameters that correlate with biofilm formation from time-lapse images. This method does not require the user to be a computational expert and is not just limited to *C. albicans* and biofilm formation.

To better understand boric acid chemical properties, I examined the differential response of boric acid and fluconazole on *Candida* isolates with different morphologies in Chapter 3. I screened 235 clinical isolates of *C. albicans*, *Candida glabrata* and *Candida parapsilosis* for planktonic susceptibility and tolerance (the ability of a subpopulation to grow slowly at inhibitory drug concentrations). I found that there were inconsistent but significant differences among species, but that population-level variation for both drugs was broader for fluconazole in all species. Out of the 235 isolates, only one *C. parapsilosis* isolate was resistant to boric acid, suggesting that boric acid resistance and tolerance are quite rare. I also looked at the drug response of both drugs against biofilm formation of eight *C. albicans* isolates and mature biofilms of 68 *C. albicans* isolates, and I showed that fluconazole did not inhibit hyphal formation and biofilm formation (although it decreased biofilm formation by 0-50%), and mature biofilms were resistant to fluconazole. By contrast, boric acid inhibited hyphal and biofilm formation in a dose-dependent manner and eradicated mature biofilms.

In Chapter 4, I evolved 12 replicates from eight *C. albicans* isolates in the lab to increasing concentrations of boric acid. I surprisingly found that evolved replicates exhibited increased tolerance but not resistance. Combined, this thesis demonstrates that boric acid is effective at inhibiting planktonic and biofilm *Candida* cells, and that boric acid tolerance is evolvable. These results give us important baseline information about how boric acid works, that we can use in future studies on females with vulvovaginal candidiasis.

ACKNOWLEDGEMENTS

To my supervisor, Aleeza, thank you for always being there for me, for continuously pushing me to do better, and for constantly killing my darlings. The lab dynamics and values that you have set are amazing, and I do consider myself lucky to be part of your lab and to be your first graduate student. I would not have asked for a better graduate experience.

I would like to also thank my advisory committee, Silvia Cardona and Steven Harris, for their valuable scientific inputs, support and encouragement. Of course, I cannot forget my microstats peeps who always helped. Thank you, Rebekah Kukurudz, for being my coffee and brunch buddy, for always helping me with my huge DDA experiments and for being as excited as I am for decorating our lab door each year. I would not have done them without your help. I would like to also thank people in the microbiology department. They made my move to Winnipeg a lot easier and made graduate school a lot of fun. During my degree, I knocked on the door of each lab asking for help at least once, and I was never turned down. I would not have asked for a better welcoming and friendly environment to be part of. I would like to thank Karen Eusebio for her support, for always having coffee and lunch with me and for always bringing me her baked goods.

I would like to thank my family who without them I would not be here today. My parents, Ezz and Hala, thank you for being my support system throughout my career. My sister, Shaimaa, thank you for always cheering me up and for always introducing me to new good movies. Thank you to my second family, Manar, Mohamed, Murad and Fadi. You guys made me realize that we do not have to be blood related to be a family. Manar, although we were in two different continents, you always managed to be there for me.

This thesis is dedicated to my parents.

لقد كنتم ملاذي.

TABLE OF CONTENTS

ABSTRACT ---- **2**
ACKNOWLEDGEMENTS ---- **4**
PERMISSIONS ---- **8**
LIST OF TABLES ---- **9**
LIST OF FIGURES ---- **10**
LIST OF ABBREVIATIONS ---- **11**
CHAPTER 1 INTRODUCTION ---- 12
1.1 Vulvovaginal candidiasis ---- **12**
1.2 *Candida* species ---- **13**
1.3 Why does recurrence occur? ---- **15**
1.4 Boric acid as a therapeutic alternative ---- **17**
1.5 Why does boric acid work? ---- **18**
1.6 Hypotheses ---- **19**
CHAPTER 2 HIGH-THROUGHPUT COMPUTATIONAL ANALYSIS ---- 20
2.1 Abstract ---- **20**
2.2 Introduction ---- **21**
2.2 BASIC PROTOCOL 1: SAMPLE PREPARATION ---- **23**
2.3 BASIC PROTOCOL 2: TIME-LAPSE MICROSCOPY ---- **26**
2.4 BASIC PROTOCOL 3: BATCH FILE RENAMING ---- **28**
2.5 BASIC PROTOCOL 4: MACHINE LEARNING ANALYSIS OF EVOS IMAGES WITH ORBIT ---- **32**
2.6 BASIC PROTOCOL 5: PARAMETRIZATION OF ORBIT OUTPUT IN R ---- **38**
2.7 BASC PROTOCOL 6: VISUALIZATION OF LOGISTIC FITS IN R ---- **44**
2.8 REAGENTS AND SOLUTIONS ---- **48**
2.9 COMMENTARY ---- **49**
2.9.1 BACKGROUND INFORMATION ---- 49
2.9.2 CRITICAL PARAMETERS and TROUBLESHOOTING ---- 50
2.9.3 ANTICIPATED RESULTS ---- 53
2.9.4 TIME CONSIDERATIONS ---- 54
2.10 Acknowledgments ---- **55**
2.11 Author Contributions ---- **55**
2.12 Conflict of Interest ---- **56**
CHAPTER 3 DIFFERENTIAL RESPONSE OF *CANDIDA* SPECIES ---- 57
3.1 Abstract ---- **57**
3.2 Introduction ---- **58**
3.3 Results ---- **60**
3.3.1 Variation in Drug Susceptibility and Tolerance ---- 60
3.3.2 BA Inhibits *C. albicans* Hyphal Formation ---- 63
3.3.3 BA Eradicates *C. albicans* Mature Biofilms ---- 66
3.4 Discussion ---- **68**
3.5 Conclusion ---- **70**
3.6 Material and Methods ---- **71**
3.6.1 Isolates ---- 71
3.6.2 Disk Diffusion Assay ---- 71
3.6.3 Boric Acid levels ---- 71
3.6.4 Biofilm Formation Drug Response ---- 72
3.6.5 Microscopic Image Analysis ---- 73
3.6.6 Biofilm Eradication ---- **73**
3.6.7 Statistical Analysis ---- 74
3.7 Acknowledgments ---- **74**
CHAPTER 4 BORIC ACID ADAPTATION IN *CANDIDA ALBICANS* ---- 75

4.1 Abstract ---------- **75**
4.2 Introduction ---------- **75**
4.3 Methods ---------- **76**
4.3.1 Isolates ---------- 76
4.3.2 Pilot Boric Acid Evolution Experiment ---------- 76
4.3.3 Modified Boric Acid Evolution Experiment ---------- 77
4.3.3 Susceptibility and Tolerance ---------- 78
4.4 Results and Discussion ---------- **79**
DISCUSSION ---------- 85
CONCLUSION ---------- 88
BIBLIOGRAPHY ---------- 89
SUPPLEMENTARY MATERIAL FOR CHAPTER 3 ---------- 100
SUPPLEMENTARY MATERIAL FOR CHAPTER 4 ---------- 104

PERMISSIONS

Figures, tables and passages within this thesis have been adapted from published works in academic journals that I have authored.

Chapter 2:

Authors retain copyright as per John Wiley & Sons publications policy.

Copyright © Wiley Periodicals LLC [Current Protocols e194, Volume 1, DOI: 10.1002/cpz1.194
Authors retain the right to reuse the full article in their dissertation or thesis per the John Wiley & Sons publications policy.

LIST OF TABLES

Table 2.1 Plate layout example. ---------- 30
Table 4.1 List of replicates used in susceptibility and tolerance screening. ---------- 78
Table 4.2 Isolates used in BA evolution experiment. ---------- 81
Table 4.3 Welch two-sample t-tests to compare ancestral and evolved ---------- 83

LIST OF FIGURES

Figure 1.1 *Candida* and *Saccharomyces* clade phylogeny. ---------- 14
Figure 1.2 Schematic of biofilm structure of *C. albicans*, *C. glabrata* and ---------- 15
Figure 2.1 Example plate setup for time-lapse microscopy ---------- 26
Figure 2.2 Images were captured every hour for 24 h using Evos FL 2 Imaging System. ------- 28
Figure 2.3 Orbit Image Analysis interface running on PC Windows 10. ---------- 35
Figure 2.4 Training the machine learning algorithm based on the selected classes. ---------- 36
Figure 2.5 Batch Analysis and data export. ---------- 37
Figure 3.1 Susceptibility and tolerance for FLC and BA ---------- 61
Figure 3.2 Association within and between drug response parameter and drugs ---------- 62
Figure 3.3 Biofilm formation drug responses of eight *C. albicans* isolates ---------- 64
Figure 3.4 Quantitative image analysis of time lapse images of eight *C. albicans* ---------- 65
Figure 3.5 Biofilms drug responses of 63 *C. albicans* isolates. ---------- 67
Figure 4.1 BA evolution experiment. Eight *C. albicans*. ---------- 80
Figure 4.2 Variation in susceptibility and tolerance between ancestral and evolved replicates - 84
Supplementary Material for Chapter 3
Supplementary Figure 3. 1 Association of planktonic susceptibility and biofilm biomass ---- 100
Supplementary Figure 3. 2 Association of planktonic susceptibility and biofilm activity ----- 101
Supplementary Figure 3. 3 Association of planktonic tolerance and biofilm biomass --------- 102
Supplementary Figure 3. 4 Association of planktonic tolerance and biofilm activity ---------- 103
Supplementary Material for Chapter 4
Supplementary Figure 4. 1 Trajectory of each replicate by day for *C. albicans* ---------- 104
Supplementary Figure 4. 2 Trajectory of each replicate by day for *C. albicans* ---------- 105
Supplementary Figure 4. 3 Trajectory of each replicate by day for *C. albicans* ---------- 106
Supplementary Figure 4.4 Trajectory of each replicate by day for *C. albicans* ---------- 107

LIST OF ABBREVIATIONS

BA	Boric Acid
DMSO	Dimethyl sulfoxide
FLC	Fluconazole
FoG_{20}	Fraction of growth above RAD_{20}
MH	Sabouraud Dextrose Agar
NAC	Non-albicans Clinical
OD_{600}	Optical density measured at 600 nm
PBS	Phosphate buffered saline
R/VVC	Vulvovaginal candidiasis and recurrent Vulvovaginal candidiasis
RAD_{20}	Radius where 20% of growth reduction occurs
RVVC	Recurrent vulvovaginal candidiasis
VVC	Vulvovaginal candidiasis

Chapter 1 Introduction

Over the last 30 years, the number of invasive fungal infections has increased; fungi cause as much human mortality (~1.5 million people a year) as tuberculosis and malaria (Bongomin et al., 2017; Kainz et al., 2020). *Candida* species are some of the main species responsible for most cases of serious fungal infections, and *Candida albicans* is responsible for the majority of mucosal diseases. Due to the eukaryotic nature of fungal cells, it is difficult to develop antifungal drugs that target fungal pathogens without damaging human cells (Seneviratne and Rosa, 2016). The current arsenal of antifungal drugs are limited to only a few classes: azoles, polyenes, fluoropyrimidines, echinocandins, allylamines, and flucytosine (Pappas et al., 2016; Sanglard et al., 2009).

1.1 Vulvovaginal candidiasis

Vulvovaginal candidiasis (VVC) is a pathological condition of the lower female reproductive tract caused by *Candida* species, particularly *C. albicans* which accounts for 85-90% of the VVC cases (Rosati et al., 2020; Willems et al., 2020; Martin Lopez, 2015). Unlike other invasive fungal infections, VVC is a disease of both immunocompetent and immunocompromised females (Rosati et al., 2020). It is the second most common cause of vaginitis after bacterial vaginosis. Approximately 75% of females will have a VVC infection at least once, and the symptoms they typically experience include vaginal discharge, severe itching, inflammation, and pain (Sobel, 2007; Willems et al., 2020). VVC patients usually respond well to fluconazole (150 mg oral dose) and are able to clear out the infection (Pappas et al., 2016; van Schalkwyk et al., 2015). However, a small but significant number of females (~8% of females globally) will experience recurrent VVC (RVVC), which is defined as at least four episodes of VVC in one year (Denning et al., 2018; Pappas et al., 2016). Compared to females with other chronic vaginal diseases, RVVC patients report the greatest negative impact on work and social life. It is expected that the number of females who experience RVVC will increase from 138 million to 158 million females by 2030, with a global economic burden of over 14 billion dollars a year (Nyirjesy et al., 2006; Denning et al., 2018). Unfortunately, even with the high incidence and significant effect on the quality of life, VVC and RVVC received less consideration from researchers than other forms of Candida infections since they are rarely life-threatening (Achkar and Fries, 2010; Willems et

al., 2020). The lack of attention that VVC and RVVC received is what motivated us to do the work described in this thesis.

1.2 *Candida* species

The genus *Candida* has been used as an umbrella term to refer to yeast that can cause human infections and lacks a conventional sexual cycle (Ene et al., 2021). The genus is compromised of approximately 200 species belonging to over 13 phylogenetically distinct clades. They are among the most common fungal pathogens and can cause vaginitis, oral candidiasis, cutaneous candidiasis, candidemia and systematic infections (Wächtler et al., 2012). *Candida albicans*, *Candida glabrata, C. parapsilosis* and *C. tropicalis* account for over 95% of *Candida* infections (Turner and Butler, 2014; Gabaldón et al., 2016). Although *C. albicans* is the primary causative agent of VVC and RVVC, non-albicans *Candida* (NAC) species can also be involved (Bhattacharjee, 2016; Hashemi et al., 2019). The frequency of NAC species is increasing with *C. glabrata* having the highest frequency rate followed by *C. parapsilosis* and *C. tropicalis* (Linhares et al., 2001; Cetin et al., 2007; Okungbowa et al., 2003). Among the four, *C. glabrata* has the highest incidence of azole resistance (Oxman et al., 2010; Pfaller et al., 2014).

C. albicans and *C. parapsilosis* belong to the CTG clade (Figure 1.1) (Butler et al., 2009). *C. glabrata* belongs to a group of species that have undergone whole-genome duplication (WGD) and is more closely related to *Saccharomyces cerevisiae* than it is to *C. albicans* (Fitzpatrick et al., 2006). The nomenclature for *C. glabrata* is currently transitioning to *Nakaseomyces glabrata* (Kidd et al., 2021). Therefore, we use the term NAC species to refer to "non-albicans clinical" species rather than "non-albicans *Candida*" species as has been done previously.

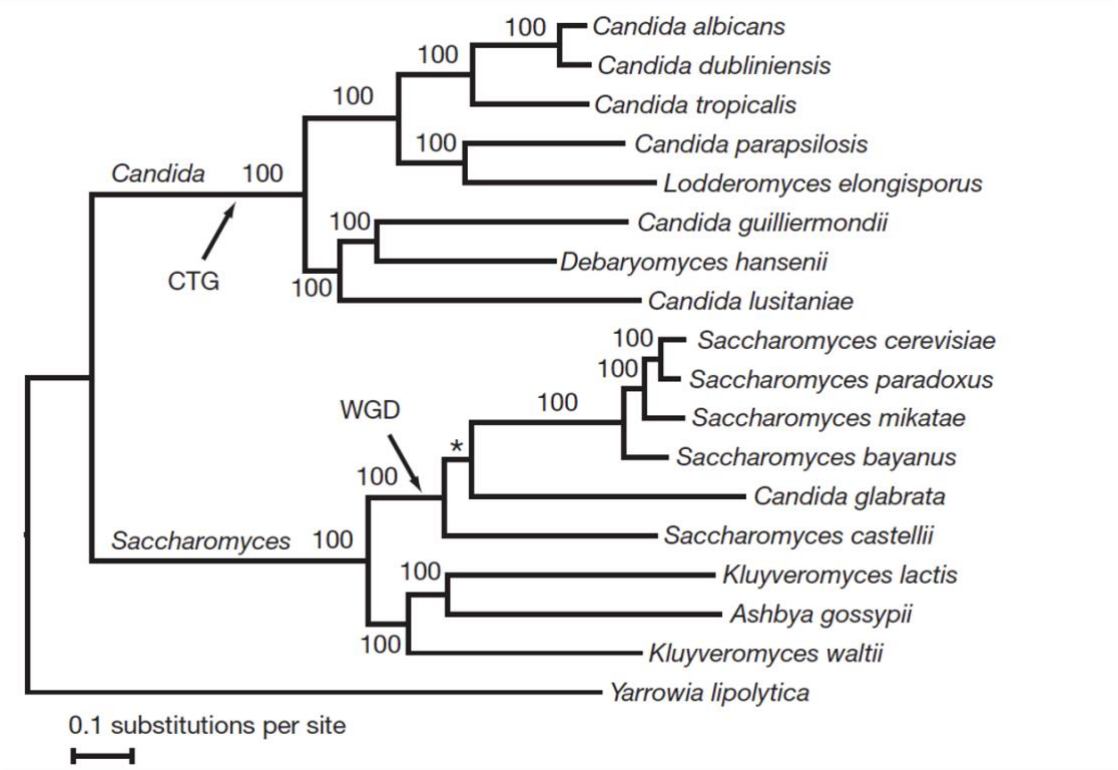


Figure 1.1 *Candida* and *Saccharomyces* clade phylogeny. *C. albicans* and *C. parapsilosis* both belong to the CTG clade. *C. glabrata* is more closely related to *S. cerevisiae* than *C. albicans*. The phylogenetic tree was constructed using both peptide and coding nucleotide sequences.
This figure was obtained from (Butler et al. 2009).

C. albicans has the most morphological plasticity; depending on the environment, it can grow as yeast cells, pseudohyphae and true hyphae (Gabaldón et al., 2016). *C. glabrata* is not polymorphic and can only grow in the yeast form while *C. parapsilosis* can produce yeast and pseudohyphae (Larone and Larone, 1987). This morphological variation among these three species is translated in how they form biofilms (Figure 1.2). Among the three, *C. albicans* is the best biofilm producer and its biofilms are composed of a dense network of yeast, pseudohyphal, and hyphal cells embedded in an extracellular matrix made of polysaccharide materials (Ramage et al., 2002; Kuhn et al., 2002). *C. glabrata* biofilms are composed of yeast cells embedded in an extracellular matrix that exhibit high levels of carbohydrates and proteins (Silva et al., 2009). On the other hand, *C. parapsilosis* biofilms are made of mainly yeast cells and some pseudohyphal cells, and they are embedded in minimal, if any, extracellular matrix (Kuhn et al., 2002). Although we use the term *Candida* as an umbrella term to refer to these three species, it is important to keep

in mind that there is a lot of differences among them and that these differences could be implicated in the persistence of infection.

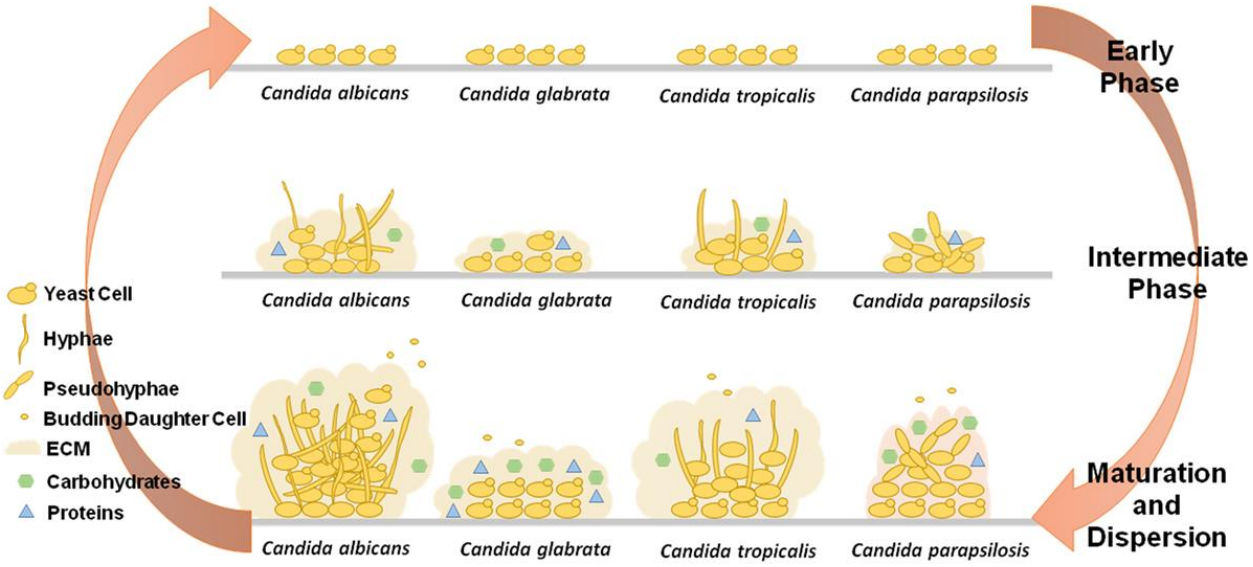


Figure 1.2 Schematic of biofilm structure of *C. albicans*, *C. glabrata* and *C. parapsilosis*. *C. albicans* is the best biofilm producer. This figure was obtained from (Cavalheiro and Teixeira 2018).

1.3 Why does recurrence occur?

No clear explanation exists for why some females experience RVVC while others do not (Willems et al., 2020). However, there is some explanation for why fluconazole (FLC) could fail in RVVC patients. Susceptibility tests and clinical breakpoints for FLC are well established for *Candida* species (Wayne, 2002, 2004). However, clinical protocols determine drug response by only quantifying fungal drug resistance, which is typically measured as the minimum inhibitory concentration (MIC) after 24 h of growth (Wayne, 2002, 2004), and they have previously ignored drug tolerance, which is defined as the ability of a subpopulation of drug-susceptible isolates to grow slowly at inhibitory drug concentrations (Gerstein et al., 2016; Rosenberg et al., 2018; Berman and Krysan, 2020; Levinson et al., 2021). However, tolerance has recently been shown to be a good proxy for predicting fluconazole efficacy in patients with *C. albicans* bloodstream infections (Rosenberg et al., 2018). Hence, tolerance is an important parameter that should not be ignored, and it could play an important role in RVVC.

Most *C. albicans* isolates are susceptible to FLC, and the emergence of FLC-resistant isolates as a consequence of frequent use of FLC is considered rare (Sobel, 2005, 2016). However,

continuous exposure to FLC (i.e., RVVC maintenance therapy) can induce resistance in *C. albicans* (Marchaim et al., 2012). Acquired resistance was also observed in clotrimazole, another azole drug, in RVVC patients who were on clotrimazole maintenance therapy (Arastehfar et al., 2021). Furthermore, experimental evolution from a sensitive *C. albicans* isolate grown continuously in FLC for over 330 generations showed that resistance can be acquired (Cowen et al., 2000). Thus, acquired resistance could play an important role in RVVC, and we should determine the adaptability of *Candida* species to different antifungal drugs.

Moreover, *Candida* species do not live alone. In healthy females, *Candida* can live in symbiosis with the vaginal microbiota. Disruptions to the host or the bacterial community can lead to overgrowth of *Candida* and/or changes in the host defense mechanisms (Sobel, 2007). Lactobacilli (specifically *Lactobacillus crispatus*, *L. jensenii*, and *L. iners*) are the dominant bacterial organisms in the normal microflora of healthy females (Vásquez et al., 2002). These species produce lactic acid, H_2O_2 and anti-microbial compounds which prevent *Candida* growth (Klebanoff et al., 1991; Boskey et al., 2001; Voravuthikunchai et al., 2006). One critical attribute to the pathogenesis of *C. albicans* is its morphological plasticity (i.e., yeast to hyphal transition) (Mayer et al., 2013; Noble et al., 2017). Recently, *Lactobacillus* species was shown to produce β-carbolines, which inhibited *C. albicans* yeast to hyphal transition in *in vitro* models and biofilm formation in *in vitro* and murine models (MacAlpine et al., 2021). It has not yet been determined whether these compounds are produced in the vagina, but it seems to be likely (MacAlpine et al., 2021). In sum, the breakdown of the symbiotic relationship between the vaginal normal flora and yeast could influence the yeast to hyphal transition, which could explain why some females experience VVC.

Clinical assessments of yeast in the context of VVC have ignored biofilms (Donlan, 2001). It has been suggested that biofilms are involved in VVC and RVVC (Rodríguez-Cerdeira et al., 2019; Harriott et al., 2010; Wu et al., 2020). This has been debated though (Sobel, 2015), and a recent study demonstrated the absence of biofilms in vaginal biopsies from VVC patients (Swidsinski et al., 2019). Cells in biofilms are protected by the extracellular matrix which in return confers more resistance to antifungal drugs compared to their planktonic counterparts. *C. albicans* biofilms are resistant to FLC, amphotericin B, caspofungin, nystatin and voriconazole (Fanning and Mitchell, 2012). A study showed that mannan and β-1,6 glucan present in the extracellular matrix of *C. albicans* biofilms contribute to the impermeability of FLC through the biofilm

structure (Fanning and Mitchell, 2012). Moreover, biofilms of *C. albicans* isolates from females with RVVC are insensitive (resistant) to FLC (Sherry et al., 2017) Therefore, if biofilms play an important role in RVVC then measuring how they are influenced by different drugs is an important avenue of resaerch that should not be overlooked.

1.4 Boric acid as a therapeutic alternative

Boric acid (BA, H_3BO_3) is an inorganic weak acid that is available as an odorless white powder (Heckelman et al., 1996). BA was first made in 1702 by Wilhelm Homberg who mixed borax, mineral acids, and water and produced the BA crystals by evaporating the water (Jolly, 1991). Homberg termed BA *Sal sedativum Hombergi* (sedative salt of Homberg") because of the BA soothing effect on the skin. BA was used for the first time as a topical antiseptic in 1875 by Joseph Lister (Lister, 1945). It was then used in powders, ointments, and lotions and was considered by dermatologists as a low toxicity substance (Fisher, 1956). Later on, BA was shown to have bacteriostatic and fungistatic properties, and physicians started utilizing 600 mg BA suppositories to treat VVC (Prutting and Cerveny, 1998).

The Infection Disease Society of America and the Society of Gynecologists and Obstetricians of Canada guidelines recommend BA intravaginal suppositories (300-600 mg daily × 14 days) as an alternative treatment when first-line treatment (typically fluconazole) fails, especially when NAC species are involved (Pappas et al., 2016; van Schalkwyk et al., 2015). *In vitro* studies have shown that BA at concentrations ranging from 4-10 mg/mL inhibits *Candida albicans* at rates of 97.2-100% (Kalkanci et al., 2012; De Seta et al., 2009; Larsen et al., 2018). BA MIC has been measured before in planktonic cells (De Seta *et al*., 2009: 71 *C. albicans* isolates and 2 *C. glabrata*; Otero *et al*., 2002: 25 *C. glabrata*, eight *C. parapsilosis*, one *C. parapsilosis* and one *C. tropicalis*). NAC species, particularly *C. glabrata*, was found to have a slightly higher intrinsic resistance to BA (De Seta et al., 2009; Otero et al., 2002). However, the clinical break points for BA are not defined. *In vivo* studies showed that treatment with BA led to rapid relief of symptoms and a negative culture after 14 days of treatment (Sobel et al., 2003; Ringdahl, 2000; De Seta et al., 2009; Iavazzo et al., 2011) and this is consistent with clinical reports of females suffering from recurrent infection (Dr. Vanessa Poliquin, pers. comm.). Studies have shown that using one to two 600 mg BA intravaginal suppositories daily for 1-2 weeks led to blood concentrations of < 1 μg/mL (blood concentrations < 200μg/mL are considered safe), suggesting that there is little absorption of BA across the vaginal wall (Iavazzo et al., 2011).

1.5 Why does boric acid work?

The exact mechanism of action of BA is still unknown (Prutting and Cerveny, 1998; De Seta et al., 2009). One theory proposed is that BA works because it is a weak acid (i.e., it acidifies the environment) (Prutting and Cerveny, 1998; Shinohara and Tasker, 1997). However, De Seta *et al.* (2009) showed that other acids (i.e., acetic acid, citric acid, succinic acid, and tartaric acid) did not inhibit *C. albicans*. Rather they showed that sodium borate, an alkaline, is intrinsically more effective against *Candida* than BA, suggesting that boron is likely to be the factor inhibiting *Candida* (De Seta et al., 2009). It has also been suggested that BA works by inhibiting oxidative metabolism, but whether this inhibition contributes to therapeutic efficacy remains unknown (De Seta et al., 2009). Furthermore, BA was shown to inhibit hyphal formation by disrupting the cytoskeleton of hyphae and changing the actin distribution from the apical to the isotropic pattern (Pointer et al., 2015). This reorganization of actin leads to the loss of Spitzenkörper, a complex multi-component structure at the apex of the hyphae responsible for hyphal directionality and morphogenesis, and polarisome, a multi-protein complex that regulates hyphal growth at polarized growth sites in yeast, leading to the broadening of hyphal tips and the halt of hyphal growth (Pointer et al., 2015; Steinberg, 2007). BA has also been shown to reduce the biomass of mature biofilm compared to drug-free controls (De Seta et al., 2009); however, whether this reduction was due to eradication effects (disruption of the biofilm structure post BA exposure) or static effects (inhibiting further growth of the biofilm post BA exposure) compared to the BA-free controls was not determined. Unlike FLC, we do not know whether continuous exposure to BA can give rise to BA resistant (or tolerant) isolates *in vitro* or *in vivo*.

In this thesis, I sought to compare FLC and BA drug responses in *Candida* species. In order to study how BA affects the early phases of biofilm formation, I first developed a tool to extract parameters from time-lapse microscopy images that correlate with the ability of planktonic cells to form biofilms (Chapter 2). In Chapter 3, I screened 235 clinical isolates of *Candida* isolates (165 *C. albicans*, 50 *C. glabrata*, and 20 *C. parapsilosis*) for planktonic susceptibility and tolerance. I used the tool developed in Chapter 2 to examine the response of both drugs on eight *C. albicans* biofilms during the early phases of biofilm formation. I also looked at BA drug response of mature biofilms of 68 different *C. albicans* isolates. Finally, in Chapter 4, I describe an experiment where I continuously exposed replicates from eight *C. albicans* isolates to increasing concentrations of BA in an effort to evolve BA-resistant and/or tolerant isolates. My

work shows that BA is effective against planktonic and biofilm *Candida* cells and that there might be barriers to developing BA adaptability. These results demonstrate multiple pathways by which BA may be an effective treatment against *Candida* species.

1.6 Hypotheses

1. Boric acid will be more effective than fluconazole at inhibiting growth of planktonic cells, biofilm formation, and at eradicating mature biofilms.
2. Continuous exposure to increasing concentrations of boric acid will give rise to resistant and/or tolerant *Candida albicans* isolates.

Chapter 2 High-Throughput Computational Analysis of Biofilm Formation from Time-Lapse Microscopy

2.1 Abstract

Candida albicans biofilm formation in the presence of drugs can be examined through time-lapse microscopy. In many cases, the images are used qualitatively, which limits their utility for hypothesis testing. We employed a machine learning algorithm implemented in the Orbit Image Analysis program to detect the percent area covered by cells from each image. This is combined with custom R scripts to determine the growth rate, growth asymptote, and time to reach the asymptote as quantitative proxies for biofilm formation. We describe step by-step protocols that go from sample preparation for time-lapse microscopy through image analysis parameterization and visualization of the model fit.

Basic Protocol 1: Sample Preparation

Basic Protocol 2: Time-lapse microscopy: Evos protocol

Basic Protocol 3: Batch file renaming

Basic Protocol 4: Machine learning analysis of Evos images with Orbit

Basic Protocol 5: Parametrization of Orbit output in R

Basic Protocol 6: Visualization of logistic fits in R

KEYWORDS:

Candida, image analysis, drug response, Orbit, R

2.2 Introduction

Biofilm formation is an important virulence factor in *Candida albicans* (Chandra et al., 2001; Douglas, 2003; Fanning and Mitchell, 2012; Mayer et al., 2013; Cavalheiro and Teixeira, 2018). There are three distinct developmental stages of biofilm formation: 1) adherence of the yeast cells, 2) an intermediate phase of dimorphic switching from yeast to hyphae and formation of the matrix, and 3) the formation of the three-dimensional mature biofilm architecture (Kojic and Darouiche, 2004; Cavalheiro and Teixeira, 2018). *C. albicans* biofilms are the leading cause of medical device-acquired nosocomial infections because they have the ability to adhere to and grow on different types of medical devices, such as prostheses, cardioverter defibrillators, catheters, and cardiac devices (Douglas, 2003; Elving et al., 2002; Potera, 1999; Kojic and Darouiche, 2004). *C. albicans* biofilms have been reported to be highly resistant to a variety of antifungal drugs including fluconazole, itraconazole, amphotericin B, nystatin, and chlorhexidine (Chandra et al., 2001; Fanning and Mitchell, 2012; Sherry et al., 2017; Kuhn et al., 2002; Hawser and Douglas, 1995). There are well-developed in vitro biofilm protocols to study antifungal resistance by examining drug penetration in mature biofilms (Gulati et al., 2018; Pierce et al., 2010). These assays measure the antifungal drug response by evaluating the biofilm biomass by optical density (Fox et al., 2015; Lohse et al., 2017), metabolic activity (Nett et al., 2011; Kuhn et al., 2002; Melo et al., 2011), or direct observation through confocal scanning microscopy (Fox et al., 2015; Chandra et al., 2001). However, fewer protocols exist to examine the earlier developmental stages, i.e., to determine whether drugs inhibit adherence and/or the intermediate phases of biofilm formation (Abdelmegeed and Shaaban, 2013; Nagy et al., 2014; McCall et al., 2019).

Time-lapse microscopy is the technique to capture a sequence of images at regular time intervals (Collins et al., 2019). Time-lapse microscopy has previously been used to examine the growth rate of biofilms qualitatively by visually evaluating the effect of the drug (Kawai et al., 2017) or quantitatively by measuring the thickness of biofilms grown in the presence of drug (Kaneko et al., 2013). However, time-lapse images are often only examined qualitatively. When the large number of images created by a typical time-lapse are quantified manually for parameters that correspond with biofilm formation ability, it can be very time consuming and subjective. Although numerous analysis tools are available for image analysis, such as CellProfiler (Carpenter et al., 2006), ImageJ (Lind, 2012) and Nuerostudio (Rodriguez et al., 2008), these tools are designed for specific and typically singular purposes, such as cell counting, cell detection of

specific cell types (e.g., human cells) and/or work with a specific type of microscopic images (e.g. fluorescent images).

Here, we developed a method that quantifies biofilm formation from the earliest phases, i.e., before adherence, in a high-throughput, quantitative, and unbiased fashion. To accomplish this, we combined 96-well time-lapse microscopy of bright-field images with Orbit image analysis. Orbit is an open-source software (available at https://www.orbit.bio/) that incorporates a machine learning algorithm that can be trained to detect and quantify cells, and provides a built-in mechanism to analyze a large number of images (Stritt et al., 2020). Orbit does not require the user to have extensive prior knowledge of image analysis or scripting and does not depend on having a huge training set of images. We use Orbit to quantify the area of each well that is covered by cells at each time point. We then developed custom scripts in the R programming language (R Core Team, 2020) to fit a logistic equation to % area over time, to determine the growth rate (slope during exponential phase), % area at the growth asymptote, and to determine the time it takes to reach the asymptote. Finally, we provide a script to visualize the model fit. We describe how we have used this protocol to examine biofilm formation of *C. albicans* in the presence of the broad spectrum antimicrobial boric acid, though note that biofilm formation of any species in any desired environment is possible.

Basic protocol 1 describes the growth conditions required to go from freezer stock to sample preparation for the time-lapse microscopy, basic protocol 2 describes Evos FL Auto 2 set up and how images were taken, basic protocol 3 describes how to batch rename images using Bulk Rename Utility and R, basic protocol 4 describes Orbit set up and how a model was trained to detect the cells, basic protocol 5 describes how important parameters (% area at the asymptote, slope and time to reach the asymptote) were extracted from Orbit output using the R programming language, and basic protocol 6 describes a how to visualize the logistic fit of the % area and the other important parameters extracted from basic protocol 5. Overall, this approach allows us to extract quantitative parameters from qualitative data, which will facilitate a novel method to interpret time-lapse microscopic data and expand our understanding of biofilm formation in the presence of antifungal drugs. The R scripts detailed here are included as supporting material (.R files), alongside an example of their use (.PDF files). The scripts and example image files for practice are also located as a github repository, accessible at https://github.com/acgerstein/biofilm-formation.

2.2 BASIC PROTOCOL 1: SAMPLE PREPARATION

Basic protocol 1 describes sample preparation for use in time-lapse microscopy for one biological replicate from eight strains of interest, each grown in five different concentrations of two different drugs. Any desired 96-well configuration is possible (e.g., 10 concentrations of a single drug, or five concentrations of a single drug with two different types of base media). Basic Protocols 2-5 describe the results from one clinical isolate of *C. albicans* (P75016) grown in five different concentrations of boric acid as an example.

The initial growth from freezer stocks is done in yeast extract peptone dextrose (YPD) in this example, as this medium is the standard for general laboratory growth. 96-well plate preparation for the time-lapse assay is done in RPMI-1640, a standard environment for biofilm growth assays. These environments can be adjusted as desired for the particular experimental goals. Depending on the specific isolates examined and the media type used, the growth period may need to be optimized to ensure robust growth prior to the initiation of the time-lapse protocol. This part of the protocol is based on the biofilm formation assay described in Pierce et al. (Pierce et al., 2010).

Materials

YPD liquid media (see recipe in Reagents and Solutions)

Candida albicans strain(s) of interest (The protocol has been tested on *C. albicans* strains SC5314, FH1, P87, GC75, P78048, P75016, P76055, T101)

0.01 M Phosphate buffered saline (PBS; see recipe in Reagents and Solutions)

RPMI-1640 media (See recipe in Reagents and Solutions)

Stock solution of drug or stress of interest (at least 2× desired maximum concentration)

15 mL centrifuge tubes (Fisherbrand, Catalog number: 14955238)

Sterile pipette tips (Ranin, Catalog number: 30389299)

Aliquoting pipet (VistaLab, Catalog number: 2000-0005)

10 mL glass serological pipette (Fisherbrand, Catalog number: 14955234)

30 °C shaking incubator (Eppendorf, Catalog number: M1299-0094)

Centrifuge (Thermo Scientific, ST16, Catalog number: 75004240)

Vortex (Thermo Scientific, Catalog number: S28673)

Spectrophotometer (Life Technologies Inc., Multiskan Sky Microplate Spectrophotometer, Catalog number: 51119600)

Microcentrifuge tubes (Fisherbrand, Catalog number: 02682002)

96-well microtiter plate PS F-bottom (Greiner Bio-One, Catalog number: 655161)

200 µL Multichannel pipette (Ranin, Pipet-Lite Multi Pipette L12-200XLS+, Catalog number: 17013810)

Clear seal (Thermo Scientific, Catalog No.14-245-18)

Polystyrene Microplate Lids (Greiner Bio-One, Catalog number: 656176)

Parafilm M Wrapping Film (Fisher Scientific, Catalog number: S37441)

37 °C incubator (Thermo Scientific, Catalog number: 51033557)

1. Inoculate 10 µL of desired *C. albicans* strain from glycerol stock into 10 mL of YPD in a 15 mL falcon tube.

   Inoculation can also be done from freshly grown colonies streaked from freezer stock onto YPD plates.
2. Place the falcon tube in a shaker (200 rpm) or rotator drum at 30 °C and incubate for 24 h.

   Some strains may take longer than 24 h to grow.
3. Centrifuge at 3000 g and remove the supernatant.

   An easy way of removing the supernatant is by inverting the falcon tube over a liquid waste container. Do that quickly and cover the falcon tube right away.
4. Add 10 mL of PBS to the falcon tube and vortex for at least 10 seconds on the highest speed to resuspend the colony.
5. Centrifuge at 3000 g and remove the supernatant.
6. Repeat step 4 & 5 three times to wash the cells. After the third PBS wash, resuspend again in 10 mL PBS.
7. Transfer 100 µL of the washed cultures to a single well of a 96-well microtiter plate.
8. Measure optical density and standardize in 1.5 mL microcentrifuge tubes to OD_{600} of 0.005 in 1 mL of RPMI-1640.

   Use $C_1V_1 = C_2V_2$ for your calculation. For example, if the OD_{600} of your culture is 0.6, and you want to standardize to 0.005 in 1 mL of RPMI-1640, then $(0.6)(V_1) = (0.005)(1000)$. Therefore, $V_1 = 8.33\ \mu L \simeq 8\ \mu L$, and you would transfer 8 µL of the overnight culture to 992 µL RPMI-1640.

9. Add 100 µL of RPMI-1640 to all wells of columns 1-9 of a flat-bottom 96-well microtiter plate (Figure 2.1).
10. Add 200 µL of RPMI-1640 to column 12. Add 200 µL of RPMI-1640 + 2× the desired final concentration of drug A to all wells of column 11 and add 200 µL of RPMI-1640 + 2× the desired final concentration of drug B to all wells of column 10.
11. Using a pipettor, do a serial dilution by transferring 100 µL of column 11 to column 9. Mix by pipetting up and down 3-4×. Transfer 100 µL from column 9 to column 7 and mix again. Keep doing that for all of the odd numbered columns until column 3 (REMEMBER to stop at column 3). After mixing column 3, discard the extra 100 µL.
12. Repeat step 11 for column 10 and transfer and mix with even numbered columns. REMEMBER to stop at column 2. After mixing column 2, discard the extra 100 µL.

    Note: All of the wells of columns 1-11 should now contain 100 µL of media. Column 1 and 12 should have no drug. Odd numbered columns (3-11) contain drug A, with the highest concentration in column 11 and the lowest concentration in column 3. Even numbered columns (2-10) contain drug B, with the highest concentration in column 10 and the lowest concentration in column 2 (Figure 2.1).
13. Transfer 100 µL of standardized culture to all wells of columns 1-11 of a flat-bottom 96-well microtiter plate (Fisher Scientific). Column 12 should not contain culture (Figure 2.1).

    Note: Keep in mind that this will dilute the culture and the drug concentration by 2-folds. For example, if the BA concentration put in column 11 is 6.4 mg/mL, the final FLC concentration after transferring 100 µg/mL of culture will be 3.2 mg/mL. Similarly, the final well OD_{600} should be 0.0025.
14. Cover with a sterilized lid and seal with parafilm.

    Note: To ensure that you are not covering the bottom of the plate with parafilm, use scissors to cut parafilm to the desired thickness to only cover the sides of the plate.

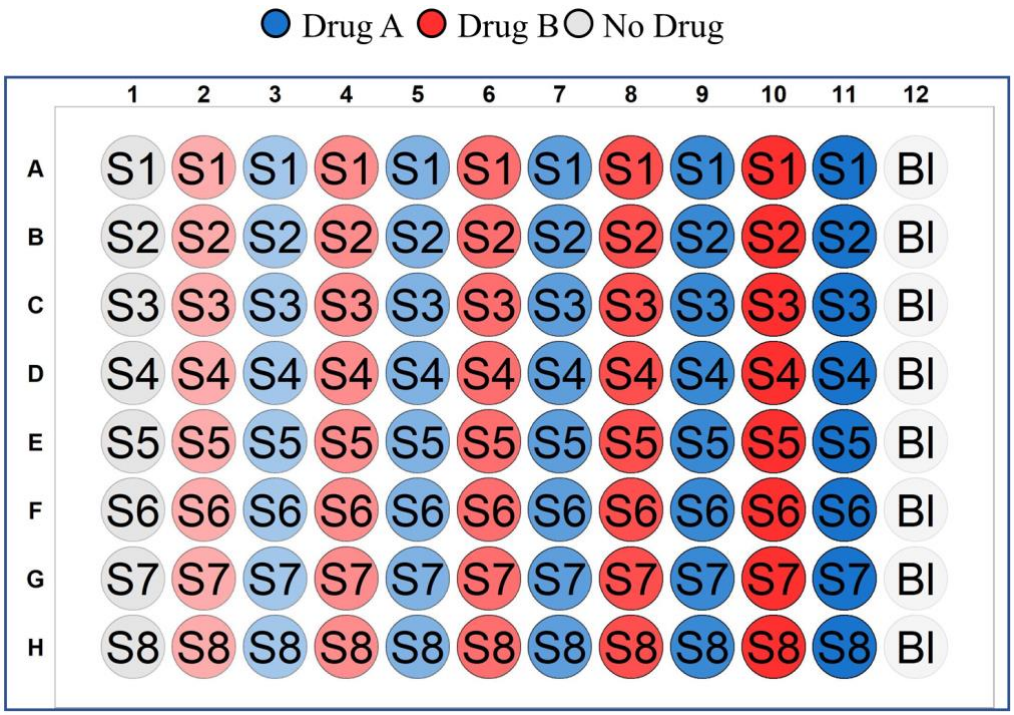


Figure 2.1 Example plate setup for time-lapse microscopy with eight different strains (S1-S8) and two different drugs (Drug A and B). To ensure the strains are growing as expected, include wells that contain no drug (column 1). As a contamination check, include blank wells with medium but without cells (column 12; "Bl"). The gradient of the colors from high to low saturation represent the decreasing concentration of drug with each dilution (column 3 has the lowest concentration of drug A and column 2 has the lowest concentration of drug B).

2.3 BASIC PROTOCOL 2: TIME-LAPSE MICROSCOPY

The Evos FL Auto 2 (Thermo Scientific) was used to take images every 1 h for 24 h. Between images the plate was kept in a 37 °C incubator. The Evos can be set up to incubate and automatically scan a 96-well plate for 24 h without manual intervention if the onstage incubation is available.

Any microscopy system capable of taking high resolution images can be used in lieu of the Evos FL Auto 2 Imaging System.

Materials

Hardware- a computer with at least 4GB RAM

-Evos FL Auto 2 (Thermo Scientific, Catalog number: AMAFD2000)

Software- EVOS FL Auto 2 Imaging System

1. Turn on the machine.
2. Place the 96-well plate containing your samples on the stage.

Note: Make sure you are using the 96-well plate vessel on the microscope.

3. Open EVOS FL Auto 2 Imaging System and click on the **Vessel** (top right). Click on **Well Plates** and select **Well Plate** for the **holder** and **96 Well** for the **Plate**. Click **Done** to finish your vessel set up.
4. Click on a well that contains your sample, select **10×** for your **Objective** and **Trans** for your **Light source.**
5. Bring the cursor of the **Bright** to the middle and click on **AutoFocus**. When your sample comes into focus, click on **Capture.**

   Note: After focusing, you can adjust the brightness to suit your needs.
6. To set up a scanning protocol, click on the **Automate tab**. Go to **Hardware** -> **Edit** and select **20×** for **Objective** and **Trans** for **Channels**. Click on **Done** when you finish picking your parameters.
7. To adjust the scan area, click on **Select scan areas** -> **Assign scan area** and select the desired area of the plate to be scanned and click **Done.** Click on **Pattern** and enter **1** in the **W** and **H fields of view.** Check the **Stitching** box and click on **Create.**
8. Open **AutoFocus** and **Z Stacks** and click on **review**. Check the **Use Autofocus** box and select **Single Channels.** Make sure that **Trans** is selected in the **Channel** option and the **Z-Offsets** box is checked. Select **Every field** option for the **AutoFocus Frequency.** Click **Done** to save your settings.
9. Click on **Image Save Settings** -> **Edit.** Specify the location where you wish to save your images and click on **Done.** You can also save the scan protocol you created for future use by clicking on **Save** in the **Automate tab.**

   *If you wish to use the same protocol in future, in the Automate tab click on **Load** and navigate to the folder containing your saved protocol. Select the desired protocol and click **Open.***
10. Click on **Run** to scan your plate.

    This is the 0 h (t0) reading. Every new scan will be exported into its own unique folder. Images will be named after their position (i.e., images of well G11 will be named "G11.TIF"). The default naming convention for Evos is scan.date-time (e.g., scan.2021-02-16-16-22-15). It is recommended that you change the name of the folder that contains your images to a name that indicates the time point.

11. Incubate the plate statically at 37 °C for 24 h and take images hourly using Evos FL Auto 2. As long as no one else is using the machine and changes the settings, at each desired time point, click **Run** to scan your plate. If the settings are changed between images just reopen the saved protocol (step 23).

    Note: If on-stage incubation is set up then the plate will stay in the machine and readings can be automatically taken every hour.

12. If you are doing a 24 h time-lapse, you will have 25 folders by the end of your experiment, which each contain 96 images (example images in Figure 2.2).

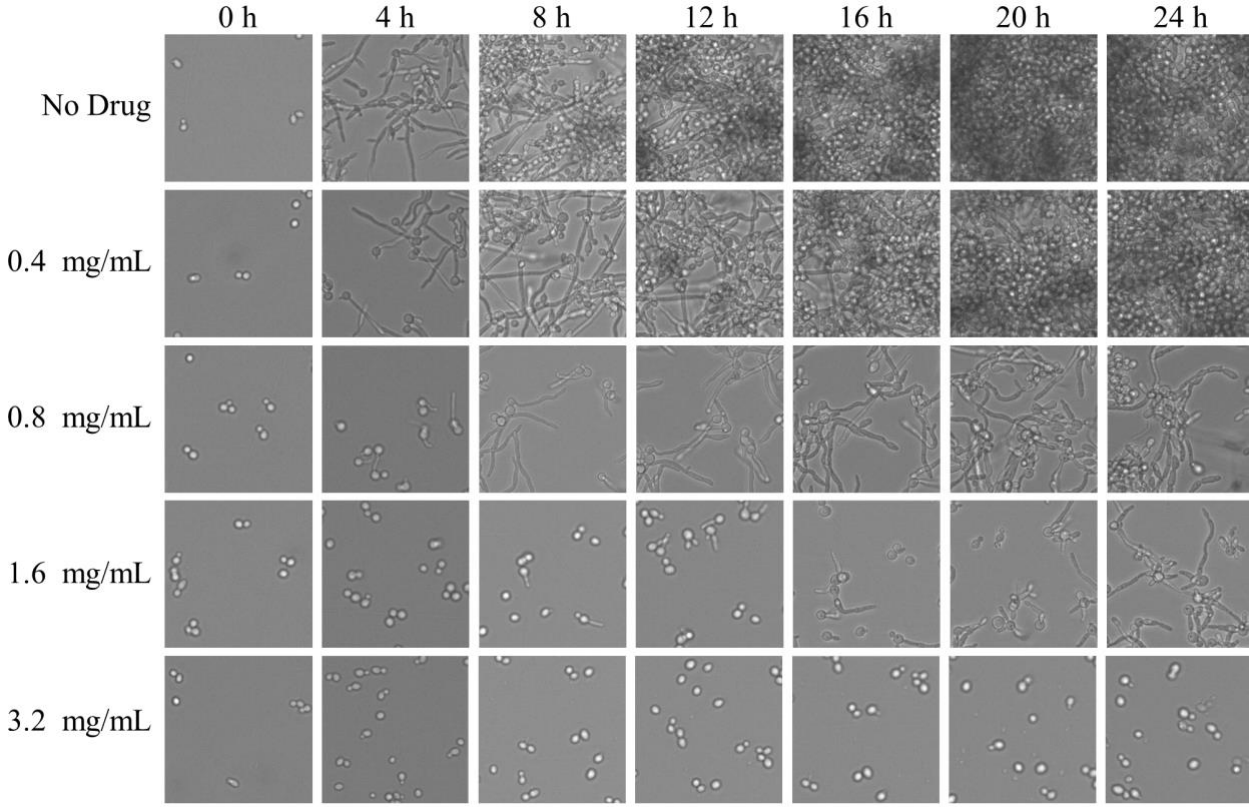


Figure 2.2 Images were captured every hour for 24 h using Evos FL 2 Imaging System. Shown are sample images of a clinical *Candida albicans* strain grown in RPMI-1640 + boric acid at 37°C.

2.4 BASIC PROTOCOL 3: BATCH FILE RENAMING

Time-lapse of a 96-well plate with images taken every hour for 24 hours produces 2304 images; this number will be even larger if the experiment is repeated to get additional biological replicates. The Evos auto names images by their position and splits different time points into different folders (t0-t24); all images will need to be put into one folder for Basic Protocol 4. Renaming each image manually is a time-consuming and tedious task that is prone to typos. Described below is an

efficient way to automate file renaming using a combination of the free Windows filename program "Bulk Rename Utility" and the R Programming Language.

Materials

Hardware- a computer with at least 4GB RAM.

Software- Bulk Rename Utility (https://www.bulkrenameutility.co.uk/).

- R (https://www.r-project.org/).
- RStudio (https://www.rstudio.com/products/rstudio/download/).
- tidyverse package (Wickham et al., 2019).

Files- TIFF images from Evos output (other image formats should also be fine).

- .csv file that contains plate layout (see Table 2.1 for an example)
- BP3-BatchRenaming.R (Supporting Information).

1. Download Bulk Rename Utility from https://www.bulkrenameutility.co.uk/. Follow the installation instructions.

   Note: The installer has both the 32-bit and the 64-bit version. Bulk Rename Utility is only available for Windows 7, 8, and 10. Files can be bulk-renamed in Mac through Finder.
2. Open Bulk Rename Utility and go to the folder that contains your images.

   For example, go to the folder that has the images from time point 1. On a Mac, open Finder and go to the folder that contains your images.
3. In the **Add (7)** panel, write underscore + the time point in the **Suffix**. Select all of the images in the folder and click **Rename.**

   *Before clicking rename, check the **New Name** column and make sure this is what the name should look like. The names of the files should be well position + time point + image file format (for example, G11_t01.TIF).*

   *On a Mac, click on **Action —> Rename Items —> Add text** to add the appropriate time-point as a suffix as above.*
4. Repeat step 3 for all of the folders that contain the different time points.
5. Put all of the images into one folder.

   Now all of the images have unique names and will not overwrite each other when put together in one folder.

Before proceeding to the next step, you will need to install R and RStudio if you have not already done so. You will also need to create a .csv file that contains your plate layout (Table 2.1). You

will be using that .csv file to rename your files. You can add more or less information to the file names by adding or removing columns. For example, you can add a 'Replicate' column or remove the 'Drug' column. At the end of Protocol 4, your files will look something like this: Calb_DrugA_2_t01.TIF (Strain_Drug_Concentration_timepoint.TIF). **It is strongly recommended you keep a backup of your images in case you misname them.**

Table 2.1 Plate layout example.

Well	Strain	Drug	Concentration
A01	SC5314	ND	0
A02	SC5314	Drug-A	2
A03	SC5314	Drug-B	0.4
A04	SC5314	Drug-A	4
A05	SC5314	Drug-B	0.8
A06	SC5314	Drug-A	8

6. Open RStudio and load the tidyverse library.
   `library(tidyverse)`
   If this is the first time you are using tidyverse, you will need to install the package using the `install.packages("tidyverse")`*. You only need to install the package once; however, you will need to load the tidyverse library every time you exit your R session.*
7. Load the .csv file that contains your plate layout. Click on **Import Dataset —**> **From Text (readr) —**> **Browse.** Find the plate layout file and click **Open.** In the **Import Options**, change the name to a simple name such as plate_layout. Click on **Import** when you are done.
8. Go to **Session —**> **Set Working Directory —**> **Choose Directory.** Open the folder that contains the images you want to rename and click **Open.**
9. Run `list.files(pattern = "*.TIF")` and make sure that the files returned in the R console are the ones you want to rename.
   If your images are not TIF files, change the pattern to match your image format (For example, if you have jpg files, your code would change to: `list.files(pattern = "*.jpg")`

10. Create a dataframe (Evos_tbl) that contains a column ("EvosNames") with the image names (e.g., A01_t01.TIF):

```
Evos_tbl <- tibble(EvosNames =
                     unlist(list.files(pattern = "*.TIF" )))
```

11. Create a dataframe (Evos_separate) with a separate column for each piece of information (i.e., one column for well, one column for time point, and one column with the image type). This information is then attached to the dataframe Evos_tbl created in step 36.

```
Evos_separate <- Evos_tbl %>%
  separate(EvosNames,
           into = c("well", "time point", "image")) %>%
  cbind(Evos_tbl)
```

12. Join `plate_layout` dataframe with `Evos_separate`. Create a new column ("NewFullName") that combines the strain, drug, concentration, and time point columns. The final dataframe, `Full`, is then selected to keep only 2 columns; column 1, "EvosNames", will contain the existing file names and column 2, "NewFullName", will contain the corresponding new name (strain_drug_concentration_time point).

```
Full <- Evos_separate %>%
  merge(plate_layout, by = "well" ) %>%
  unite(col = "NewFullName", c(strain, drug,
                               concentration, time point),
        sep = "_", na.rm = TRUE) %>%
  select(EvosNames, NewFullName)
```

13. Rename the files using the `Full` dataframe.

```
file.rename(from = Full$EvosNames,
            to = paste0(Full$NewFullName, ".TIF"))
```

After running this line, R will look for the file names matching the EvosNames column and will replace it with the corresponding new name. If there is an image that has a name not listed in `EvosNames`, it will not be renamed. If your images are not TIF files, change ".TIF" in the paste0 argument to the image format you are using (for example, if your images are .jpg, then change it to `paste0(Full$NewFullName, ".jpg")`. By the end of this step, all of your images will have a new name.

2.5 BASIC PROTOCOL 4: MACHINE LEARNING ANALYSIS OF EVOS IMAGES WITH ORBIT

Time-lapse experiments of 96-well plates produce a large number of images. Analyzing those images by eye is time consuming and potentially subjective. We developed a novel quantitative pipeline to measure parameters that correlate with adherence and biofilm formation. Orbit Image Analysis is a user-friendly tool that uses machine learning to detect cells of interest. In this protocol, Orbit is trained to detect fungal cells and calculate the % area covered by cells from time-lapse microscopy images.

Materials

Hardware- a computer with at least 8GB RAM

Software- Orbit Image Analysis version 3.64 or higher

Files- TIFF images from Evos output (other image formats should also be fine)

Download and install Orbit

1. Go to https://www.orbit.bio/download/ and look for your OS and press download (if you are using a 32bit OS, download the JAR version)
2. Lunch orbit_xxx_exe and follow the installation instructions

Importing images and defining classes

3. Open Orbit by double-clicking the icon. Orbit will ask whether you want to configure an Omero image server; press **No** if you do not have one (Figure 2.3A). When Orbit asks whether a local filesystem fallback is used, press **Continue** (Figure 2.3B).
4. Go to **Image —**> **Open Image from File System —**> Select a few images or an image that contains all of the cell types that need to be detected (Figure 2.3C &D). Click **Open** when you are done.

   Typically, 3 images are sufficient for training: one from t0, one that has an intermediate concentration of cells (usually t08) and one that is highly saturated with cells (usually t24).
5. In the menu bar, go to **Model —**> **Classes** (or press **F2**). Define the different classes in your images (e.g., Background and Fungi). The default is 3 classes: **Background**, **Celltype1** and **Celltype2**. To rename a class, click on the class to be renamed, write the new name, and press **rename class**. You can add a class by pressing on **add class** or remove one by pressing

on **remove class**. Press **OK** when you are done with defining classes. In this protocol, the images have two classes: Background and Fungi (Figure 2.4A).

Training and saving a model

6. Select class Background from the drop-down class menu (top-left). From the menu bar, go to **Classification** and choose **Polygon**. You have to mark representative regions of Background (Figure 2.4A & B). When you are defining the background, try to come close to the cells.
7. Repeat step 6 but change the class to Fungi. When you are defining class Fungi, try as much as possible to not include background in the selected regions.
8. Repeat steps 6 & 7for all opened images.
9. Press on **Train (F7)** to train a model to detect the defined classes.
   Note: Training will be done only on opened images. If you close an image that had the different classes regions selected, it will not be included in the training.
10. Go to **Help** and click on **Show Log** and check the quality of your model.
11. Go back to the **Classification** panel and click on **Classify (F9)**. Drag the Opacity slider to check whether Orbit detected the right objects (Figure 2.4C).
    If you are not happy with the detection model, repeat step 6-11. Select more regions representative of your cells and background. Double check that you are using the right class when using the polygon and marking your cells and background. A common mistake is marking your cells with the polygon tool while selecting the wrong class from the drop-down class menu.
12. Open an image that was not included in the training, click on **Classify**, and check whether the model that has been created can still accurately identify cells. Use the opacity slider to check the quality of your detection model.
    *If you are not satisfied with the model, repeat step 6-12. It is recommended that you include the image that Orbit had trouble detecting cells in in your opened images to include it in the training model. Open a different image when the training is done and click on **Classify** to check if the newly created model is better. Keep in mind that every time you click **Train**, you are overwriting the previous model and any image you close will not be included in the new model.*

13. Go to **Model** and click on **Save Model as (Figure 2.4D).**

    *You can load your saved model anytime using **Open Model**.*

Batch analysis

14. Go to **Batch** and click on **Local Execution** (Figure 2.5A). Select all of the images to be analyzed and click on **Open** (Figure 2.5B). Orbit will ask you whether the model you are applying is a ratio quantification model, click on **Yes** (Figure 2.5C). This step may take up a few hours, and you can check that it is running by going to **Help —> Show Log**. Orbit will eventually pop up a window with the classification results (Figure 2.5D). Copy the results to an excel file and save it as a comma-delimited (.csv) file (Figure 2.5E). The quantification model calculates the % area covered by cells for each time-lapse image.

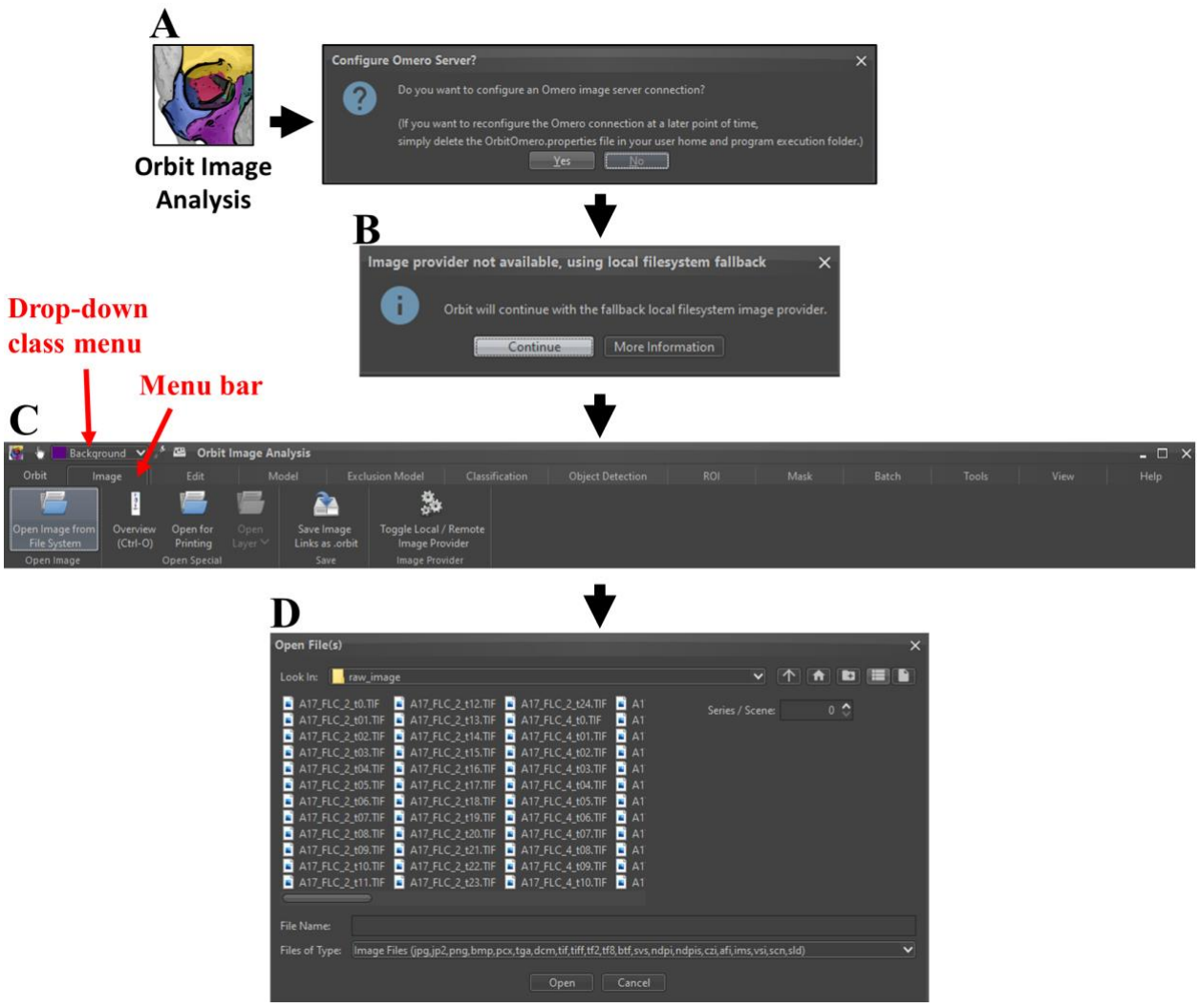


Figure 2.3 Orbit Image Analysis interface running on PC Windows 10. (A) Open Orbit and click on No when the "Configure Omero Server?" message pops up. (B) Click on Continue when "Image provider not available, using a local filesystem fallback" message pops up. (C) Now you are in the main Orbit interface with the drop-down class menu on the top left and the menu bar just below. (C and D) To open an image, select Image from the menu bar and click on Open Image from File System. Select the image/images and click Open.

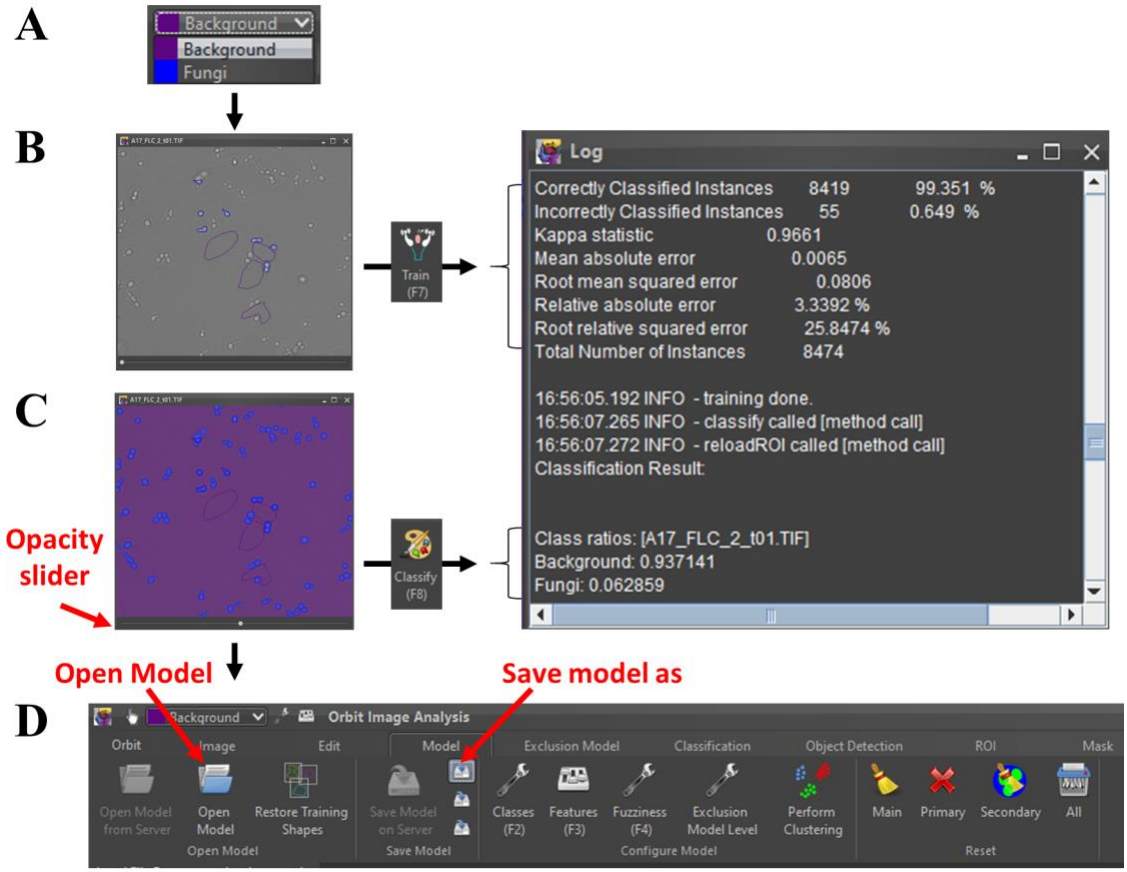
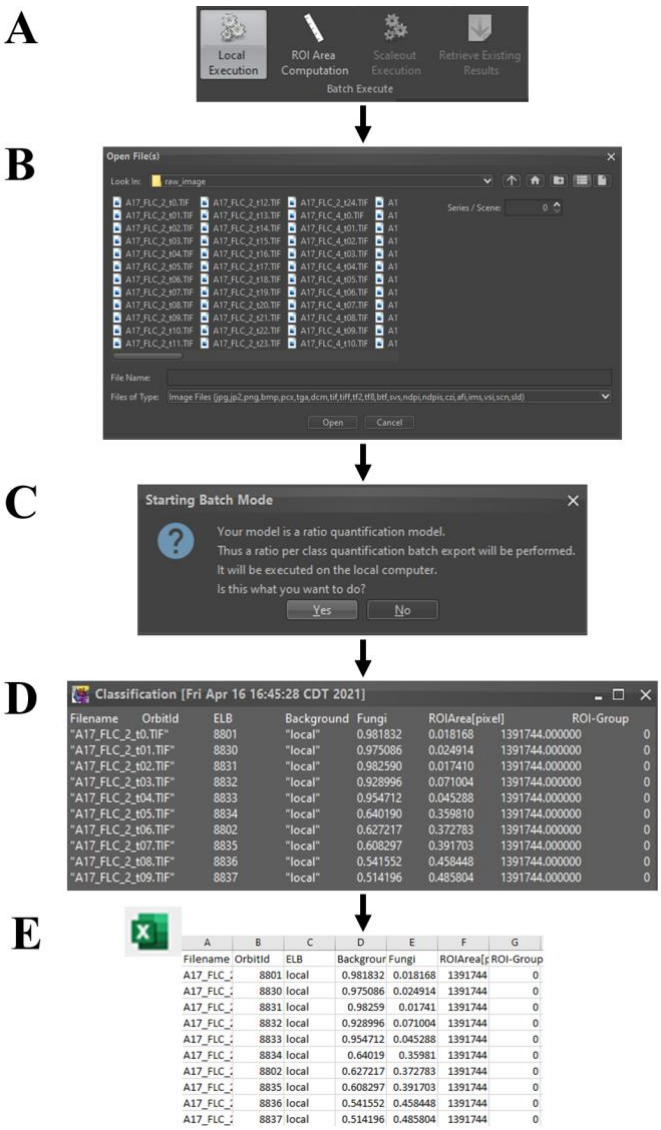


Figure 2.4 Training the machine learning algorithm based on the selected classes. A & B) Select representative regions for background (purple) and fungal cells (blue) using the polygon tool. Train a classification model by clicking on Train. The log output indicates model fit; in this case, 99.3% correctly of instances were correctly classified. C) Test the model by clicking on Classify; use the opacity slider to check if the model is capable of differentiating between the background and cells. The log output indicates the % area covered by fungal cells and the percent area of the background. D) Save the model by going to Model in the menu bar and clicking on Save model as.



Filename	OrbitId	ELB	Background	Fungi	ROIArea[pixel]	ROI-Group
"A17_FLC_2_t0.TIF"	8801	"local"	0.981832	0.018168	1391744.000000	0
"A17_FLC_2_t01.TIF"	8830	"local"	0.975086	0.024914	1391744.000000	0
"A17_FLC_2_t02.TIF"	8831	"local"	0.982590	0.017410	1391744.000000	0
"A17_FLC_2_t03.TIF"	8832	"local"	0.928996	0.071004	1391744.000000	0
"A17_FLC_2_t04.TIF"	8833	"local"	0.954712	0.045288	1391744.000000	0
"A17_FLC_2_t05.TIF"	8834	"local"	0.640190	0.359810	1391744.000000	0
"A17_FLC_2_t06.TIF"	8802	"local"	0.627217	0.372783	1391744.000000	0
"A17_FLC_2_t07.TIF"	8835	"local"	0.608297	0.391703	1391744.000000	0
"A17_FLC_2_t08.TIF"	8836	"local"	0.541552	0.458448	1391744.000000	0
"A17_FLC_2_t09.TIF"	8837	"local"	0.514196	0.485804	1391744.000000	0

	A	B	C	D	E	F	G
	Filename	OrbitId	ELB	Backgrour	Fungi	ROIArea[p	ROI-Group
	A17_FLC_2	8801	local	0.981832	0.018168	1391744	0
	A17_FLC_2	8830	local	0.975086	0.024914	1391744	0
	A17_FLC_2	8831	local	0.98259	0.01741	1391744	0
	A17_FLC_2	8832	local	0.928996	0.071004	1391744	0
	A17_FLC_2	8833	local	0.954712	0.045288	1391744	0
	A17_FLC_2	8834	local	0.64019	0.35981	1391744	0
	A17_FLC_2	8802	local	0.627217	0.372783	1391744	0
	A17_FLC_2	8835	local	0.608297	0.391703	1391744	0
	A17_FLC_2	8836	local	0.541552	0.458448	1391744	0
	A17_FLC_2	8837	local	0.514196	0.485804	1391744	0

Figure 2.5 Batch Analysis and data export. A) After creating a successful model, run a batch analysis by going to Batch and clicking on Local Execution. B) Select all of the images to be analyzed. C) Click on Yes when a "Starting Batch Mode" message pops up. D) When the analysis is done, a "Classification" output window will pop up. D) Select the classification output using Ctrl + A and E) copy to Excel. Save the excel file as a comma-delimited (.csv) file.

2.6 BASIC PROTOCOL 5: PARAMETRIZATION OF ORBIT OUTPUT IN R

In this protocol, the growthcurver R package (Sprouffske, 2020) is used to fit a logistic equation to the % area data output from Basic Protocol 4. From the logistic fit determine for each well, we extract relevant parameters that correlate with biofilm formation: growth rate (measured as the slope of cellular growth, measured as % area covered); growth plateau (the asymptote of % area covered); and time to reach the asymptote. Prior to running the logistic fit function, the data are cleaned using functions from the tidyverse R metapackage (Wickham et al., 2019). Here we show how the Orbit data is cleaned, how to extract the asymptote and slope, and how to calculate the time to reach the asymptote.

Materials

Hardware- a computer with at least 4GB RAM

Software- R (https://www.r-project.org/).

- RStudio (https://www.rstudio.com/products/rstudio/download/).
- The tidyverse package (Wickham et al., 2019).
- The growthcurver package (Sprouffske, 2020).

Files- .csv file that contains Orbit output. (see OrbitOutput_SampleData.csv found in Supporting Information for mock Orbit sample)

- BP5-OrbitParameterization.R (Supporting Information)

1. Open RStudio. Go to **View —**> **Panes —**> **Show All Panes**

   Depending on your set up, this may be an unnecessary step as all panes may already be showing.

2. Go to **Session —**> **Set Working Directory —**> **Choose Directory** and find the folder that contains the Orbit output .csv file. Select the folder and click **Open.**

   Any files and images you will save will be saved to that working directory.

3. Load the tidyverse and growthcurver libraries

   ```
   library(tidyverse)
   library(growthcurver)
   ```

   If this is the first time using these libraries, you will have to install them first:

   ```
   install.packages("tidyverse")
   install.packages("growthcurver")
   ```

4. Under the **Environment** panel, click on **Import Dataset —**> **From Text(readr)**. Click on **Browse** and look for the folder containing your Orbit output .csv file. Select the file and click on **Open**. At the bottom left, find **Import Options** and change the **Name** to **df** (which stands for dataframe). Click on **Import** when you are done. Under the Environment panel, you should be able to see df data that just got imported.

   A pop-up view window of the dataset will appear after you click Import. Double check that the right data is being imported and being read correctly.

   You can also import datasets programmatically using a read_csv() function call.

5. The file name format described in Basic Protocol 3 contains information about: strain, drug, drug concentration, and the time point the image was captured. Separate this information into different columns using tidyverse functions. The end result is a dataframe (`df_cleaned`) that contains columns for each component of your file name and % area covered by cells.

```
df_clean <- df %>%
  separate(Filename, c("strain", "drug", "concentration",
                       "timepoint"), sep = "_") %>%
  separate(timepoint, c("timepoint", "image_format")) %>%
  separate(timepoint, c("t", "time"), sep = "t") %>%
  select(strain, drug, concentration, time, Fungi) %>%
  rename("area" = "Fungi") %>%
  mutate_each(funs(as.numeric), time)
```

   If the file name format is different from what is described in Basic Protocol 3, the code needs to be tweaked. For example, if your file name does not contain "drug" and "concentration", change the code to:

```
df_clean <- df %>%
  separate(Filename, c("strain",
                       "timepoint"), sep = "_") %>%
  separate(timepoint, c("timepoint", "image_format")) %>%
  separate(timepoint, c("t", "time"), sep = "t") %>%
  select(strain, time, Fungi) %>%
  rename("area" = "Fungi") %>%
  mutate_each(funs(as.numeric), time)
```

6. Create a new dataframe (`df_0`) where the % area at the first time point (t0) has been subtracted from all time points.

   To fit a logistic equation, the % area at the first time point has to be equal to zero. The subtracted area will be added back after model fitting.

```
t0 <- df_clean %>%
  filter(time == 0)

df_0 <- merge(df_clean, t0, by = c("strain", "drug",
                                   "concentration")) %>%
  select(!time.y) %>%
  mutate(area = area.x - area.y) %>%
  select(c(strain, drug, concentration, time.x, area)) %>%
  rename("time" = "time.x")
```

7. Convert `df_0` from a long dataframe to a wide dataframe (`df_0_wide`). This way each column contains the data for all time points from each well, which is required for the next step.

```
df_0_wide <- df_0 %>%
  unite(sample, strain, drug, concentration) %>%
  pivot_wider(names_from = sample, values_from = area)
```

8. Obtain the summary metrics of the logistic fit to each well by running the `SummarizeGrowthByPlate()` function (from the growthcurver R package), saved in the `logfit_params0` dataframe. View `logfit_params0` to see the resulting dataframe: "sample" corresponds to the file name, "r" is the slope of the logistic fit (rate of growth), "k" is the asymptote of the logistic fit, and "t_gen" is the generation time (time it takes for a population to double in size).

```
logfit_params0 <- SummarizeGrowthByPlate(df_0_wide)
view(logfit_params0)
```

9. Create a new dataframe `logfit_params` that combines the `t0` with `logfit_params0` dataframes, separates the sample column into strain, drug and drug concentration, contains and adds back the subtracted area from time point zero (t0) to the asymptote (k).

```
logfit_params <- unite(t0, sample, strain, drug,
```

```
                        concentration) %>%
  merge(logfit_params0) %>%
  group_by(sample) %>%
  mutate(k = area + k) %>%
  select(!time & !area) %>%
  separate(sample, into = c("strain", "drug",
                            "concentration"), sep = "_")
```

10. Check the notes column of logfit_params. If the `SummarizeGrowthByPlate()` function was unable to fit a logistic equation to a given well it will say "cannot fit data", rerun Step 60 and exclude those wells.

    For example, if you want to remove sample Calb_FLC_16:

```
df_0_wide <- df_0 %>%
    unite(sample, strain, drug, concentration) %>%
    filter(!sample == "Calb_FLC_16") %>%
    pivot_wider(names_from = sample, values_from = area)
```

    If you want to remove multiple samples, adjust the filter function to include the samples you want to remove:

```
filter(!sample %in% c("S2_FLC_1", "S7_FLC_2", "S11_FLC_1"))
```

11. Create a new dataframe, df_predicted_plate, that contains predicted y values (predicted % area based on the best fitting logistic equation) for each model fit (obtained by applying the `SummarizeGrowth`() function to all wells). This is used for plotting.

```
models_all <- lapply(df_0_wide[2:ncol(df_0_wide)],
     function(x) SummarizeGrowth(df_0_wide$time, x)
)

df_predicted_plate <- data.frame(time = df_0_wide$time)

for (i in names(df_0_wide[2:ncol(df_0_wide)])){
  df_predicted_plate[[i]] <-
    stats:::predict(models_all[[i]]$model)
  }
```

12. Create a dataframe, `df_0_logfit`, that contains the % area and predicted % area from the logistic fit.

```
df_0_logfit <- cbind(
  pivot_longer(df_0_wide, !time,
               names_to = "sample",
               values_to = "area"),
  pred_area = pivot_longer(df_predicted_plate, !time,
     names_to = "sample",
     values_to = "pred_area")[,3]) %>%
  separate(sample,
     c("strain", "drug", "concentration"), "_")
```

13. Create another data frame `df_final` that adds the subtracted t0 % area back to the area and predicted % area columns.

```
df_final <- merge(df_0_logfit, t0,
                  by = c("strain", "drug",
                         "concentration")) %>%
  select(!time.y) %>%
  rename("time" = "time.x") %>%
  group_by(strain, drug, concentration, time) %>%
  summarise(area = area.x + area.y,
            pred_area = pred_area + area.y)
```

14. Save `df_final` as a .csv file.

```
write_csv(df_final,
          file = "example_data_predicted.csv")
```

The file will be saved to the folder you set as your working directory in step 55. Note the file you save can be named whatever you like.

15. Create a new dataframe, `logfit_params_corrected`, contains the previously calculated logistic fit parameters and uses the predicted areas calculated above to determine the time it took to reach the asymptote. If you have wells with no or low growth, two additional columns, `k_corrected` and `r_corrected` are used to account for poor or incorrect model fit. Respectively, they set the % area at asymptote (k) to be equal to the %

area at the end time point and the rate of growth (r) to be equal to 0. `t_asym` (the time it takes to reach k) is also adjusted to be equal to the final time point + 4 (this is used for visualization, below). If you have robust growth in all wells, data in the `k_corrected` and `r_corrected` columns should be the same as in the `k` and `r` columns. Save `logfit_params_corrected` as a .csv file.

```
logfit_corrected <- logfit_params %>%
  select(strain, drug, concentration, k, r) %>%
  merge(df_final, by = c("strain", "drug",
                         "concentration")) %>%
  mutate(k_corrected = replace(k, round(k, digits = 2) > 1,
                           pred_area[which(time == "24")]),
         r_corrected = replace(r, k < 0.15, 0),
         k = round(k, digits = 2),
         pred_area = round(pred_area, digits = 2)) %>%
  group_by(strain, concentration, drug) %>%
  summarise(t_asym = time[which.min(abs (pred_area - k))],
            k_corrected = mean(k_corrected),
            r_corrected = mean(r_corrected)) %>%
  mutate(t_asym = replace(t_asym, r_corrected == 0, 28))

logfit_params_corrected <- merge(logfit_corrected,
                                 logfit_params,
                                 by = c("strain", "drug",
                                        "concentration"))
write_csv(logfit_params_corrected,
          file = "example_data_logfit.csv")
```

If your experiment is not 24 h, change the number in `pred_area[which(time == "24")]`) *to the experiment length (e.g.,* `pred_area[which(time == "48" )]`).
If you have wells with low or no growth and your experiment is not 24 h, change "28" in `mutate(t_asym = replace(t_asym, r_corrected == 0, 28))` to the length

of your experiment + 4 (e.g., for a 48 h experiment, `mutate(t_asym = replace(t_asym, r_corrected == 0, 52))`).

The file will be saved to the folder you set as your working directory in step 55.

Note the file you save can be named whatever you like.

2.7 BASC PROTOCOL 6: VISUALIZATION OF LOGISTIC FITS IN R

Visualization of the data is an important step in data analysis; it makes it easy to identify patterns, provide valuable insights about the data, and is required to communicate the results to your intended audience. In this protocol, `ggplot()` (part of the tidyverse package) will be used to visualize the output data from Basic Protocol 5.

Materials

Hardware- a computer with at least 4GB RAM

Software- R and RStudio

- The tidyverse package (Wickham et al., 2019).

Files- The two .csv files output from Basic Protocol 5

- BP6-LogFitParamsVis.R (Supporting Information)

1. Open RStudio and go to **Session —> Set Working Directory —> Choose Directory** and find the folder that contains the Basic protocol 5 output .csv files. Select the folder and click **Open.**

   You can skip this step if you are on the same R session used in Basic Protocol 5.

2. Load the tidyverse library

   ```
   library(tidyverse)
   ```

   You can skip this step if you are on the same R session used in Basic Protocol 5. You only need to load the tidyverse library

3. Read in the .csv file you saved in steps 14 and 15 in Basic Protocol 5. You will be using those files for visualizing your data.

   *import the data using **Import Dataset —> From Text(readr)**, remember to change the name in the **Import Options** to `df_final` and `logfit_params_corrected`. You can skip this step if you are on the same R session used in Basic Protocol 5.*

4. Plot the % area covered by cells for each time point (one panel for each strain) and a line of the logistic fit using `ggplot()`.

```
df_final %>%
  ggplot(aes(x = time, y = area, color = concentration,
             group = concentration))+
  geom_point() +
  geom_line(aes(y = pred_area)) +
  scale_x_continuous(breaks = seq(0, 24, 4)) +
  facet_wrap(~strain)+
  xlab("Time (hours)") +
  ylab("Area % Covered by Cells") +
  scale_color_gradient(low = "blue", high = "red") +
  theme_bw()
```

If you have multiple conditions (e.g., drugs) and you want a separate panel for each, you can change the `facet_wrap` *function to, e.g.,* `facet_grid(drug ~ strain)`*. If your incubation time is not 24 h, change 24 in* `scale_x_continuous()` *to your incubation time.* For example, if your incubation time is 48 h, change `scale_x_continuous()` *to* `scale_x_continuous(breaks = seq(0, 48, 4))`.

5. Plot the parameters that were extracted from the logistic fit (asymptote, slope, and time to reach the asymptote):

```
# plot the asymtotes
logfit_params_corrected %>%
  ggplot(aes(x = concentration, y = k_corrected,
             group = strain)) +
  geom_point(size = 2) +
  geom_line() +
  facet_wrap(~strain) +
  xlab("BA Concentration (mg/mL)") +
  ylab("% Area at Asymptote") +
  theme_bw()

# plot the slopes
logfit_params_corrected %>%
```

```
  ggplot(aes(x = concentration, y = r_corrected,
             group = strain)) +
  geom_point(size = 2) +
  geom_line() +
  facet_wrap(~strain) +
  xlab("BA Concentration (mg/mL)") +
  ylab("Slope") +
  theme_bw()

# plot the time to reach the asymptote
logfit_params_corrected %>%
  ggplot(aes(x = concentration, y = t_asym,
             group = strain)) +
  geom_point(aes(shape = t_asym > 24), size = 2) +
  geom_line() +
  scale_y_continuous(breaks = seq(0, 28, 4),
                     labels = c(seq(0 , 24, 4), "> 24"),
                     limits = c(0, 28)) +
  scale_shape_manual(values = c(16, 1)) +
  facet_wrap(~strain) +
  xlab("BA Concentration (mg/mL)") +
  ylab("Time to Asymptote (h)") +
  theme_bw() +
  theme(legend.position = "none")
```

If you have multiple conditions (e.g., drugs) and you want a separate panel for each, you can change the `facet_wrap` *function to, e.g.,* `facet_grid(drug ~ strain)`.

When plotting time to reach the asymptote, if your experiment is not 24 h, change "24" in the `geom_point()` *and* `scale_y_continuous()` *functions to the appropriate numbers (as in Basic Protocol 5). For example, if your experiment is 48 h, change to* `geom_point(aes(shape = t_asym > 48), size = 2)`

and `scale_y_continuous()` *to* `scale_y_continuous(breaks = seq(0, 52, 4), labels = c(seq(0 , 48, 4), "> 48"), limits = c(0, 52))`. *The* `geom_point()` *code changes the point type for wells with poor or low growth to be a different point type than other wells (point types are specified in the* `scale_shape_manual()` function. *If all wells have robust growth, the "limits" flag in the* `scale_y_continuous()` *function can be changed to, e.g.,* c(0, 24)(*for a 24 h experiment).*

6. Save the plots you have made by clicking on **Export** in the Plots panel (typically on the bottom right) and click on **Save as Image**. You can change the file name and image format, width and height of the plot you wish to save. Click on **Directory** to select the folder you want to save your image to and click **Open** after selecting the folder. Click **Save** to save the image.

   Use the arrows in the Plots panel to navigate through your plots. You have to repeat this step for each plot.

2.8 REAGENTS AND SOLUTIONS

Ampicillin Stock, 1000x

750 ug of Ampicillin sodium salt (Fisher BioReagents, Catalog number: BP176025)

7.5 mL of dH2O

Aliquot into 750 μL

Chloramphenicol Stock, 1000x

187.5 mg of Chloramphenicol (Fisher BioReagents, Catalog number: BP904-100)

7.5 mL of 95% ethanol (Greenfield Global, Catalog number: P025EA95)

Glucose, 40%

20 mL of dH2O

Dissolve 15 g dextrose (Fisher Chemical, Catalog number: D16500) using stir bar

Bring volume to 37.5 mL using dH2O

Autoclave

Aliquot into 750 μL

Phosphate-buffered saline (PBS), 0.01M

2 tablets of PBS tablets (BioReagents, Catalog number: BP308100)

400 mL of dH2O

Autoclave

RPMI-1640 medium

10.4 g of RPMI-1640 powder (Sigma-Aldrich, Catalog number: R6504)

15.0 g Dextrose (Fisher Chemical, Catalog number: D16500)

17.3 g of MOPs (Fisher BioReagents, Catalog number: BP308-100)

pH to 7 using NaOH (Fisher Chemical, Catalog number: S318-500)

Filter sterilize

YPD liquid medium

15 g Bacto Peptone (gibco, Catalog number: DF0118-17-0)

7.5 g Yeast Extract (gibco, Catalog number: 288610)

120 mg Adenine Hemisulfate (Thermo Fisher Scientific, Catalog number: A1696409)

60 mg Uridine (Sigma-Aldrich, Catalog number: U3750)

712.5 mL dH2O

Autoclave

Add 750 µL of 1000× ampicillin stock (See recipe)

Add 750 µL of 1000× Chloramphenicol stock (See recipe)

Add 37.5 mL of 40% glucose stock when ready to use (See recipe)

2.9 COMMENTARY

2.9.1 BACKGROUND INFORMATION

Sample preparation

Common growth conditions that work for a large number of strains have been used to grow the culture from frozen. YPD is an inexpensive, easy to make rich medium that can be stored for a long time and is commonly used to grow strains from frozen. RPMI-1640 is a standard media used in susceptibility testing. Compared to other media, RPMI-1640 enhances hyphal formation and induces biofilm growth in *C. albicans* (Kucharíková et al., 2011; Weerasekera et al., 2016). The described growth conditions result in consistent biofilms between different biological replicates. The sample preparation for biofilm formation was adapted from (Pierce et al., 2010) with minor modifications. Since the goal was to examine the drug effect on biofilm formation (not just drug penetration of preformed biofilms), the cells were treated with drug from the beginning to examine how biofilms form under biofilm-stimulating conditions.

Time-lapse microscopy and Orbit Image Analysis

C. albicans forms highly structured biofilms under biofilm stimulating conditions, and the drug response of the early steps of biofilm formation can be visualized using time-lapse microscopy. Time-lapse is a powerful tool that provides spatiotemporal data, and if done using a microscope capable of scanning a 96-well plate, it is a high throughput tool for studying cells. When combined with image analysis, time-lapse can provide both qualitative and quantitative data. Orbit Image Analysis is a new open-source analysis tool that can extract quantitative data from time-lapse images. It includes a machine learning algorithm that can be easily trained to detect cells (Stritt et

al., 2020). It can be downloaded on any computer with at least 8 GB RAM. This facilitates image analysis on a personal computer.

R for renaming, parametrization, and visualization

The R programming language is widely used in many disciplines, including biology and statistics. It is a powerful tool to clean, analyze, and visualize data. It is free and can run on all the major operating systems. R packages are extensions of the core R functionality that are always available for free. We use the tidyverse and growthcurver packages (Wickham et al., 2019; Sprouffske, 2020). The tidyverse is a metapackage (collection of R packages), which includes dpylr, the main tidyverse package used for cleaning the data in Basic Protocol 5, and ggplot2, which is used for visualization in Basic Protocol 6. The growthcurver package is used to fit a logistic equation to the % area data and extract important parameters from the Orbit output, including the asymptote and the slope in Basic Protocol 5. Custom scripts in Basic Protocol 5 & Basic Protocol 6 are provided for additional parameterization (growth rate, % area at asymptote, time to reach the asymptote), and to give an example of the visualization that is possible.

2.9.2 CRITICAL PARAMETERS and TROUBLESHOOTING

Sample preparation

Sterile technique is critical for Basic Protocol 1. It is important to include blank wells to ensure the media has not been contaminated. It is recommended to always start with growing up culture from freezer stocks as mutations (including chromosomal aneuploidy) can arise rapidly in *C. albicans* cultures. In most cases, culture for biofilm assays should typically be grown for less than 18 h from stationary phase or frozen culture, however, if culture is not visible in liquid YPD, a longer growth period may be necessary. To ensure accurate spectrophotometer readings it is often required to dilute the overnight culture. Actual OD_{600} values vary depending on the strain, species, and growth conditions. In the biofilm assay, cells in the control column (no drug) should exhibit robust and rapid growth, and the blank column should remain cell-free for the duration.

Time-lapse microscopy

It is important to use the same machine and scanning protocol for biological replicates. If the scanning protocol is done manually as described here (i.e., the plate was manually taken out of an

incubator every 1 h for a scan), ensure the incubation temperature is consistent. The interval between readings should also be kept as constant as possible. If the microscope has an autofocus option, for consistency it should be used for every scan, not just the first reading. *C. albicans* clinical strains in some environments (e.g., no drug) form hyphae within the first hour, thus it is important to minimize the time between setting up the 96-well plate and the first microscope scan of the plate. It is thus recommended that you set the scanning protocol before beginning using a mock plate that contains some cells.

Batch file renaming

Renaming files through Bulk Rename Utility and R is irreversible, thus it is important to keep a backup of the images that are being renamed in case of error. Consider doing a mock test on a subset of files before renaming all of your raw images. Some of the common mistakes in renaming through R are not setting the working directory to the folder containing the images to be renamed, not loading the tidyverse library, not installing the tidyverse library for the first time, and not changing the image format (e.g., from .TIF to .jpg). See the file BP3-BatchRenaming.pdf (Supporting Information) to see how the script should work. It is recommended that you avoid spaces or special characters in image file names to ensure code compatibility.

Orbit Model training

Image analysis in Orbit and the quality of the detection model is highly dependent on the image quality. Focus, illumination, magnification and scanning time intervals should be kept consistent between biological replicates. The polygon object selection step is critical for the accuracy of the model. Use the slider to check the detection model that you created, and ensure that the model properly differentiates between the cells and the background. If you are not satisfied with the detection model, tweak your selections (i.e., select more cells and more background regions) and train the model again. Model quality will also depend on cell saturation. Sometimes when the whole field of view is covered by cells, Orbit will detect the cells as background (which will influence the logistic fit parameterization). To help address this, highly saturated images should be included in the model training. It is important to test the model on images that are not included in the training set before proceeding to the batch analysis step. If you are using a macOS, you

might experience a very slow response of Orbit if you are using .TIF images. To address this issue, convert the .TIF files to .jpg files.

Parametrization and visualization using R

Parameters such as slope and % area at the asymptote are extracted using the growthcurver package and parameter fits are visualized using the tidyverse package. If this is your first time using these packages, ensure they are installed and loaded. Remember that packages need to be loaded in every R session (this is a common error). If the predicted logistic does not fit the data properly, check whether you initially forgot to subtract the t0 % area and whether you added the subtracted t0 % area back to both the predicted % area and the measured % area. Similarly, if the plotted asymptote by eye does match the value in the `logfit_params_corrected` data set, check whether you added the t0 % area to the asymptote (k) column. Sometimes `SummarizeGrowthByPlate()` will give an unrealistically high asymptote reading ($k > 1$); this indicates that either you have not collected enough data for the model to fit properly. To address this, either run a longer experiment, or you can use the data in the k_corrected column from the `logfit_params_corrected` dataframe. In the k_corrected column, k values > 1 are replaced with the k values from at 24 h. Another potential issue with the algorithm used to calculate the growth rate (`SummarizeGrowthByPlate()`) is that occasionally high growth rates (r) appear for wells that visually appear to have minimal or no growth. The r_corrected column in the `logfit_params_corrected` dataframe records $r = 0$ when $k < 0.15$ at 24 h.

STATISTICAL ANALYSIS:

The goal of these protocols is to calculate parameters from time lapse images that correlate with the ability to form biofilms. With those parameters (growth rate, % area at asymptote, time to reach asymptote) standard statistical analyses can be conducted. The specific tests will depend on the experimental framework. For example, if you are testing whether strain background influences biofilm formation in the presence of the same drug (and have measured biological replicates), you could use an ANOVA with strain as the predictor variable and any of the calculated parameters as the response.

2.9.3 ANTICIPATED RESULTS

Culturing & sample preparation

With some exceptions and depending on the strain, cultures should visually appear saturated (visible clumps of cells at the bottom of the tube) in liquid YPD after overnight growth. After 24 h incubation with drug in the biofilm assay, cells in the control column (no drug; column 1 in Figure 2.1) should have a lot of growth visible while the blank column (column 12 in Figure 2.1) should have no growth. Depending on specifics of the strain and the drug environment, you may or may not see growth in experimental wells.

Time-lapse microscopy

C. albicans biofilms are highly structured; they contain yeast and hyphal cells. Generally, at 0 h, all of the cells should be in the yeast form (Figure 2.2). After 1 h, hyphae should be visible in the control column (column 1). Depending on the drug, concentration, and media, hyphae might be seen in the drug-treated columns in as little as 1 hour or not at all after 24 h. If the Evos FL Auto 2 is used with the autofocusing feature, all of the images are expected to be in focus even when cells are highly saturated. For each time point, the images taken will be saved in a separate folder and will be named after the position (i.e., images from well A01 will be named A01.TIF).

Orbit Image Analysis

The results of this step should reflect what you see by eye (i.e., if you see few cells in the field of view, Orbit should give a low % area, whereas if it visually appears that cells are covering the whole field of view, Orbit should give you > 90% area). If the results do not reflect what you see, check the section Critical Parameters for some suggestions on how to troubleshoot this step.

R for renaming, parametrization and visualization

The expected results of each protocol step alongside the code can be seen in Supporting Information BP3-BatchRenaming.pdf, BP5-OrbitParameterization.pdf, and BP6-LogFitParamsVis.pdf.

2.9.4 TIME CONSIDERATIONS

Culturing

The time required for starting a culture from frozen will vary depending on the number of strains and growth conditions. Starting culture straight from frozen as described for Basic Protocol 1 for 8 strains will take ~5-10 minutes.

Sample preparation for time-lapse microscopy

The time required to set up a 96-well plate will vary depending on the number of strains, the growth environment, and the number of 96-well plates. If the conditions are similar to what is described in Basic Protocol 1, the washing step takes ~30 minutes, standardization takes ~15 minutes, putting the media into the 96-well plate and performing the drug dilutions takes ~10 minutes and transferring cultures into the right wells and sealing the plate takes ~10 minutes.

Time-lapse microscopy

The time required for setting up time-lapse microscopy will vary depending on the machine. If you use the scanning protocol described in Basic protocol 2 it takes ~15 minutes to set up. Note that the protocol can be set up prior to the actual experimental day. Loading in the protocol on the experiment day takes less than 5 minutes. The 96-well plate scans in under 5 minutes. The time that will be spent on the microscope will depend on whether the machine's on-stage incubator is used. If the incubator is used, then after setting up the protocol and starting the experiment you just come back the next day to take the plate out. If you manually take the plate out of the incubator, put it on the microscope, scan it and place it back into the incubator this requires ~5 minutes every 1h for 24h (or whatever your incubation time is).

Batch file renaming

If you are dealing with 2304 images (as described here), adding a time point suffix to the files using Bulk Rename Utility and combining the images in one folder should take ~20 minutes. Tweaking the R script and renaming the images through R will take ~30 minutes the first time, but will take less time (5 - 10 minutes) once you are familiar with the script and how to use R.

Orbit training

Training Orbit takes ~30 minutes the first time you are using the software. This will decrease with program familiarity. The time spent on batch analysis by the program will vary depending on the number of images and the computer. Note that Orbit recommends having a 32 GB RAM (and 64 GB if possible) computer. However, a 5-year-old 8 GB RAM PC was capable of running the analysis and took ~ 3 h to analyze 2304 images. Make sure your computer is plugged in.

R parametrization and visualization

The time spent on this step will depend on your familiarity with R. It is recommended that you read the supporting documents BP5-OrbitParameterization.pdf and BP6-LogFitParamsVis.pdf for a description of what the different code chunks do and to see the expected output. If this is your first-time using R, it could take several hours to understand the functions and steps taken in Basic Protocol 5 and Basic Protocol 6. Once you are familiar with R and have adapted the script (if necessary) to the specifics of your experiment, it should take ~15-20 minutes the next time you do a similar analysis.

2.10 Acknowledgments

We thank Kamaldeep Chhoker for the Evos FL Auto 2 training. This work was supported by a Discovery Grant to A.C.G. from the Natural Sciences and Engineering Research Council of Canada (NSERC). O.E.S was supported by a University of Manitoba Graduate Fellowship (UMGF).

2.11 Author Contributions

Ola Salama: conceptualization, data curation, formal analysis, funding acquisition, investigation, methodology, project administration, software, validation, visualization, writing-original draft, writing-review and editing; Aleeza Gerstein: conceptualization, formal analysis, funding acquisition, methodology, project administration, resources, software, supervision, writing review and editing.

2.12 Conflict of Interest

The authors declare no conflict of interest. Data Availability Statement The data that support the findings of this study are available from the corresponding author upon reasonable request. The scripts and example image files for practice are located in a github repository, accessible at https:// github.com/ acgerstein/ biofilm-formation.

Chapter 3 Differential response of *Candida* species morphologies and isolates to fluconazole and boric acid

3.1 Abstract

Candida albicans is the most prevalent cause of vulvovaginal candidiasis ('yeast infection') and recurrent vulvovaginal candidiasis, though the incidence of non-albicans yeast species is increasing. The azole fluconazole is the primary antifungal drug used to treat R/VVC yet isolates from some species have intrinsic resistance to fluconazole, and recurrent infection can occur even with fluconazole-susceptible populations. The second-line broad-spectrum antimicrobial drug, boric acid, is an alternative treatment that has been found to successfully treat complicated VVC infections. Far less is known about how boric acid inhibits growth of yeast isolates in different morphologies compared to fluconazole. We found significant differences in drug resistance and drug tolerance (the ability of a subpopulation to grow slowly in high levels of drug) between *C. albicans*, *C. glabrata*, and *C. parapsilosis* isolates, with the specific relationships dependent on both drug and phenotype. Population-level variation for both susceptibility and tolerance was broader for fluconazole than boric acid in all species. Unlike fluconazole, which neither prevented hyphal formation nor disrupted mature biofilms, boric acid inhibited *C. albicans* hyphal formation and reduced mature biofilm biomass and metabolic activity in all isolates in a dose-dependent manner. Variation in planktonic response did not generally predict biofilm phenotypes. Overall, our findings illustrate that boric acid is broadly effective at inhibiting growth across many isolates and morphologies, which could explain why it is an effective treatment for R/VVC.

3.2 Introduction

Vulvovaginal candidiasis (VVC), a pathological condition of the lower female reproductive tract, affects ~75% of females at least once in their life (Sobel et al., 1998; Sobel, 2007). Although patients usually respond well to the first-line treatment (typically fluconazole) (van Schalkwyk et al., 2015; Pappas et al., 2016), ~8% of females globally will experience recurrent VVC, which can have a significant negative impact on quality of life (Pappas et al., 2016; Denning et al., 2018). *Candida albicans* has been the primary cause (75-90%) of VVC, yet the frequency of other species, particularly *C. glabrata* followed by *C. parapsilosis*, is increasing (Linhares et al., 2001; Cetin et al., 2007; Okungbowa et al., 2003). In light of the transition to rename *C. glabrata* as *Nakaseomyces glabrata* ,(Kidd et al., 2021), we use the acronym NAC to refer to "non-albicans clinical" species, rather than "non-albicans *Candida*" species as has been done historically.

Boric acid (BA) intravaginal suppositories are recommended and have found success as a second-line treatment for NAC infections and when recurrence occurs on first-line treatment, typically fluconazole (FLC) (Pappas et al., 2016; van Schalkwyk et al., 2015; Sobel et al., 2003; Iavazzo et al., 2011). Despite this success, BA remains a second-line treatment because its exact mechanism of action is unknown and much less work has evaluated its broad efficacy and possible long-term effects (Prutting and Cerveny, 1998; De Seta et al., 2009). The minimum inhibitory concentration of BA was previously measured in a relatively small number of *C. albicans*, *C. glabrata*, and *C. parapsilosis* isolates (De Seta et al., 2009; Otero et al., 2002), yet unlike FLC (and many other antifungal drugs), there are no standard clinical methods for drug resistance testing, nor have breakpoints been established for BA planktonic resistance. Furthermore, variation among isolates in fungal drug tolerance, the ability of a subpopulation of drug-susceptible isolates to grow slowly at inhibitory drug concentrations (Gerstein et al., 2016; Rosenberg et al., 2018; Berman and Krysan, 2020; Levinson et al., 2021), has largely been ignored, yet recent studies are beginning to implicate tolerance as a factor in predicting drug efficacy (Rosenberg et al., 2018; Levinson et al., 2021; Berman and Krysan, 2020).

Morphological plasticity is an important virulence trait in many contexts for *Candida* species (Noble et al., 2017). The yeast to hyphal transition is critical for biofilm stability, penetration of host epithelial cells, and escape from host phagocytes (Gulati and Nobile, 2016; Wilson et al., 2016). Hyphal formation is also important for biofilm formation in *C. albicans* (*C.*

glabrata do not form hyphae and *C. parapsilosis* forms pseudohyphae) (Cavalheiro and Teixeira, 2018). The involvement of biofilms in RVVC is still being debated (Harriott et al., 2010; Wu et al., 2020). However, hyphal forms were recently detected in vaginal lavage fluid from an RVVC patient (McKloud et al., 2021). I*n vivo* mice models showed that *C. albicans* can form biofilms on the vaginal mucosa (Harriott et al., 2010; Wu et al., 2020) and genes involved in hyphal morphogenesis biofilm formation were detected in vaginal lavage (McKloud et al., 2021). FLC was shown previously not to inhibit hyphal formation (Ha and White, 1999). However, low BA concentrations (0.02 mg/mL) can disrupt the cytoskeleton of hyphae by changing the actin distribution from the apical to the isotropic pattern (Pointer et al., 2015), and higher BA concentrations (10 mg/mL or 50 mg/mL) were shown to inhibit hyphal formation in two *C. albicans* isolates (De Seta et al., 2009). BA has also been found to reduce the biomass of mature biofilms relative to biofilms growing without drug (De Seta et al., 2009); it was unclear, however, whether this reflected the drug simply stopping further growth, or whether boric acid acted to reduce the biofilm below pre-drug treatment levels.

To quantify the diversity of BA phenotypic responses among different species, we compared FLC and BA planktonic susceptibility and tolerance among 235 clinical isolates of *C. albicans*, *C. glabrata* and *C. parapsilosis*. We also quantify the impact of FLC and BA on *C. albicans* yeast to hyphal transition (leading to biofilm formation), and on *C. albicans* mature biofilms. We found significant differences among species for drug resistance and tolerance, and a consistent increase in the variance among isolates for both drug response phenotypes in FLC compared to BA. We also found that unlike FLC, BA is effective at inhibiting the yeast-to-hyphal transition and thus biofilm formation, and can effectively break apart mature biofilms. Combined, this demonstrates multiple pathways where BA is more effective at inhibiting *Candida* species growth compared to fluconazole.

3.3 Results

3.3.1 Variation in Drug Susceptibility and Tolerance

Fluconazole (FLC) and boric acid (BA) drug susceptibility and tolerance were measured for 235 *Candida* isolates (165 *C. albicans*, 50 *C. glabrata*, 20 *C. parapsilosis*) using *diskImageR*, a computational analysis tool that quantifies drug response from imagers of disk diffusion assays (Gerstein et al., 2016). Susceptibility was measured as RAD_{20} (the radius where 20% of growth reduction occurs), while tolerance was measured as FoG_{20} (the fraction of the population that is able to grow above RAD_{20} after 48 h). *C. albicans* isolates on average had higher susceptibility than *C. glabrata* but lower susceptibility than *C. parapsilosis*, and higher tolerance than either in FLC (Figure 3.1, left panels; Kruskal-Wallis rank-sum test; susceptibility: $\chi^2 = 63.43$ df = 2, $P < 0.0001$, species differences determined by post-hoc pairwise Wilcoxon tests with the (Benjamini and Hochberg, 1995) *P* adjustment; tolerance: $\chi^2 = 82.04$, df = 2, $P < 0.0001$). In BA, *C. albicans* isolates had higher susceptibility than both NAC species, and lower tolerance than *C. glabrata* (susceptibility: $\chi^2 = 39.8$, df = 2, $P < 0.0001$; tolerance: $\chi^2 = 97.9$, df = 2, $P < 0.0001$). The magnitude of isolate variation in BA was significantly less than in FLC for both *C. albicans* and *C. glabrata*, the two species with a sufficiently large sample size (Fligner-Killeen test of homogeneity; susceptibility: *C. albicans*, $\chi^2 = 23.4$, df = 1, $P < 0.0001$; *C. glabrata*, $\chi^2 = 7.8$, df = 1, $P = 0.005$; tolerance: *C. albicans*, $\chi^2 = 116.59$, df = 1, $P < 0.0001$; *C. glabrata*, $\chi^2 = 4.94$, df = 1, $P = 0.03$).

There was a significant positive correlation for FLC susceptibility and tolerance within isolates of the same species: isolates that had lower susceptibility (i.e., higher resistance levels) also tended to have higher tolerance (Figure 3.2A, Spearman's rank correlation, for *C. albicans:* rho = -0.197, S = 571000, $P = 0.02$ *C. glabrata*: rho = -0.49 , S = 29249, $P < 0.0001$, *C. parapsilosis*: rho = -0.73, S = 2295, $P < 0.0001$). In BA, the correlation was significant for *C. glabrata* and *C. parapsilosis* (Figure 3.2B, *C. glabrata*, rho = -0.42, S = 27802, $P = 0.003$; *C. parapsilosis*, rho = -0.63, S = 2173, $P = 0.003$) but not *C. albicans* (rho = 0.07, S = 444639 $P = 0.420$). There was no correlation in susceptibility and tolerance between drugs, indicating that the mode of action for BA differs from that of FLC, as the isolates that are less susceptible or more tolerant in one drug do not tend to have improved growth in the other (Figure 3.2C&D, Spearman's rank correlation, susceptibility, *C. albicans*: S = 500605, $P = 0.56$; *C. glabrata*: S = 19549, $P =$

0.99; *C. parapsilosis:* S = 975, *P* = 0.26; tolerance , *C. albicans:* S = 490557, *P* = 0.74; *C. glabrata*: S = 15401, *P* = 0.14; *C. parapsilosis:* S = 1332, *P* = 0.995).

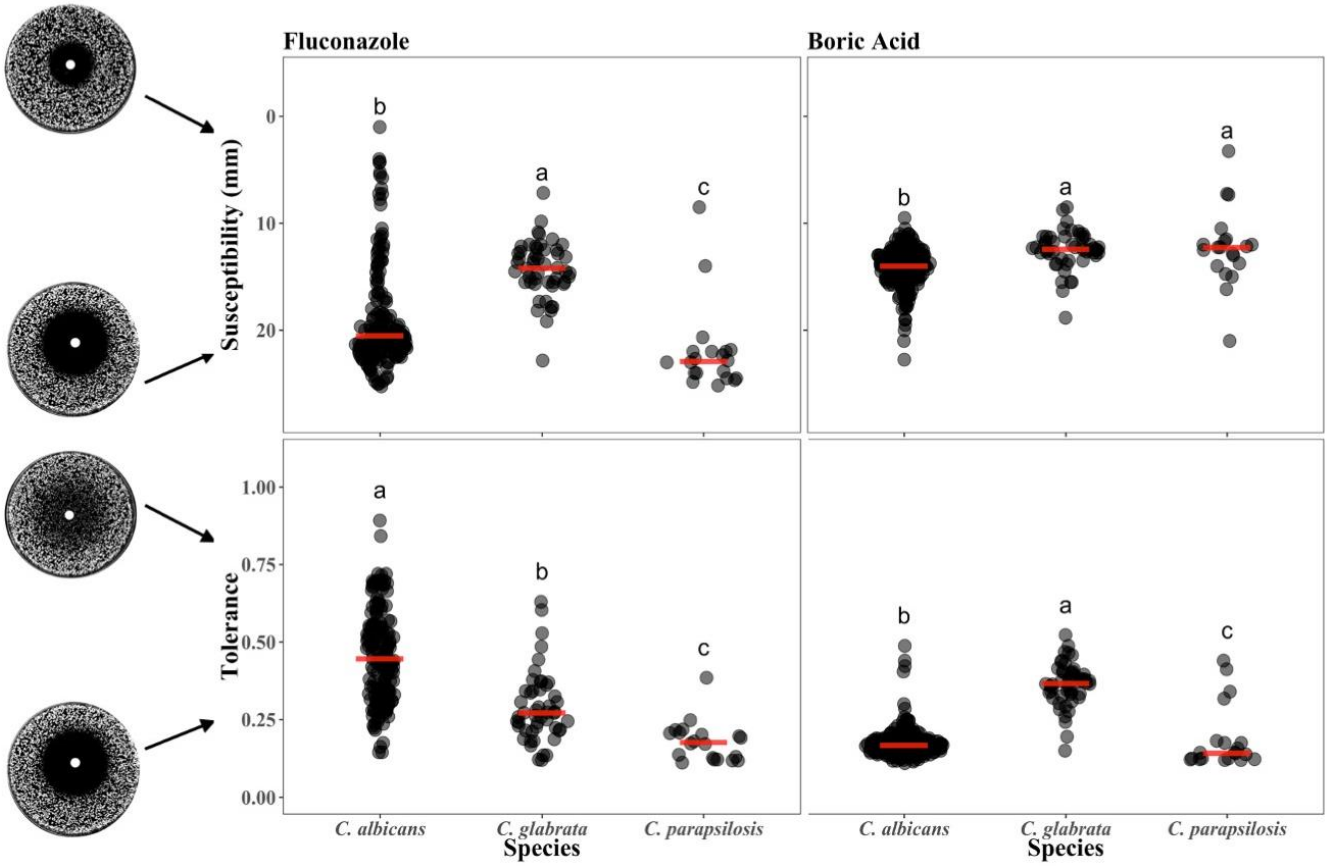


Figure 3.1 Susceptibility and tolerance for FLC and BA was quantified for 165 *C. albicans*, 50 *C. glabrata*, and 20 *C. parapsilosis* isolates. Note that susceptibility is measured as RAD_{20} and the y-axis is reversed so that the less susceptible (more resistant) isolates are towards the top. Tolerance is measured as FoG_{20}. Letters indicate the statistical differences among-species in each panel from a post-hoc pairwise Wilcox test with the Benjamini and Hochberg (1995) p-value adjustment; when species do not share a letter, they are significantly different from each other ($P < 0.05$).

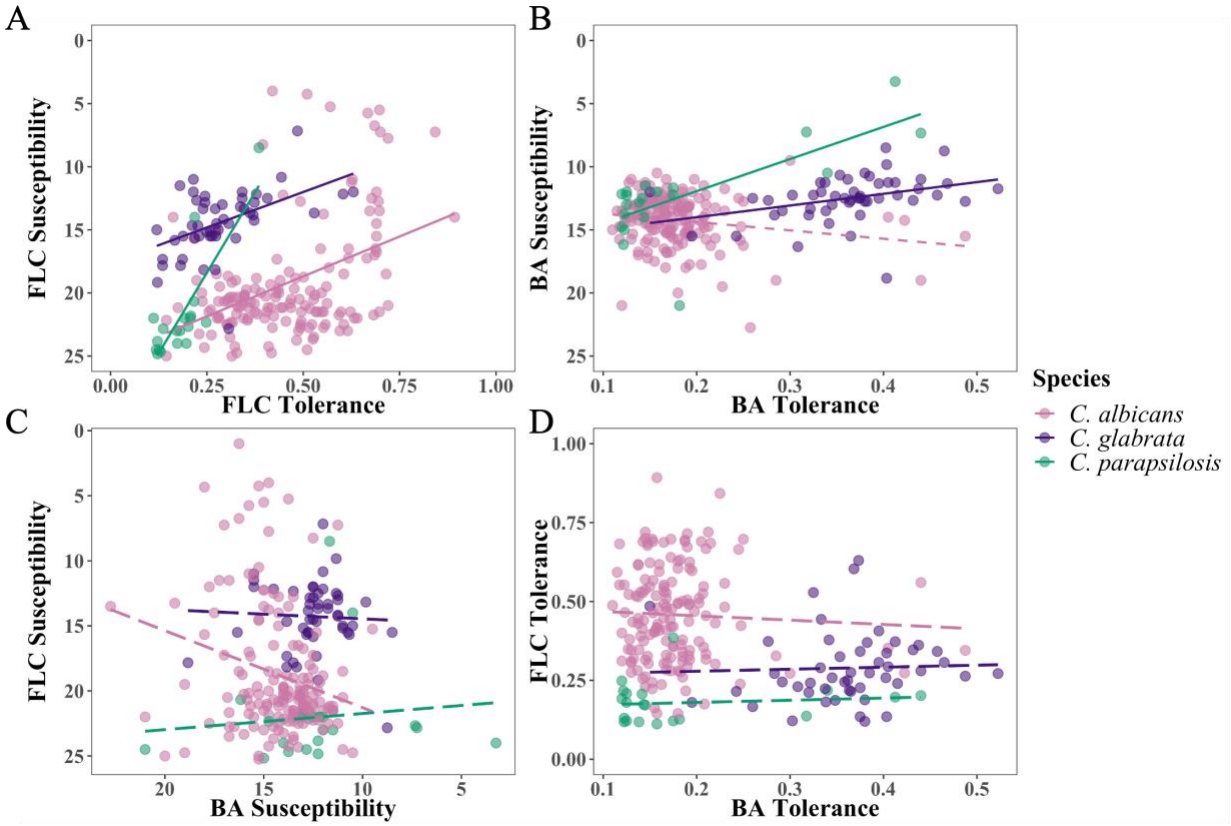


Figure 3.2 Association within and between drug response parameter and drugs. (A) susceptibility and tolerance in FLC, (B) susceptibility and tolerance in BA, (C) susceptibility in FLC and BA, (D) tolerance in FLC and BA. Solid lines indicate a significant correlation ($P < 0.05$) from a Spearman's rank correlation test.

3.3.2 BA Inhibits *C. albicans* Hyphal Formation

We used time-lapse microscopy to examine the ability of eight phylogenetically diverse *C. albicans* isolates to form hyphae and begin biofilm formation in the presence of drug (Figure 3.3). Visual inspection of images indicated it took only 1-2 hours for all isolates to form hyphae regardless of the FLC concentration (Figure 3.3B). By contrast, BA affected hyphal formation in a highly dose-dependent manner. In low levels of BA (0.4 and 0.8 mg/mL), there was very little variation in the time to first hyphal formation among isolates. As the level of BA increased, the time to hyphal formation as well as the variation among isolates increased. No hyphae were observed by 24 h at the highest level of BA.

To further quantify biofilm formation from the time-lapse images, we used a computational pipeline that we recently developed that uses machine learning in the Orbit Image Analysis program (Stritt et al., 2020) and custom R scripts. The pipeline computationally quantifies the percent area covered by cells in each image, and uses this to calculate the biofilm growth rate, the time to reach the growth asymptote (i.e., growth plateau), and percent area covered at the asymptote. At the highest FLC concentration, populations retained 50-100 % of percent area covered by cells at the asymptote relative to no drug (Figure 3.4A) and had a reduced but still relatively high growth rate (Figure 3.4B). There was not a clear trend among isolates in the time required to reach the asymptote (Figure 3.4C). Consistent with the identified variation by eye in the time to hyphal formation, BA reduced the percent area covered by cells at the growth asymptote, decreased the growth rate and increased the time to reach the growth asymptote in a dose-dependent manner (Figure 3.4A-C). Interestingly, there was more variation in percent area at the growth asymptote, growth rate, and time to reach the growth asymptote among isolates in FLC compared to BA. There was no correlation between FLC drug responses and BA drug responses (Spearman's rank correlation, percent area covered by cells: S = 1399899, $P = 0.48$; time to reach the growth asymptote S = 1346887, $P = 0.89$; growth rate: S = 1275866, $P = 0.5447$). Overall, unlike FLC, BA effectively inhibits hyphal formation and biofilm formation in a dose-dependent manner.

.

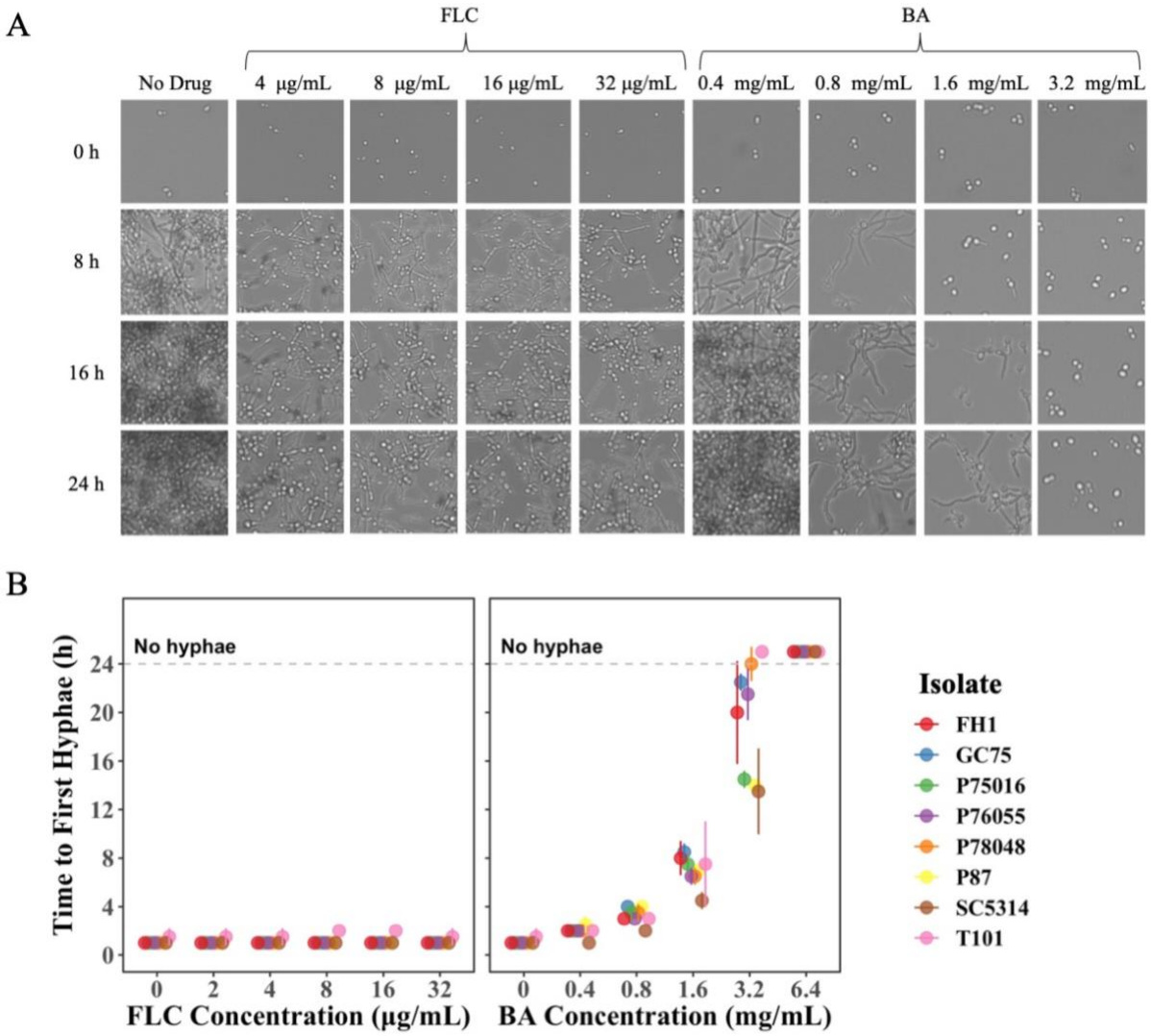


Figure 3.3 Biofilm formation drug responses of eight *C. albicans* isolates. Fungal cells were initially cultured in liquid YPD at 30 °C, washed and standardized to OD_{600} of 0.01 in RPMI. Cells were inoculated into various concentrations of FLC or BA. The plate was incubated at 37 °C and (A) manually taken out every 1 h for 24 h for scan using Evos FL Auto 2 inverted microscopy. (B) Time to the first hyphal formation was measured by manually going through the images and identifying the hour where the first hypha was observed. Values presented for each isolate are the mean of two biological replicates ± SD.

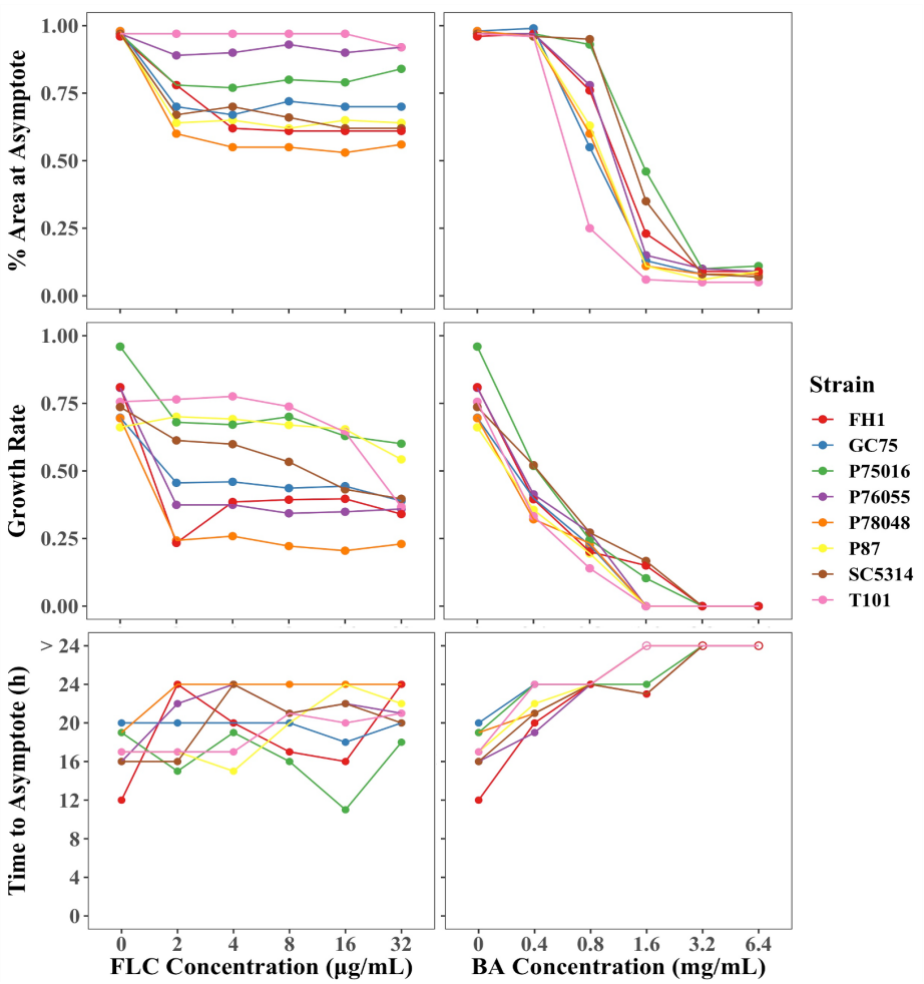


Figure 3.4 Quantitative image analysis of time lapse images of eight *C. albicans* isolates. Orbit Image Analysis was used to calculate the % area covered by cells for all the images and custom R scripts was used to calculate % area at the asymptote, growth rate and time to reach the asymptote. BA affected biofilm formation in a dose dependent manner; (A) it reduced % area at the asymptote, (B) decreased the growth rate, and (C) increased time to reach the asymptote unlike FLC. Values presented are the mean of two biological replicates.

3.3.3 BA Eradicates *C. albicans* Mature Biofilms

The ability of drugs to break apart mature *C. albicans* biofilms formed in absence of drug was evaluated by quantifying both biomass and activity. As previously shown by others (Melo et al., 2011; Sherry et al., 2017; Wu et al., 2020), mature biofilms were largely impervious to FLC; post-drug biomass was higher than the measured pre-drug biomass for all levels of FLC (Figure 3.5; linear mixed-effect model implemented in the lmer R package (Kuznetsova et al., 2017), with change in biomass as the response variable, level of the drug as the predictor and isolate as a random effect, p-value obtained through the analysis of variance test with Satterthwaite's method for degrees of freedom; $F_{1,342} = 2.98$, $P = 0.09$). There was a negative association between FLC concentration and biofilm activity (linear mixed-effect model with change in activity as the response variable, level of the drug as the predictor, and isolate as a random effect, $F_{1,342} = 32.46$, $P < 0.0001$), driven by activity at the highest level of FLC (model with FLC 32 μg/mL removed from the dataset: $F_{1,285} = 0.0937$, $P = 0.76$).

Similar to biofilm formation, BA significantly affected biofilm biomass and activity in a dose-dependent manner (Figure 3.5; biomass, $F_{6,342} = 249.94$, $P < 0.0001$; activity, $F_{6,342} = 249.94$, $P < 0.0001$). Interestingly, the biomass of 48% of isolates and the activity of 57% of isolates increased at 0.4 mg/mL BA relative to no drug, suggesting that BA can stimulate growth at a low concentration. The biofilm biomass at high BA concentrations relative to a biofilm grown without drug was reduced for all isolates. The activity of the remaining biofilm at the highest BA levels for some isolates increased above that of the preceding lower drug level, likely because BA degraded the biofilm matrix allowing XTT to better penetrate the cells.

Planktonic drug responses were partially predictive of biofilm responses, albeit in an inconsistent manner. Isolates with higher planktonic growth tended to have a higher biofilm activity but not higher biomass, while lower susceptibility (higher resistance) did not predict either biofilm biomass or activity (Supplementary Material for Chapter 3 Figure 3.1-3.4; linear mixed-effect model with the FLC planktonic response as the predictor variables and isolate as a random effect; change in biomass as the response variable: susceptibility, $F_{1,57} = 1.59$, $P = 0.21$, tolerance, $F_{1,54} = 1.28$, $P = 0.26$; change in activity as the response variable, susceptibility, $F_{1,57} = 2.51$, $P = 0.12$, tolerance, $F_{1,54} = 5.76$, $P = 0.02$). By contrast, reduced BA planktonic susceptibility was associated with higher biofilm activity but not biomass, while tolerance was associated with neither (susceptibility, change in biomass, $F_{1,57} = 1.04$, $P = 0.31$, change in activity, $F_{1,57} = 5.55$,

P = 0.02; tolerance, change in biomass, $F_{1, 57}$ = 0.0004, P = 0.98; change in activity, $F_{1, 57}$ = 0.07, P =0.79). Hence, isolate differences in planktonic drug responses are likely not a good predictor for how a specific isolate will respond to drug when in a biofilm.

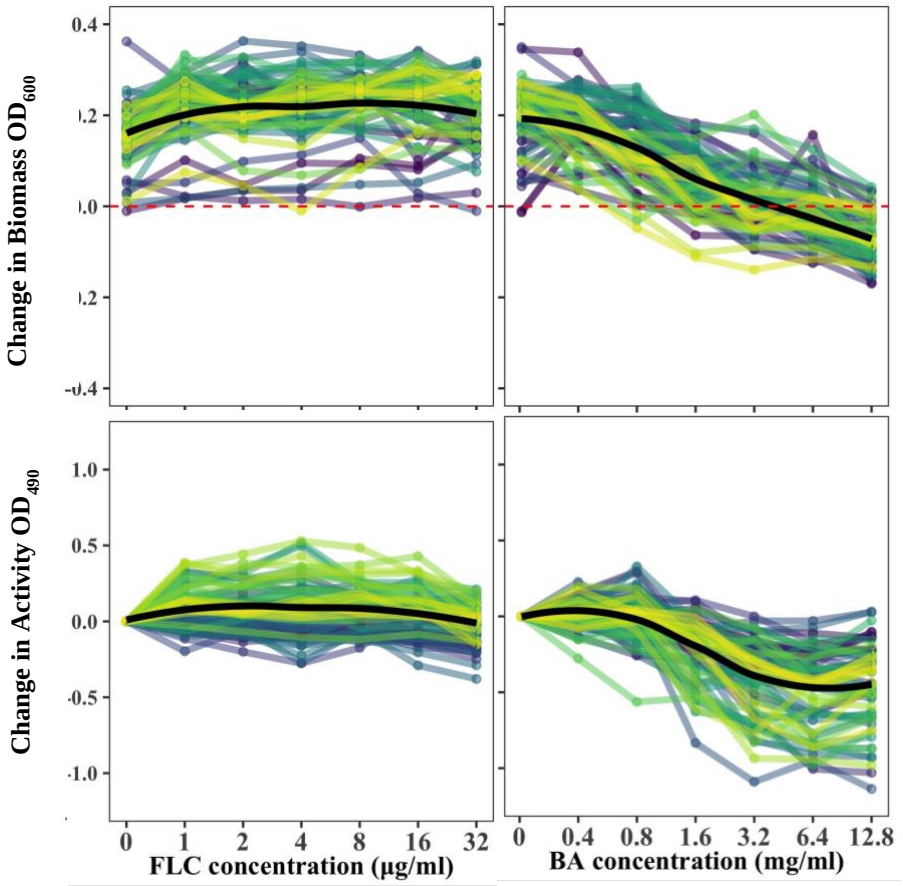


Figure 3.5 Biofilms drug responses of 63 *C. albicans* isolates. In all panels, the black line indicates the mean across all isolates at each concentration. The line colors are arbitrary and used to visualize different isolates. Biofilms were insensitive to FLC regardless of the FLC concentration. BA eradicated mature biofilms in a dose-dependent manner and reduced activity. Values presented are the means of three biological replicates.

3.4 Discussion

We screened isolates of *Candida* species to enhance our understanding of how diverse isolates in multiple morphologies respond to boric acid (BA), an effective drug for treating complicated vulvovaginal candidiasis (VVC). We directly compared responses against fluconazole (FLC), the first-line treatment. Consistent with previous work, compared to *C. albicans*, we found that *C. glabrata* on average had lower susceptibility to both FLC (Bhattacharjee, 2016; Hashemi et al., 2019) and BA (De Seta et al., 2009; Otero et al., 2002) Our work is also in agreement with previous work that found no correlation between FLC and BA susceptibility in 76 *C. albican* isolates (Pointer et al., 2015), implying that the mode of action of FLC is different from that of BA. In both *C. albicans* and *C. glabrata*, we found that the distribution of susceptibility values was broader in FLC than BA. Rosenberg *et al.* (2018) measured susceptibility in 19 *C. albicans* isolates in seven antifungal drugs and similarly found FLC had the broadest distribution (Rosenberg et al., 2018). Our work suggests BA resistant isolates may be rare as only one *C. parapsilosis* isolate out of 235 *C. albicans, C. glabrata* and *C. parapsilosis* isolates had considerably higher resistance than other isolates. Additional screening with a larger isolate collection is required to establish clinical breakpoints of BA resistance.

We also found significant variation among species and a wider breadth of responses in FLC compared to BA for drug tolerance. There is a growing acknowledgment that fungal drug tolerance may be associated with treatment failure and infection persistence. One study showed that *C. albicans* isolates from patients with persistent candidemia had a higher tolerance to FLC than isolates from patients with non-persistent candidemia (Rosenberg et al., 2018). Increased tolerance was also found to be a good predictor of FLC efficiency in patients with *C. albicans* bloodstream infections (Levinson et al., 2021).

Interestingly, using the CLSI disk diffusion assay protocol (Sheehan et al., 2004), we found that FLC drug susceptibility and tolerance were significantly correlated for all three species, while BA drug susceptibility and tolerance were significantly correlated for *C. glabrata* and *C. parapsilosis*. This result differs from a previous screen of 219 *C. albicans* isolates that found no correlation between FLC susceptibility and tolerance when isolates were grown up on YPD and tested on casitone plates at 30 ℃ (Rosenberg et al., 2018). Although the mechanisms of tolerance have not yet been well resolved, assay medium and temperature has previously been shown to significantly influence fungal drug susceptibility and can dramatically affect drug

tolerance (Gerstein et al., 2016). The drivers and clinical importance of tolerance is an area of active interest and research.

The involvement of morphological changes in symptomatic vulvovaginal candidiasis is also an area of current interest. The yeast to hyphal transitionis an important virulence trait in many infection contexts, and compounds that inhibit hyphal formation in *C. albicans* significantly reduce virulence in multiple contexts (Meng et al., 2019; Zhao et al., 2018; Wilson et al., 2016). Our results show that *C. albicans* forms hyphae in the first 2 h regardless of FLC concentration, in alignment with previous research (Ha and White, 1999). Through the new quantitative platform we developed, we similarly found that percent area covered at the asymptote, biofilm growth rate, and time to reach the growth asymptote are also not correlated with FLC concentration, though we did uncover significant variation among isolates for these phenotypes. BA is clearly superior to FLC at the inhibition of hyphal formation, with the speed of morphological transition and subsequent biofilm formation influenced by BA in a dose-dependent manner. Hyphal formation was previously reported before to be responsible for vaginal inflammation (Moyes et al., 2011; Peters et al., 2014), and hyphae contribute to the invasive growth of *C. albicans* (Gulati and Nobile, 2016), suggesting that inhibiting the yeast to hyphal transition could help explain why BA is an effective treatment against complicated VVC.

If a biofilm has formed in the absence of a drug (e.g., prior to a symptomatic infection), penetration of drugs through the extracellular matrix is critical for eradication (Rodríguez-Cerdeira et al., 2019). We found that *C. albicans* biofilms are insensitive to FLC, consistent with past work (Sherry et al., 2017; Melo et al., 2011). Conversely, we found that BA can reduce biomass and activity of mature biofilms in a dose-dependent manner, and therefore is likely capable of penetration. Approximately 40% of the extracellular matrix of *C. albicans* is composed of polysaccharides and the major carbohydrates present is glucose (~40%) (Al-Fattani and Douglas, 2006; Cavalheiro and Teixeira, 2018). Saccharides (especially glucose) have a strong affinity for borate (Peters, 2014), thus we think that BA likely penetrates the extracellular matrix of the biofilm by breaking the matrix apart. Compared to planktonic cells, *C. albicans* cells in a biofilm have a significantly higher β-1,3 glucan content in their cell wall, which has been implicated in FLC impermeability (Nett et al., 2007). We observed an increase in activity at high BA concentrations even though the biomass was decreasing. We think that this increase in activity is artificial and due to how the XTT activity assay works. Mitochondrial succinoxidase, cytochrome P450 systems,

and flavoprotein oxidases convert XTT to a colored formazan (Altman, 1976). If high concentrations of BA degrade the extracellular matrix, then more XTT will get inside the cells, which is read out as increase in activity. Our future work will thus directly investigate the ability of BA to penetrate the cell wall of different *Candida* morphologies.

3.5 Conclusion

Our work provides baseline data for multiple ways boric acid is an effective drug against diverse isolates of *Candida* species. We find that planktonic susceptibility and tolerance are more similar among isolates in boric acid than fluconazole. Boric acid is also effective at slowing or stopping the yeast-to-hyphal transition and biofilm growth in *C. albicans*, as well as able to penetrate and degrade mature biofilms. Planktonic responses in fluconazole and boric acid were not correlated, and nor did planktonic and biofilm phenotypes. Combined, this work advances our understanding of multiple biological fronts about why boric acid may be an effective treatment against vulvovaginal candidiasis.

3.6 Material and Methods

3.6.1 Isolates

235 Candida isolates were used in this study. 155 of these isolates were clinically isolated (85 *C. albicans*, 50 *C. glabrata*, and 20 *C. parapsilosis*) and provided by the Health Sciences Centre (HSC) in Winnipeg, Canada. 80 additional *C. albicans* isolates from our lab freezer inventory were also examined.

3.6.2 Disk Diffusion Assay

To screen for drug susceptibility and tolerance, the CLSI document M44 guidelines for antifungal disk diffusion susceptibility testing were followed with slight modifications (Sheehan et al., 2004). Briefly, isolates were streaked from frozen glycerol stocks into Sabouraud Dextrose Agar (SDA) and incubated for 48 h at 37 °C. Colonies were resuspended in 200 µL of PBS and were standardized to an optical density (OD_{600}) of 0.01 in 1 mL PBS. 100 µL of the standardized cells were spread in duplicates onto 15 mL Muller Hinton (MH) plates using sterile beads. 5 mg BA disks were prepared by transferring 10 µL of preheated 500 mg/mL BA in Dimethyl sulfoxide (DMSO) stock to blank antimicrobial disks (6 mm, Fisher Scientific). Single disks containing either 5 mg BA or 25 µg FLC (6 mm, Fisher Scientific) were placed in the center of the MH plates. Plates were then incubated at 37 °C for 48 h, and individual photographs were taken of each plate every 24 h and 48 h. Images were edited using ImageJ (Schneider et al., 2012) according to recommendations specified in diskImageR vignette V2 146 (Gerstein, 2016). Disk diffusion analysis to measure drug susceptibility and drug tolerance was done using diskImageR package and the R script available at https://github.com/acgerstein/diskImageR/blob/master/inst/walkthrough.R (Gerstein et al., 2016). Susceptibility was measured from 48 h images as RAD_{20} (the radius where 20% growth of reduction occurs) while tolerance was measured as FoG_{20} (the fraction of growth above RAD_{20}).

3.6.3 Boric Acid levels

We picked the concentrations of BA based by measuring the minimum inhibitory concentration (MIC) for the isolates used in biofilm formation and eradication was determined using the CLSI M27-A2 guidelines with some modifications. Briefly, isolates used in biofilm

formation and biofilm eradication screening were streaked from frozen stocks on SDA plates and were incubated overnight at 37 °C. Colonies were suspended in PBS and were standardized to an OD_{600} of 0.01 in 1 mL of RPMI-1640. 100 μL of the standardized culture were transferred to a 96-well plate (Greiner Bio-One) containing two-fold dilutions of BA with the maximum concentration of 50 mg/mL (maximum solubility of BA in RPMI) in column 1, column 11 containing no drug and column 12 containing just RPMI-1640. MIC_{50} were determined by taking OD_{600} after 24h and 48h. The MIC_{50} of all isolates was either 0.39 or 0.78 mg/mL and the MIC was 1.56 mg/mL. We decided to pick two levels above and below the MIC and to round the concentrations to one decimal place (i.e., 0.4, 0.8, 1.6, 3.2 and 6.4 mg/mL).

3.6.4 Biofilm Formation Drug Response

The ability to form a biofilm in the presence of a drug of eight *C. albicans* isolates was measured as previously described in (Salama and Gerstein, 2021). Briefly, 100 μL of RPMI-1640 was added to all the wells of columns 1-9 and 12 of a flat-bottom 96-well microtiter plate (Greiner Bio-One). 200 μL of RPMI-1640 + 12.8 mg/mL BA was added to all wells of column 11 and 200 μL of RPMI-1640 + 64 μg/mL FLC was added to all wells of column 10. A 2 fold serial dilution for each drug was done so that odd-numbered columns (11-3) contain dilutions of BA, even-numbered columns (10-2) contain dilutions of FLC, and columns 1 and 12 contain no drug. *Candida albicans* isolates SC5314 (ATCC MYA-2876), FH1 (Marr et al., 1997), P87 (Wu et al., 2007), GC75 (Wu et al., 2007), P78048 (Wu et al., 2007), P75016 (Wu et al., 2007), P76055 (Wu et al., 2007) and T101 (Odds et al., 2007) isolates were grown overnight 30 °C in liquid YPD from frozen glycerol stocks. These isolates were picked because they span the phylogenetic diversity of *C. albicans*. Overnight cultures were washed with PBS and standardized to OD_{600} of 0.005 in 1.5 mL RPMI-1640. 100 μL of the standardized cultures were inoculated into the 96-well microtiter plate that contains our drugs. The plate was sealed with a clear seal (Thermo Scientific) and polystyrene microplate lid (Greiner Bio-One), and parafilm was used to seal the sides of the plate. The plate was incubated at 37 °C and images were taken manually every 1 h for 24 h using Evos FL Auto 2 inverted microscopy (Thermo Scientific).

3.6.5 Microscopic Image Analysis

Time to form hyphae was recorded manually by going through the images and taking note of the time of the first hypha that was observed. Important parameters (% area at the asymptote, growth rate, time to reach the asymptote) that correlate with biofilm formation ability were extracted using a high throughput automated method (Salama and Gerstein, 2021). Briefly, Orbit Image Analysis (Stritt et al., 2020) was trained on 14 images and a detection model with 99.3% correctly classified instances was created. This detection model was used to calculate the % area covered by cells for all of the images. Custom R scripts (Salama and Gerstein, 2021) were used to extract % area at the asymptote, growth rate, time to reach the asymptote from Orbit output.

3.6.6 Biofilm Eradication

Biofilms were prepared as described previously with slight modifications (Pierce et al., 2010). Briefly, overnight cultures of 68 different *C. albicans* isolates were prepared by inoculating 10 μL of frozen glycerol stocks in 500 μL YPD (Yeast Peptone Dextrose) liquid medium in a microplate shaker (about 200 rpm) at 30 °C overnight. Isolates were then standardized to OD_{600} of 0.01 in 1.5 mL RPMI-1640 broth and aliquots of 100 μL of the standardized culture were inoculated into flat-bottom 96-well microtiter plates (Fisher Scientific). The plates were then covered with a sealing membrane, sterilized lids, and the sides of the plates were sealed with parafilm. The plates were incubated statically at 37 °C for 24h. Mature biofilms were washed 3 times with phosphate buffer saline (PBS) to remove the non-adherent cells, and OD_{600} was taken to quantify the pre-drug biomass of the biofilms.

The examined drug concentrations ranged from 0.4 mg/mL to 12.8 mg/mL for BA and from 1 μg/mL to 32μg/mL for FLC. The biofilm antifungal susceptibility testing was done according to (Pierce et al., 2010) with slight modifications. Briefly, the mature biofilms were treated with either BA or FLC and incubated statically with the drug for 24 h at 37 °C. The drug-treated biofilms were washed 3 times with PBS, and OD_{600} was taken to quantify the post-drug biomass of the biofilms. The biomass of the biofilms was normalized by subtracting the biomass of the biofilms pre-drug exposure from the biomass of the biofilms at each concentration. The metabolic activity was determined using the calorimetric 2,3-Bis-(2-Methoxy-4-Nitro-5-Sulfophenyl)-2*H*-Tetrazolium-5-Carboxanilide (XTT) assay, which measures mitochondria

reduction of the tetrazolium salt reagent; briefly, mature biofilms were incubated with 100 uL of XTT for 2 h in 37 °C, and OD_{490} was taken to quantify the metabolic activity. Biofilm activity was normalized by subtracting the activity at no drug concentration from the activity at each drug concentration. We excluded 4 isolates from our analysis because they failed to form biofilms during the pre-drug exposure phase.

3.6.7 Statistical Analysis

Values for susceptibility and tolerance screening represent the average of three biological replicates with one or more technical replicates each. Values for hyphal and biofilm formation represent the average of two biological replicates with one technical replicate each. Values for biofilm eradication represent the average of three biological replicates with one technical replicate each. Error bars throughout represent standard error.

All statistical tests performed and graphs generated were done using R programming language (R Core Team, 2020). Since our data is not normally distributed, we used rank-based measures. When comparing susceptibility and tolerance among species for each drug, we used Kruska-Wallis rank-sum test and determined significance using post-hoc pairwise Wilcoxon tests with the (Benjamini and Hochberg, 1995) *P*. We looked at homogeneity of group variances using Flinger-Killeen test of homogeneity. We used Spearman's rank correlation when looking at the correlation between planktonic drug responses. We used linear mixed-effect models from lmerTest R package (Kuznetsova et al., 2017) to determine if planktonic drug responses would influence biofilm drug responses. In all cases, the specific statistical test is indicated inline. Significance was assigned for $P < 0.05$.

3.7 Acknowledgments

We thank Dr. Markus Stein (clinical microbiologist, Diagnostic Services of Manitoba) who provided us with HSC isolates. The research was funded by a start-up grant from the University of Manitoba to ACG, and a University of Manitoba fellowship to OES. We thank members of the Gerstein and Bakker Labs at The University of Manitoba for their thoughtful comments.

Chapter 4 Boric Acid Adaptation in *Candida albicans*

4.1 Abstract

Boric acid (BA), a broad-spectrum antimicrobial, has been used as a treatment for vulvovaginal candidiasis when patients relapse on the primary antifungal drug, fluconazole. *Candida albicans* is the most common cause of vulvovaginal candidiasis. Little is known about the propensity of *C. albicans* to develop BA resistance or tolerance (the ability of a subpopulation to grow slowly in high levels of drug). Here, we evolved 12 replicates from eight different *C. albicans* isolates to BA to examine whether resistance and/or tolerance to BA would evolve. After 22 transfers to increasing drug concentrations, we found that all replicates went extinct, but observed significant differences in extinction timing among isolate backgrounds. Surprisingly, evolved isolates became less resistant yet more tolerant to BA. This experiment suggests that the evolution of BA drug tolerance may be more evolvable than resistance in *C. albicans*.

4.2 Introduction

Vulvovaginal candidiasis (VVC) affects ~75% of females at least once in their life (Sobel, 2007). VVC patients usually respond well to the first-line azole drug treatment fluconazole. However, a small but significant number of females experience recurrent VVC (RVVC), which is defined as three or more episodes of VVC in one year (Pappas et al., 2016). *Candida albicans* is the most prevalent causative of VVC and RVVC; however, other species including *C. glabrata*, *C. parapsilosis* and *C. tropicalis* can also be involved (Zhang et al., 2014; Wang et al., 2016; Hedayati et al., 2015). Continuous exposure to antifungal drugs (such as to treat recurrent infection) can trigger genetic changes in susceptible populations that modulate the ability of the cells to withstand drug stress. Fungal drug response can be assessed by looking at fungal drug susceptibility, typically measured as the minimum inhibitory concentration after 24 h of growth. Recently fungal drug tolerance, which is defined as the ability of a subpopulation to overcome the drug stress and grow slowly at inhibitory drug concentrations after 48 h, has also been potentially implicated in clinical failure (Gerstein et al., 2016; Rosenberg et al., 2018; Berman and Krysan, 2020; Levinson et al., 2021).

Acquired resistance is considered rare in recurrent vaginal infections (Kelly et al., 1996; Sobel, 2016), however, studies have shown that fluconazole resistance in *C. albicans* can arise due to continuous exposure to fluconazole during fluconazole maintenance therapy for patients with

RVVC (Marchaim et al., 2012). Tolerance has been rarely measured as a response, yet may be common, particularly with long-term drug exposure. A recent *in vitro* study showed that changes in fluconazole tolerance were prevalent in *C. albicans* replicates that were grown continuously in fluconazole, and that changes in tolerance were acquired independent of changes in resistance (Gerstein and Berman, 2020).

Boric acid (BA) is a broad-spectrum antimicrobial that is used as an alternative treatment for RVVC when first-line treatment (typically fluconazole) fails (Pappas et al., 2016; van Schalkwyk et al., 2015). We previously found that BA planktonic susceptibility and tolerance are very similar among isolates and that BA resistance is quite rare (only one *C. parapsilosis* isolate out of 235 *C. albicans, C. glabrata* and *C. parapsilosis* isolates was resistant to BA) (Salama & Gerstein, in prep). A number of studies have previously used *in vitro* experimental evolution of *C. albicans* in fluconazole to elucidate some of the genetic mechanisms that confer fluconazole resistance (Todd et al., 2019). Here, we conducted the first study to determine whether continuous exposure to BA would give rise to BA resistant or tolerant isolates. We found that continuous BA exposure *in vitro* induces tolerance but not resistance in *C. albicans*, motivating future work to examine whether this also occurs in clinical settings.

4.3 Methods

4.3.1 Isolates

Candida albicans isolates SC5314 (ATCC MYA-2876), FH1 (Marr et al., 1997), P87 (Wu et al., 2007), GC75 (Wu et al., 2007), P78048 (Wu et al., 2007), P75016 (Wu et al., 2007), P76055 (Wu et al., 2007) and T101 (Odds et al., 2007) were selected to span the genetic diversity of *C. albicans* (Gerstein and Berman, 2020). Here, 'ancestral replicates' refers to replicates prior to BA exposure while 'evolved replicates' refers to replicates evolved in BA.

4.3.2 Pilot Boric Acid Evolution Experiment

C. albicans isolates were streaked from frozen glycerol stocks on Sabaroud Dextrose Agar (SDA) plates and incubated overnight at 37 °C. A scoop of culture was transferred to 200 μL phosphate saline buffer (PBS), standardized to OD_{600} 0.01. Twelve replicates were then initiated from each ancestral isolate by transferring 5 μL of standardized culture to the twelve wells in the first row of a 96-well plate containing 200 μL RPMI (each ancestral isolate in its own plate). Plates

were incubated overnight at 37 °C and then 5 µL of overnight culture was transferred to RPMI + 0.4 mg/mL BA. Plates were incubated without shaking at 37 °C. Plates were taken out every 24 h for an OD reading. When OD_{600} reached 0.3 (indicating significant growth above the background), 100 µL of BA exposed culture was transferred to fresh RPMI + 0.4 mg/mL BA. When the culture again reached OD_{600} 0.3, 100 µL was transferred into fresh medium. The culture was always transferred twice in medium with the same drug concentration followed by a transfer into medium containing double the previous amount. Wells that did not show growth after seven days were considered extinct. Drug-exposed cultures were frozen down every second transfer, i.e., prior to increasing the drug concentration. 53% of the replicates were lost by the fifth transfer (t05) which contained 1.6 mg/mL BA, and all of them were lost by the seventh transfer, which contained 3.12 mg/mL BA.

4.3.3 Modified Boric Acid Evolution Experiment

After the initial experimental run, the experimental evolution protocol was modified; only results from the modified experiment are presented. Culture (95 out of 96 replicates) that was frozen after two transfers in 0.8 mg/mL BA (i.e., t4) were grown overnight at 37 °C in RPMI + 0.8 mg/mL BA (Supplementary Material for Chapter 4 Figure 4.1-4.4). The increment increase of BA concentration was adjusted in the modified protocol to increase more linearly in an attempt to reduce the extinction rate and proceeded from 0.8 mg/mL to: 1.0 mg/mL, 1.25 mg/mL, 1.5 mg/mL, 1.75 mg/mL, 2 mg/mL, 3 mg/mL, and 4 mg/mL. No replicate survived in 4 mg/mL BA. Once a concentration of 1.5 mg/mL was reached, the number of transfers was changed from two transfers per drug concentration to five transfers. After the last transfer in 1.5 mg/mL, we transferred the culture to plates that had 1.75 mg/mL and plates that had 2 mg/mL BA. For isolates that were able to grow at 2 mg/mL within seven days (P87, P78048 and P75016), we skipped the transfers in 1.75 mg/mL BA and moved forward with the 2 mg/mL plate. Cells were frozen down at the last transfer of each drug concentration and replicates from the highest concentration frozen down were used for susceptibility and tolerance screening (Table 4.1). One of the frozen down replicates (out of two) of evolved P87 went extinct.

Table 4.1 List of replicates used in the susceptibility and tolerance screening. Replicates from the terminal BA concentration for each isolate were used.

Isolate Name	Replicates	Transfer	BA Concentration
P75016	R3, R4, R5, R6, R7, R8, R10	t20	3
P78048	R6, R7, R8, R9	t20	3
GC75	R2, R3, R4, R8, R10	t18	2
P87	R8	t15	2
T101	R5, R6, R7, R9, R10	t14	1.75
FH1	R1, R2, R3, R4	t14	1.75
SC5314	R2, R7	t14	1.75
P76055	R5	t14	1.75

4.3.4 Susceptibility and Tolerance

Ancestral and evolved isolates kept at -80 °C were streaked on Sabaroud Dextrose Agar plates and incubated at 37 °C for 48 hours. Two to three colonies were transferred to 200 µL phosphate saline buffer PBS and OD_{600} was taken. The isolates were then standardized in 1 mL of PBS to OD_{600} of 0.01. 100 µL of the standardized culture were spread on 15 mL Muller Hinton plates. Disks containing 5 mg BA were prepared by transferring 10 µL of 500 mg/mL BA in dimethyl sulfoxide (DMSO) stock to blank antimicrobial disks (6 mm, Fisher Scientific), which were placed in the middle of the plate. The plates were incubated at 37 °C for 48 h and images were taken after 48 h. Images were cropped, inverted and edited using ImageJ (Schneider et al., 2012) according to recommendations in Gerstein et al. (2016). The R package *diskImageR* (Gerstein et al., 2016) was then used to quantify susceptibility, measured as the radius of inhibition (RAD_{20}) at which 20% reduction of growth occurs, and tolerance, measured as the fraction of growth (FoG_{20}) within RAD_{20}.

4.4 Results and Discussion

The terminal drug concentration reached by isolates, and in turn the extinction rate, was influenced by isolate background and the rate that the BA concentration was increased. All replicates from all isolates were extinct by the seventh transfer into 3.12 mg/mL BA when the concentration was doubled every second transfers. In the modified protocol, where the number of transfers at each drug level was increased and incremental increase in drug concentration was decreased. 9.5% of replicates survived in 3 mg/mL (Supplementary Material for Chapter 4 Figure 4.1-4.4). We hypothesize that increasing the number of transfers provided enough time for the populations to adapt to the increasing levels of drug stress by accumulating mutations. Additional work is required to determine the genetic basis of adaptation, though previous work in fluconazole has implicated chromosomal aneuploidy in a number of cases in *C. albicans* (Selmecki et al., 2009, 2010, 2006, 2008; Gerstein and Berman, 2020). Fluconazole also induces chromosomal aneuploidy in *C. albicans* (Harrison et al., 2014). Future work is required to determine whether aneuploidy also plays a role in adaptation to BA and whether BA induces ploidy changes in *C. albicans*.

During the first three transfers of the modified evolution experiment, all of the isolates retained the ability to grow in the presence of BA (Figure 4.1). After the third transfer (into 1.25 mg/mL BA), the isolates fell into two groups: group A, which contained five isolates (PGC75, P76055, T101, SC5314 and FH1) that lost replicates quickly, and group B, which contained isolates (P87, P78048 and P75016) that were better at surviving increasing BA stress (Table 4.2). It took an average of two to three days for the replicates to grow and be transferred (see Supporting Material for Chapter 4 Figures 4.1-4.4 for all isolate trajectories).

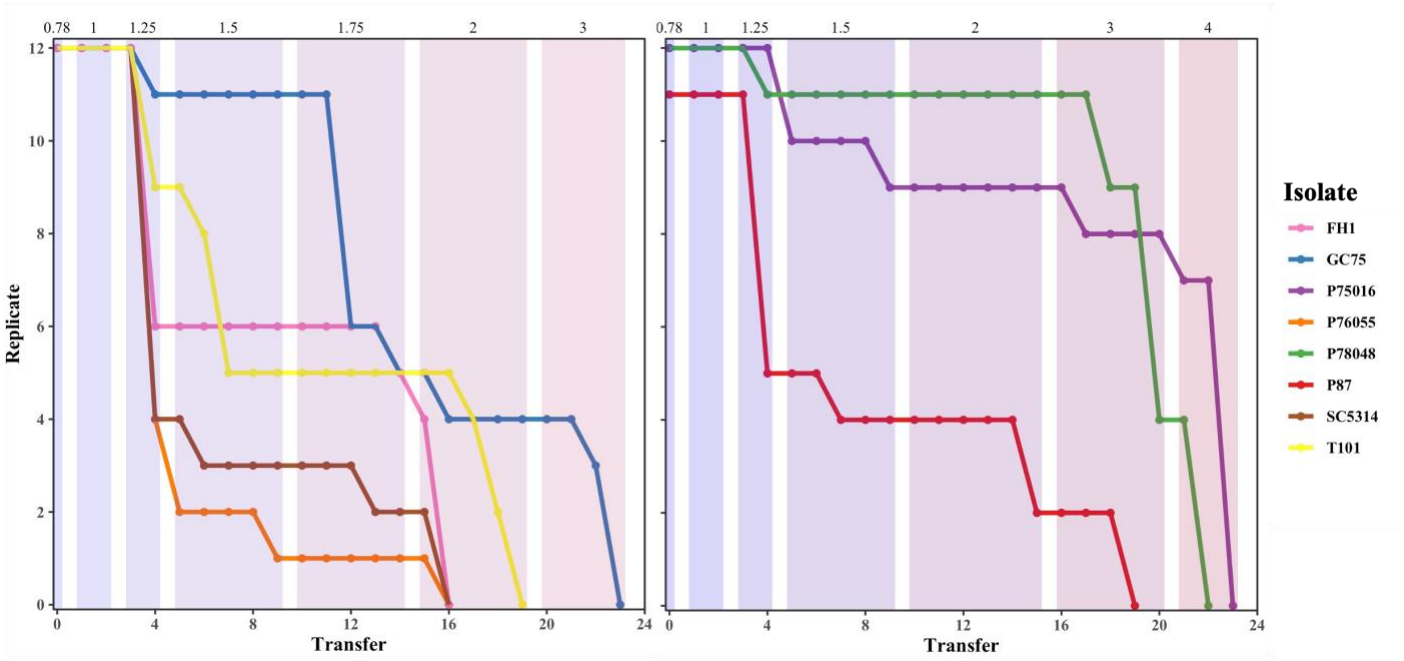


Figure 4.1 BA evolution experiment. Eight *C. albicans* isolates grown from frozen on SDA at 37 °C were transferred through various concentrations of BA in RPMI-1640 media. Numbers at the top represent the BA concentration. After 1.25 mg/mL BA, the number of transfers in each drug concentration increased from two to five. Replicates were frozen down at the last transfer of each concentration.

Table 4.2 Isolates used in BA evolution experiment.

Isolate Name	Clade	MIC50	RAD20	FoG20	Reference
P75016	4	0.8	13	0.18	Wu et al., 2007
P78048	1	0.8	15	0.17	Wu et al., 2007
GC75	4	0.8	15	0.15	Wu et al., 2007
P87	4	0.8	15	0.18	Wu et al., 2007
T101	3	0.4	19	0.13	Odds et al., 2007
FH1	3	0.8	17.5	0.16	Marr et al., 1997
SC5314	1	0.8	13	0.24	Fonzi and Irwin, 1993
P76055	2	0.8	17	0.14	Wu et al., 2007

Surprisingly, very few replicates from any isolate background improved in drug susceptibility after continuous exposure to BA, even when the terminal replicates had been growing in levels of drug that exceeded their initial MIC by 3.75× (Figure 4.2). Rather unexpectedly, a significant increase in susceptibility (i.e., decrease in resistance) was found for PGC75 and P78048 (Table 4.3, Figure 4.2). Two replicates from isolates T101 and SC5314, and one replicate from isolate FH1 had a reduced susceptibility (increased resistance). Considering each replicate independently, we found no association between evolved resistance and the terminal BA concentration that the replicates came from (linear mixed-effect model; $F_{1, 7.3} = 2.72$, $P = 0.14$). This was different from what has been previously found. A study that propagated *C. albicans* for ~330 generations in concentrations of FLC that increased each transfer to twice their most recently measured MIC found that resistance increased in three out of six populations (Cowen et al., 2000). Anderson *et al.* (2009) found that all five populations of *Saccharomyces cerevisiae* that were subjected to increasing concentrations of amphotericin B increased resistance. This suggests to us that there are barriers to acquiring BA resistance adaptability in *C. albicans*, which deserves considerable additional attention in future work.

Interestingly, most evolved replicates improved BA tolerance (Figure 4.2). Replicates from isolate PGC75, P78048 and T101 increased tolerance significantly (Table 4.3, Figure 4.2). Two replicates from SC5314 and one replicate from FH1 had a reduced tolerance. Looking at each replicate independently, we found no association between evolved tolerance and the terminal BA concentration that the replicates came from (linear mixed-effect model; $F_{1, 6.4} = 0.07$, $P = 0.8$).

Previous studies that have done a similar step-wise evolution experiment found that evolved FLC resistant *C. tropicalis* isolates (isolates that can grow in 8 and 32 μg/mL FLC) (Barchiesi et al., 2000) and evolved FLC resistant *C. albicans* (Cowen et al., 2000) when grown in FLC free media for seven days, they revert back to parental MIC. Although the replicates used in susceptibility and tolerance screening came from relatively high levels of BA, we did not see a decrease in susceptibility. This suggests that there might be an epigenetic or cellular change that allowed those replicates to grow in high levels of BA but that change was not sustained after 48 h incubation on SDA plates.

In conclusion, our results suggest that BA tolerance is evolvable and occurs relatively quickly during exposure to increasing levels of BA in the lab. These results potentially have important clinical implications. Future clinical studies will directly examine yeast isolates from vulvovaginal candidiasis patients that have taken BA to determine whether BA tolerant isolates cause treatment failure and recurrence.

Table 4.3 Welch two-sample t-tests to compare ancestral and evolved susceptibility and tolerance. Isolate P87 and P76055 had only one evolved replicate so we were not able to compare between ancestral and evolved phenotypes for these isolates.

		RAD_{20} (mm)			FoG_{20} (fraction of population)	
Isolate	Statistics	Mean Ancestral	Mean Evolved	Statistics	Mean Ancestral	Mean Evolved
P75016	$t_{13.8} = -0.1$, $P = 0.93$	13.3	13.4	$t_{8.2} = -1.8$, $P = 0.10$	0.2	0.23
P78048	$t_{4.7} = -5.3$, $P = 0.03$	13.6	16	$t_{4.1} = -3.5$, $P = 0.02$	0.15	0.19
PGC75	$t_{4.5} = -3.1$, $P = 0.03$	12.4	15.6	$t_{5.3} = -10.8$, $P < 0.0001$	0.13	0.23
T101	$t_{6.4} = 1.0$, $P = 0.33$	19.8	18.7	$t_{11.3} = -3.6$, $P = 0.004$	0.19	0.30
FH1	$t_{9.6} = 0.43$, $P = 0.68$	15	15.4	$t_{4.4} = -0.99$, $P = 0.38$	0.18	0.19
SC5314	$t_{3} = 1.2$, $P = 0.32$	18	15.4	$t_{2.2} = 1.4$, $P = 0.28$	0.29	0.24

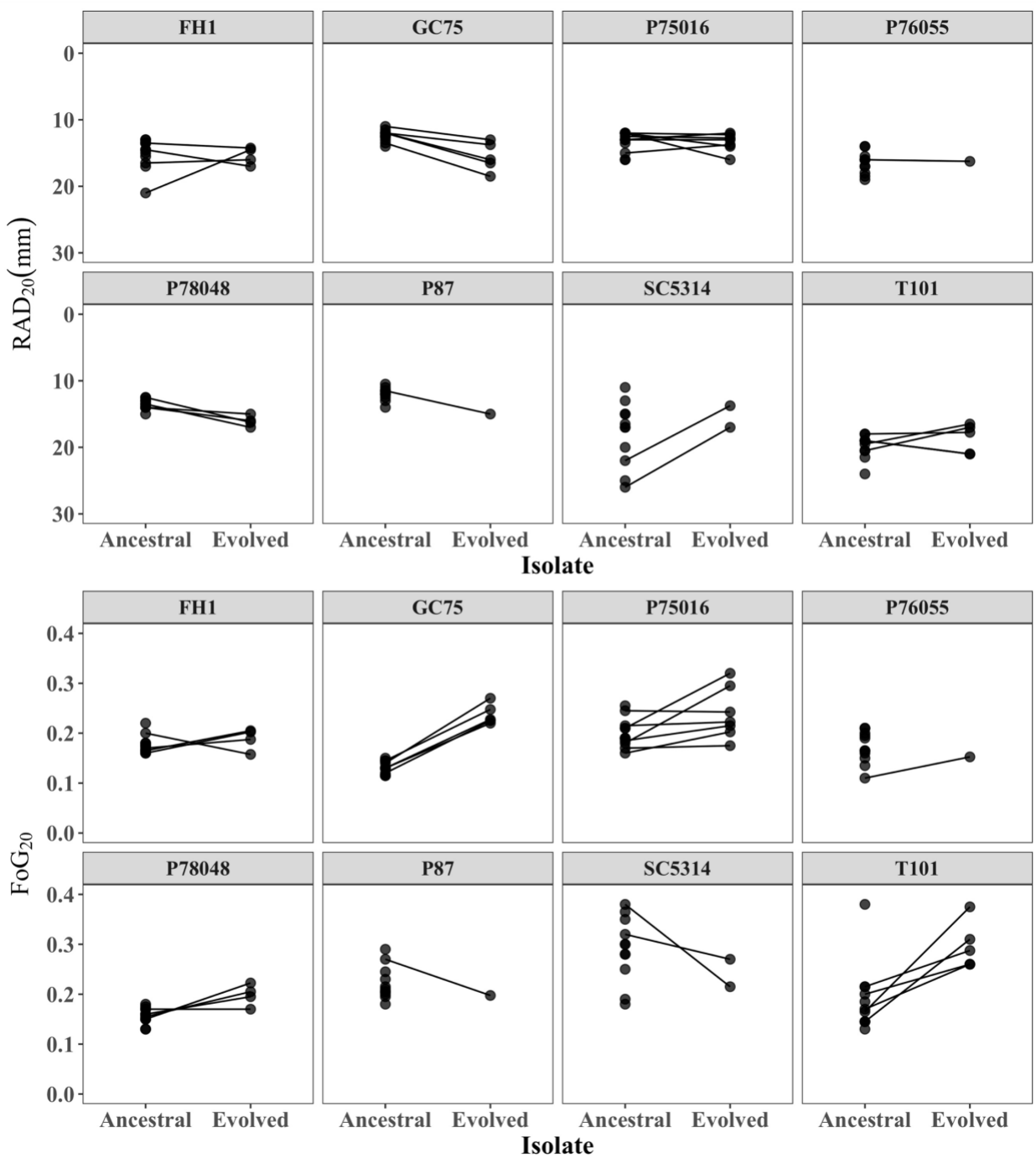


Figure 4.2 Variation in susceptibility and tolerance between ancestral and evolved replicates. The y-axis of susceptibility is reversed so more resistant replicates are towards the top. Few replicates changed in susceptibility, while tolerance often increased in evolved replicates.

Discussion

Candida albicans is the primary causative agent of vulvovaginal candidiasis (VVC), yet non-albicans yeast species can also be involved. In many infection contexts including VVC, we have a poor understanding of the factors that cause *C. albicans* to switch from a commensal species that is part of the healthy microbiome to causing symptomatic infection. A critical virulence factor for *C. albicans* in many contexts is its morphological plasticity; it is polymorphic, meaning it can grow in yeast, hyphal or pseudohyphal form and can exist as planktonic or in a biofilm. Boric acid (BA) suppositories have been used to treat VVC for the past two decades. They have been shown to be effective in inhibiting *Candida* species in complicated infections, including recurrent VVC (RVVC) and when infection is due to species that are intrinsically resistant to the primary treatment fluconazole (FLC). In this thesis, I developed a computational method that extracts parameters that correlate with biofilm formation from time-lapse images (Chapter 2). I then examined differential drug response in *Candida* species to FLC and BA (Chapter 3). Finally, I evolved *Candida albicans* isolates to BA to examine whether drug resistance or tolerance would emerge (Chapter 4).

Biofilm formation is an important virulence factor in *C. albicans* (Chandra et al., 2001; Douglas, 2003; Fanning and Mitchell, 2012; Mayer et al., 2013; Cavalheiro and Teixeira, 2018). Few protocols exist to examine the early stages of biofilm formation, and that got me interested in quantifying the drug response of *C. albicans* cells during the early phases of biofilm formation. Existing protocols that look at biofilm formation are based on visual analysis of time-lapse microscopy. The data generated are qualitative (can visually evaluate the effect of the drug) and very large; a single 96-well plate incubated for 24 h and captured every hour can generate 2304 images. In Chapter 2, I devised a computational method to analyze time-lapse images. I found an open-source tool called Orbit Image analysis (Stritt et al., 2020) that has a machine learning algorithm that I realized could be trained to detect the fungal cells in microscopic images and calculate the percent area covered by cells for each image. I then developed R scripts that use the Orbit output to extract several parameters (percent area covered by cells at the growth plateau, growth rate and time to reach the plateau) that correlate with the biofilm formation ability (Salama and Gerstein, 2021). This chapter facilitates a novel method to interpret time-lapse microscopic data and opens the door for more mechanistic studies into the underlying genetic or molecular factors that influence variation among isolates or in different environments. It also provides a

detailed method for people with no prior experience in microscopic image analysis or R programing language to analyze their microscopic data and is not restricted to use by researchers studying the same questions I am directly interested in.

The primary goal of this thesis was to capture FLC and BA differential drug response in *Candida* species. In Chapter 3, I examined 235 isolates to determine whether the planktonic drug response of BA differed from FLC, and to see if I could find any BA resistant or tolerant isolates. I used the computational tool diskImageR (Gerstein et al., 2016), which our lab uses to quantify drug resistance and tolerance from disk diffusion assay. I found that *C. glabrata*, compared to *C. albicans*, had a reduced susceptibility to FLC and BA and that the breadth of resistance and tolerance was much broader in FLC compared to BA. This is the first work that measured BA tolerance in *C. albicans*, *C. glabarata* and *C. parapsilosis*. Although the breakpoints for BA has not been defined yet, my work suggests that isolates have similar susceptibility and tolerance profiles and that resistance and tolerance to BA is rare.

It is known that the yeast to hyphal transition is an important virulence factor for *C. albicans* and is critical for forming robust biofilms. I thus wanted to determine whether BA is more effective in inhibiting hyphal and biofilm formation than FLC. I used the method developed in Chapter 2 to analyze time-lapse images of eight *C. albicans* isolates treated with increasing concentrations of FLC or BA and grown under biofilm stimulating conditions. I showed that FLC did not inhibit hyphal formation and somewhat inhibited biofilm formation. By contrast, BA inhibited hyphal and biofilm formation in a dose-dependent manner. Previous work has shown that *C. albicans* can form biofilms on the vaginal mucosa (Harriott et al., 2010; Wu et al., 2020). That made me question whether BA would also be effective against established mature biofilms. To answer this, I formed *C. albicans* biofilms and then treated the biofilms with either FLC or BA. Mirroring what I found in hyphal and biofilm formation, I found that biofilms were resistant to FLC while BA eradicated mature biofilms. Future work should look into the mechanism behind why BA is effective against mature biofilm and should investigate if it has something to do with boron's affinity to glucose.

Interestingly, boron has been shown previously to be an essential micronutrient for plants (Warington, 1923); it is essential for cell wall organization, membrane function, and metabolic activities (Blevins and Lukaszewski, 1998; Brown et al., 2002). At low BA concentrations, approximately half of the *C. albicans* isolates tested had higher biomass and higher activity

compared to biofilms in the absence of biofilms grown without drug. Low concentrations (185 μmol/L) of BA were previously shown to be strongly mitogenic, and it has been shown to stimulate growth in planktonic *Saccharomyces cerevisiae* (Bennett et al., 1999). This seems to be broadly true in eukaryotes, as similar results were seen in embryo-larval stage trout (Rowe et al., 1998; Eckhert, 1998), and Hela cells (Park et al., 2005). Treating HeLa cells with borate revealed that borate increases growth by mediating the MAPK pathway; it increases phosphorylation of MEK and ERK, which activates transcription factors important for cell growth and proliferation and inhibits apoptosis (Park et al., 2005). Future work in *C. albicans* could investigate whether this pathway is the target of BA by doing RNA-seq.

I did not find any BA resistant or tolerant isolates in my isolate screen in Chapter 3. I then tried another tactic to finding isolates with an increased resistance to BA. I set up an evolution experiment to try to evolve resistance *in vitro*. I hypothesized that if I could identify BA resistant and/or tolerant isolates I could whole-genome sequence them and potentially identify the genetic basis for BA resistance or tolerance, and potentially better understand the BA mechanism of action. Previous work showed that continuous exposure of susceptible FLC *C. albicans* replicates to FLC for over 330 generations can induce resistance (Cowen et al., 2000). Interestingly, I found that repeated exposure to BA through a similar experimental protocol induced changes in tolerance but not resistance in *C. albicans*. This could be because I waited up to seven days in between transfers and that selected for tolerance. Future work should investigate whether transferring the cells more frequently would select for BA resistance.

Due to time constraints, I focused on screening for resistance and tolerance from replicates isolated in the last transfer of the evolved experiment. Future work should look at drug responses in the isolates that were acquired from intermediate drug concentrations as well. It would also be worth investigating what happens if the number of transfers is increased at each BA concentration. I hypothesize that increasing the number of transfers per BA concentration might provide enough time for BA resistance to arise. The nature of genetic changes that arose to confer increases in tolerance has also not yet been determined. Preliminary work indicated that exposure to BA likely selected for ploidy changes, and future work is needed to investigate the nature of what arose in the BA exposed replicates.

Conclusion

I demonstrated that boric acid is effective at inhibiting planktonic *Candida* cells and that its mode of action is different than fluconazole. Unlike fluconazole, boric acid inhibits hyphal formation and eradicates mature biofilm, both in a dose-dependent manner. Surprisingly, continuous exposure to boric acid increased drug tolerance in *C. albicans* but did not select for resistance. The work in this thesis also provides critical baseline phenotypic values for future work on clinical samples from females with VVC and RVVC. Future *in vitro* work that builds directly on this thesis will be able to define the breakpoints for boric acid, determine whether boric acid works by dissolving the extracellular matrix of mature biofilm, and identify the genetic basis for boric acid tolerance.

Bibliography

Achkar, J. M., and Fries, B. C. 2010. Candida Infections of the Genitourinary Tract. *Clinical Microbiology Reviews* 23:253–273. Available at: http://dx.doi.org/10.1128/cmr.00076-09.

Al-Fattani, M. A., and Douglas, L. J. 2006. Biofilm matrix of Candida albicans and Candida tropicalis: chemical composition and role in drug resistance. *Journal of medical microbiology* 55:999–1008.

Altman, F. P. 1976. Tetrazolium salts and formazans. *Progress in histochemistry and cytochemistry* 9:1–56.

Arastehfar, A., Kargar, M. L., Mohammadi, S. R., Roudbary, M., Ghods, N., Haghighi, L., Daneshnia, F., Tavakoli, M., Jafarzadeh, J., Hedayati, M. T., et al. 2021. A High Rate of Recurrent Vulvovaginal Candidiasis and Therapeutic Failure of Azole Derivatives Among Iranian Women. *Frontiers in microbiology* 12:655069.

Barchiesi, F., Calabrese, D., Sanglard, D., Falconi Di Francesco, L., Caselli, F., Giannini, D., Giacometti, A., Gavaudan, S., and Scalise, G. 2000. Experimental induction of fluconazole resistance in Candida tropicalis ATCC 750. *Antimicrobial agents and chemotherapy* 44:1578–1584.

Benjamini, Y., and Hochberg, Y. 1995. Controlling the false discovery rate: A practical and powerful approach to multiple testing. *Journal of the Royal Statistical Society* 57:289–300.

Bennett, A., Rowe, R. I., Soch, N., and Eckhert, C. D. 1999. Boron Stimulates Yeast (Saccharomyces cerevisiae) Growth | The Journal of Nutrition | Oxford Academic. *The Journal of nutrition* 129:2236–2238.

Berman, J., and Krysan, D. J. 2020. Drug resistance and tolerance in fungi. *Nature reviews. Microbiology*. Available at: http://dx.doi.org/10.1038/s41579-019-0322-2.

Bhattacharjee, P. 2016. Epidemiology and antifungal susceptibility of Candida species in a tertiary care hospital, Kolkata, India. *Current medical mycology* 2:20–27.

Blevins, D. G., and Lukaszewski, K. M. 1998. BORON IN PLANT STRUCTURE AND FUNCTION. *Annual review of plant physiology and plant molecular biology* 49:481–500.

Bongomin, F., Gago, S., Oladele, R. O., and Denning, D. W. 2017. Global and Multi-National Prevalence of Fungal Diseases-Estimate Precision. *Journal of fungi (Basel, Switzerland)* 3. Available at: http://dx.doi.org/10.3390/jof3040057.

Boskey, E. R., Cone, R. A., Whaley, K. J., and Moench, T. R. 2001. Origins of vaginal acidity: high D/L lactate ratio is consistent with bacteria being the primary source. *Human reproduction* 16:1809–1813.

Brown, P. H., Bellaloui, N., Wimmer, M. A., Bassil, E. S., Ruiz, J., Hu, H., Pfeffer, H., Dannel, F., and Römheld, V. 2002. Boron in plant biology. *Plant biology* 4:205–223.

Butler, G., Rasmussen, M. D., Lin, M. F., Santos, M. A. S., Sakthikumar, S., Munro, C. A., Rheinbay, E., Grabherr, M., Forche, A., Reedy, J. L., et al. 2009. Evolution of pathogenicity and sexual reproduction in eight Candida genomes. *Nature* 459:657–662.

Cavalheiro, M., and Teixeira, M. C. 2018. Candida Biofilms: Threats, Challenges, and Promising Strategies. *Frontiers of medicine* 5:28.

Cetin, M., Ocak, S., Gungoren, A., and Hakverdi, A. U. 2007. Distribution of Candida species in women with vulvovaginal symptoms and their association with different ages and contraceptive methods. *Scandinavian journal of infectious diseases* 39:584–588.

Cowen, L. E., Sanglard, D., Calabrese, D., Sirjusingh, C., Anderson, J. B., and Kohn, L. M. 2000. Evolution of drug resistance in experimental populations of Candida albicans. *Journal of bacteriology* 182:1515–1522.

De Seta, F., Schmidt, M., Vu, B., Essmann, M., and Larsen, B. 2009. Antifungal mechanisms supporting boric acid therapy of Candida vaginitis. *The Journal of antimicrobial chemotherapy* 63:325–336.

Denning, D. W., Kneale, M., Sobel, J. D., and Rautemaa-Richardson, R. 2018. Global burden of recurrent vulvovaginal candidiasis: a systematic review. *The Lancet infectious diseases* 18:e339–e347.

Donlan, R. M. 2001. Biofilm formation: a clinically relevant microbiological process. *Clinical infectious diseases: an official publication of the Infectious Diseases Society of America* 33:1387–1392.

Eckhert, C. D. 1998. Boron stimulates embryonic trout growth. *The Journal of nutrition* 128:2488–2493.

Ene, I. V., Hickman, M. A., and Gerstein, A. C. 2021. The Interplay Between Neutral and Adaptive Processes Shapes Genetic Variation During Candida Species Evolution. *Current Clinical Microbiology Reports* 8:129–138.

Fanning, S., and Mitchell, A. P. 2012. Fungal biofilms. *PLoS pathogens* 8:e1002585.

Fisher, R. S. 1956. The use of boric acid in dermatologic practice. *A.M.A. archives of dermatology* 73:336–341.

Fitzpatrick, D. A., Logue, M. E., Stajich, J. E., and Butler, G. 2006. A fungal phylogeny based on 42 complete genomes derived from supertree and combined gene analysis. *BMC evolutionary biology* 6:99.

Gabaldón, T., Naranjo-Ortíz, M. A., and Marcet-Houben, M. 2016. Evolutionary genomics of yeast pathogens in the Saccharomycotina. *FEMS yeast research* 16. Available at: http://dx.doi.org/10.1093/femsyr/fow064.

Gerstein, A. 2016. diskImageR: A Pipeline to Analyze Resistance and Tolerance from Drug Disk Diffusion Assays. Available at: https://CRAN.R-project.org/package=diskImageR.

Gerstein, A. C., and Berman, J. 2020. Candida albicans Genetic Background Influences Mean and Heterogeneity of Drug Responses and Genome Stability during Evolution in Fluconazole. *mSphere* 5. Available at: http://dx.doi.org/10.1128/mSphere.00480-20.

Gerstein, A. C., Rosenberg, A., Hecht, I., and Berman, J. 2016. diskImageR: quantification of resistance and tolerance to antimicrobial drugs using disk diffusion assays. *Microbiology* 162:1059–1068.

Gulati, M., and Nobile, C. J. 2016. Candida albicans biofilms: development, regulation, and molecular mechanisms. *Microbes and infection / Institut Pasteur* 18:310–321.

Ha, K. C., and White, T. C. 1999. Effects of azole antifungal drugs on the transition from yeast cells to hyphae in susceptible and resistant isolates of the pathogenic yeast Candida albicans. *Antimicrobial agents and chemotherapy* 43:763–768.

Harriott, M. M., Lilly, E. A., Rodriguez, T. E., Fidel, P. L., and Noverr, M. C. 2010. Candida albicans forms biofilms on the vaginal mucosa. *Microbiology* 156:3635–3644.

Harrison, B. D., Hashemi, J., Bibi, M., Pulver, R., Bavli, D., Nahmias, Y., Wellington, M., Sapiro, G., and Berman, J. 2014. A tetraploid intermediate precedes aneuploid formation in yeasts exposed to fluconazole. *PLoS biology* 12:e1001815.

Hashemi, S. E., Shokohi, T., Abastabar, M., Aslani, N., Ghadamzadeh, M., and Haghani, I. 2019. Species distribution and susceptibility profiles of Candida species isolated from vulvovaginal candidiasis, emergence of C. lusitaniae. *Current medical mycology* 5:26–34.

Heckelman, P. E., Kinneary, J. F., O'Neil, M. J., Smith, A., and Others 1996. The Merck Index: an encyclopedia of chemicals, drugs, and biologicals. sidalc.net Available at: http://www.sidalc.net/cgi-

bin/wxis.exe/?IsisScript=FVL.xis&method=post&formato=2&cantidad=1&expresion=mfn=000115.

Hedayati, M. T., Taheri, Z., Galinimoghadam, T., Aghili, S. R., Yazdani Cherati, J., and Mosayebi, E. 2015. Isolation of different species of Candida in patients with vulvovaginal candidiasis from sari, iran. *Jundishapur journal of microbiology* 8:e15992.

Iavazzo, C., Gkegkes, I. D., Zarkada, I. M., and Falagas, M. E. 2011. Boric acid for recurrent vulvovaginal candidiasis: the clinical evidence. *Journal of women's health* 20:1245–1255.

Jolly, W. L. 1991. Modern Inorganic Chemistry. McGraw-Hill.

Kainz, K., Bauer, M. A., Madeo, F., and Carmona-Gutierrez, D. 2020. Fungal infections in humans: the silent crisis. *Microbial cell factories* 7:143–145.

Kalkanci, A., Güzel, A. B., Khalil, I. I. J., Aydin, M., Ilkit, M., and Kuştimur, S. 2012. Yeast vaginitis during pregnancy: susceptibility testing of 13 antifungal drugs and boric acid and the detection of four virulence factors. *Medical mycology: official publication of the International Society for Human and Animal Mycology* 50:585–593.

Kelly, S. L., Lamb, D. C., Kelly, D. E., Loeffler, J., and Einsele, H. 1996. Resistance to fluconazole and amphotericin in Candida albicans from AIDS patients. *The Lancet* 348:1523–1524.

Kidd, S. E., Halliday, C. L., McMullan, B., Chen, S. C.-A., and Elvy, J. 2021. New names for fungi of medical importance: Can we have our cake and eat it too? *Journal of clinical microbiology* 59. Available at: https://journals.asm.org/doi/10.1128/JCM.02730-20.

Klebanoff, S. J., Hillier, S. L., Eschenbach, D. A., and Waltersdorph, A. M. 1991. Control of the Microbial Flora of the Vagina by H202-Generating Lactobacilli. *The Journal of infectious diseases* 164:94–100.

Kucharíková, S., Tournu, H., Lagrou, K., Van Dijck, P., and Bujdáková, H. 2011. Detailed comparison of Candida albicans and Candida glabrata biofilms under different conditions and their susceptibility to caspofungin and anidulafungin. *Journal of medical microbiology* 60:1261–1269.

Kuhn, D. M., Chandra, J., Mukherjee, P. K., and Ghannoum, M. A. 2002. Comparison of biofilms formed by Candida albicans and Candida parapsilosis on bioprosthetic surfaces. *Infection and immunity* 70:878–888.

Kuznetsova, A., Brockhoff, P. B., and Christensen, R. H. B. 2017. lmerTest Package: Tests in Linear Mixed Effects Models. *Journal of Statistical Software* 82:1–26. Available at: http://dx.doi.org/10.18637/jss.v082.i13.

Larone, D. H., and Larone, D. H. 1987. Medically important fungi: a guide to identification. Citeseer.

Larsen, B., Petrovic, M., and De Seta, F. 2018. Boric Acid and Commercial Organoboron Products as Inhibitors of Drug-Resistant Candida albicans. *Mycopathologia* 183:349–357.

Levinson, T., Dahan, A., Novikov, A., Paran, Y., Berman, J., and Ben-Ami, R. 2021. Impact of tolerance to fluconazole on treatment response in Candida albicans bloodstream infection. *Mycoses* 64:78–85.

Linhares, L. M., Witkin, S. S., Miranda, S. D., Fonseca, A. M., Pinotti, J. A., and Ledger, W. J. 2001. Differentiation between women with vulvovaginal symptoms who are positive or negative for Candida species by culture. *Infectious diseases in obstetrics and gynecology* 9:221–225.

Lister, J. 1945. The Clinical Use of Boric Acid. *Surgery, gynecology & obstetrics* 80:651–652.

MacAlpine, J., Daniel-Ivad, M., Liu, Z., Yano, J., Revie, N. M., Todd, R. T., Stogios, P. J., Sanchez, H., O'Meara, T. R., Tompkins, T. A., et al. 2021. A small molecule produced by Lactobacillus species blocks Candida albicans filamentation by inhibiting a DYRK1-family kinase. *Nature communications* 12:6151.

Marchaim, D., Lemanek, L., Bheemreddy, S., Kaye, K. S., and Sobel, J. D. 2012. Fluconazole-resistant Candida albicans vulvovaginitis. *Obstetrics and gynecology* 120:1407–1414.

Marr, K. A., White, T. C., van Burik, J. A., and Bowden, R. A. 1997. Development of fluconazole resistance in Candida albicans causing disseminated infection in a patient undergoing marrow transplantation. *Clinical infectious diseases: an official publication of the Infectious Diseases Society of America* 25:908–910.

Martin Lopez, J. E. 2015. Candidiasis (vulvovaginal). *BMJ clinical evidence* 2015. Available at: https://www.ncbi.nlm.nih.gov/pubmed/25775428.

Mayer, F. L., Wilson, D., and Hube, B. 2013. Candida albicans pathogenicity mechanisms. *Virulence* 4:119–128.

McKloud, E., Delaney, C., Sherry, L., Kean, R., Williams, S., Metcalfe, R., Thomas, R., Richardson, R., Gerasimidis, K., Nile, C. J., et al. 2021. Recurrent Vulvovaginal Candidiasis: a Dynamic Interkingdom Biofilm Disease of Candida and Lactobacillus. *mSystems* 6:e0062221.

Melo, A. S., Bizerra, F. C., Freymüller, E., Arthington-Skaggs, B. A., and Colombo, A. L. 2011. Biofilm production and evaluation of antifungal susceptibility amongst clinical Candida

spp. isolates, including strains of the Candida parapsilosis complex. *Medical mycology: official publication of the International Society for Human and Animal Mycology* 49:253–262.

Meng, L., Zhao, H., Zhao, S., Sun, X., Zhang, M., and Deng, Y. 2019. Inhibition of Yeast-to-Hypha Transition and Virulence of Candida albicans by 2-Alkylaminoquinoline Derivatives. *Antimicrobial agents and chemotherapy* 63. Available at: http://dx.doi.org/10.1128/AAC.01891-18.

Moyes, D. L., Murciano, C., Runglall, M., Islam, A., Thavaraj, S., and Naglik, J. R. 2011. Candida albicans yeast and hyphae are discriminated by MAPK signaling in vaginal epithelial cells. *PloS one* 6:e26580.

Nett, J., Lincoln, L., Marchillo, K., Massey, R., Holoyda, K., Hoff, B., VanHandel, M., and Andes, D. 2007. Putative role of beta-1,3 glucans in Candida albicans biofilm resistance. *Antimicrobial agents and chemotherapy* 51:510–520.

Noble, S. M., Gianetti, B. A., and Witchley, J. N. 2017. Candida albicans cell-type switching and functional plasticity in the mammalian host. *Nature reviews. Microbiology* 15:96–108.

Nyirjesy, P., Peyton, C., Weitz, M. V., Mathew, L., and Culhane, J. F. 2006. Causes of chronic vaginitis: analysis of a prospective database of affected women. *Obstetrics and gynecology* 108:1185–1191.

Odds, F. C., Bougnoux, M.-E., Shaw, D. J., Bain, J. M., Davidson, A. D., Diogo, D., Jacobsen, M. D., Lecomte, M., Li, S.-Y., Tavanti, A., et al. 2007. Molecular phylogenetics of Candida albicans. *Eukaryotic cell* 6:1041–1052.

Okungbowa, F. I., Isikhuemhen, O. S., and Dede, A. P. O. 2003. The distribution frequency of Candida species in the genitourinary tract among symptomatic individuals in Nigerian cities. *Revista iberoamericana de micologia* 20:60–63.

Otero, L., Palacio, V., Mendez, F. J., and Vazquez, F. 2002. Boric acid susceptibility testing of non-C. albicans Candida and Saccharomyces cerevisiae: comparison of three methods. *Medical mycology: official publication of the International Society for Human and Animal Mycology* 40:319–322.

Oxman, D. A., Chow, J. K., Frendl, G., Hadley, S., Hershkovitz, S., Ireland, P., McDermott, L. A., Tsai, K., Marty, F. M., Kontoyiannis, D. P., et al. 2010. Candidaemia associated with decreased in vitro fluconazole susceptibility: is Candida speciation predictive of the susceptibility pattern? *The Journal of antimicrobial chemotherapy* 65:1460–1465.

Pappas, P. G., Kauffman, C. A., Andes, D. R., Clancy, C. J., Marr, K. A., Ostrosky-Zeichner, L., Reboli, A. C., Schuster, M. G., Vazquez, J. A., Walsh, T. J., et al. 2016. Clinical Practice Guideline for the Management of Candidiasis: 2016 Update by the Infectious Diseases Society of America. *Clinical infectious diseases: an official publication of the Infectious Diseases Society of America* 62:e1-50.

Park, M., Li, Q., Shcheynikov, N., Muallem, S., and Zeng, W. 2005. Borate transport and cell growth and proliferation. Not only in plants. *Cell cycle* 4:24–26.

Peters, B. M., Palmer, G. E., Nash, A. K., Lilly, E. A., Fidel, P. L., Jr, and Noverr, M. C. 2014. Fungal morphogenetic pathways are required for the hallmark inflammatory response during Candida albicans vaginitis. *Infection and immunity* 82:532–543.

Peters, J. A. 2014. Interactions between boric acid derivatives and saccharides in aqueous media: Structures and stabilities of resulting esters. *Coordination chemistry reviews* 268:1–22.

Pfaller, M. A., Jones, R. N., and Castanheira, M. 2014. Regional data analysis of Candida non-albicans strains collected in United States medical sites over a 6-year period, 2006-2011. *Mycoses* 57:602–611.

Pierce, C. G., Uppuluri, P., Tummala, S., and Lopez-Ribot, J. L. 2010. A 96 well microtiter plate-based method for monitoring formation and antifungal susceptibility testing of Candida albicans biofilms. *Journal of visualized experiments: JoVE*. Available at: http://dx.doi.org/10.3791/2287.

Pointer, B. R., Boyer, M. P., and Schmidt, M. 2015. Boric acid destabilizes the hyphal cytoskeleton and inhibits invasive growth of Candida albicans. *Yeast* 32:389–398.

Prutting, S. M., and Cerveny, J. D. 1998. Boric acid vaginal suppositories: a brief review. *Infectious diseases in obstetrics and gynecology* 6:191–194.

R Core Team 2020. R: A Language and Environment for Statistical Computing. Available at: https://www.R-project.org/.

Ramage, G., Bachmann, S., Patterson, T. F., Wickes, B. L., and López-Ribot, J. L. 2002. Investigation of multidrug efflux pumps in relation to fluconazole resistance in Candida albicans biofilms. *The Journal of antimicrobial chemotherapy* 49:973–980.

Ringdahl, E. N. 2000. Treatment of recurrent vulvovaginal candidiasis. *American family physician* 61:3306–12, 3317.

Rodríguez-Cerdeira, C., Gregorio, M. C., Molares-Vila, A., López-Barcenas, A., Fabbrocini, G., Bardhi, B., Sinani, A., Sánchez-Blanco, E., Arenas-Guzmán, R., and Hernandez-Castro, R.

2019. Biofilms and vulvovaginal candidiasis. *Colloids and surfaces. B, Biointerfaces* 174:110–125.

Rosati, D., Bruno, M., Jaeger, M., Ten Oever, J., and Netea, M. G. 2020. Recurrent Vulvovaginal Candidiasis: An Immunological Perspective. *Microorganisms* 8. Available at: http://dx.doi.org/10.3390/microorganisms8020144.

Rosenberg, A., Ene, I. V., Bibi, M., Zakin, S., Segal, E. S., Ziv, N., Dahan, A. M., Colombo, A. L., Bennett, R. J., and Berman, J. 2018. Antifungal tolerance is a subpopulation effect distinct from resistance and is associated with persistent candidemia. *Nature communications* 9:2470.

Rowe, R. I., Bouzan, C., Nabili, S., and Eckhert, C. D. 1998. The response of trout and zebrafish embryos to low and high boron concentrations is U-shaped. *Biological trace element research* 66:261–270.

Salama, O. E., and Gerstein, A. C. 2021. High-throughput computational analysis of biofilm formation from time-lapse microscopy. *Current protocols* 1:e194.

Sanglard, D., Coste, A., and Ferrari, S. 2009. Antifungal drug resistance mechanisms in fungal pathogens from the perspective of transcriptional gene regulation. *FEMS yeast research* 9:1029–1050.

van Schalkwyk, J., Yudin, M. H., and INFECTIOUS DISEASE COMMITTEE 2015. Vulvovaginitis: screening for and management of trichomoniasis, vulvovaginal candidiasis, and bacterial vaginosis. *Journal of obstetrics and gynaecology Canada: JOGC = Journal d'obstetrique et gynecologie du Canada: JOGC* 37:266–274.

Schneider, C. A., Rasband, W. S., and Eliceiri, K. W. 2012. NIH Image to ImageJ: 25 years of image analysis. *Nature methods* 9:671–675.

Selmecki, A., Forche, A., and Berman, J. 2006. Aneuploidy and isochromosome formation in drug-resistant Candida albicans. *Science* 313:367–370.

Selmecki, A., Forche, A., and Berman, J. 2010. Genomic plasticity of the human fungal pathogen Candida albicans. *Eukaryotic cell* 9:991–1008.

Selmecki, A., Gerami-Nejad, M., Paulson, C., Forche, A., and Berman, J. 2008. An isochromosome confers drug resistance in vivo by amplification of two genes, ERG11 and TAC1. *Molecular microbiology* 68:624–641.

Selmecki, A. M., Dulmage, K., Cowen, L. E., Anderson, J. B., and Berman, J. 2009. Acquisition of aneuploidy provides increased fitness during the evolution of antifungal drug resistance. *PLoS genetics* 5:e1000705.

Seneviratne, C. J., and Rosa, E. A. R. 2016. Editorial: Antifungal Drug Discovery: New Theories and New Therapies. *Frontiers in microbiology* 7:728.

Sheehan, D. J., Brown, S. D., Pfaller, M. A., Warnock, D. W., Rex, J. H., Chaturvedi, V., Espinel-Ingroff, A., Ghannoum, M. A., Moore, L. S., Odds, F. C., et al. 2004. Method for Antifungal Disk Diffusion Susceptibility Testing of Yeasts; Approved Guideline. *Pennsylvania, USA: National Committee for Clinical Laboratory Standards M27-A2*.

Sherry, L., Kean, R., McKloud, E., O'Donnell, L. E., Metcalfe, R., Jones, B. L., and Ramage, G. 2017. Biofilms Formed by Isolates from Recurrent Vulvovaginal Candidiasis Patients Are Heterogeneous and Insensitive to Fluconazole. *Antimicrobial agents and chemotherapy* 61. Available at: http://dx.doi.org/10.1128/AAC.01065-17.

Shinohara, Y. T., and Tasker, S. A. 1997. Successful use of boric acid to control azole-refractory Candida vaginitis in a woman with AIDS. *Journal of acquired immune deficiency syndromes and human retrovirology: official publication of the International Retrovirology Association* 16:219–220.

Silva, S., Henriques, M., Martins, A., Oliveira, R., Williams, D., and Azeredo, J. 2009. Biofilms of non-Candida albicans Candida species: quantification, structure and matrix composition. *Medical mycology: official publication of the International Society for Human and Animal Mycology* 47:681–689.

Sobel, J. 2005. Current treatment options for vulvovaginal candidiasis. *Women's health* 1:253–261.

Sobel, J. D. 2015. Editorial Commentary: Vaginal Biofilm: Much Ado About Nothing, or a New Therapeutic Challenge? *Clinical infectious diseases: an official publication of the Infectious Diseases Society of America* 61:607–608.

Sobel, J. D. 2016. Recurrent vulvovaginal candidiasis. *American journal of obstetrics and gynecology* 214:15–21.

Sobel, J. D. 2007. Vulvovaginal candidosis. *The Lancet* 369:1961–1971.

Sobel, J. D., Chaim, W., Nagappan, V., and Leaman, D. 2003. Treatment of vaginitis caused by Candida glabrata: use of topical boric acid and flucytosine. *American journal of obstetrics and gynecology* 189:1297–1300.

Sobel, J. D., Faro, S., Force, R. W., Foxman, B., Ledger, W. J., Nyirjesy, P. R., Reed, B. D., and Summers, P. R. 1998. Vulvovaginal candidiasis: epidemiologic, diagnostic, and therapeutic considerations. *American journal of obstetrics and gynecology* 178:203–211.

Sprouffske, K. 2020. Simple Metrics to Summarize Growth Curves [R package growthcurver version 0.3.1]. Available at: https://CRAN.R-project.org/package=growthcurver [Accessed April 26, 2021].

Steinberg, G. 2007. Hyphal growth: a tale of motors, lipids, and the Spitzenkörper. *Eukaryotic cell* 6:351–360.

Stritt, M., Stalder, A. K., and Vezzali, E. 2020. Orbit Image Analysis: An open-source whole slide image analysis tool. *PLoS computational biology* 16:e1007313.

Swidsinski, A., Guschin, A., Tang, Q., Dörffel, Y., Verstraelen, H., Tertychnyy, A., Khayrullina, G., Luo, X., Sobel, J. D., and Jiang, X. 2019. Vulvovaginal candidiasis: histologic lesions are primarily polymicrobial and invasive and do not contain biofilms. *American journal of obstetrics and gynecology* 220:91.e1-91.e8.

Todd, R. T., Wikoff, T. D., Forche, A., and Selmecki, A. 2019. Genome plasticity in Candida albicans is driven by long repeat sequences. *eLife* 8. Available at: http://dx.doi.org/10.7554/eLife.45954.

Turner, S. A., and Butler, G. 2014. The Candida pathogenic species complex. *Cold Spring Harbor perspectives in medicine* 4:a019778.

Vásquez, A., Jakobsson, T., Ahrné, S., Forsum, U., and Molin, G. 2002. Vaginal lactobacillus flora of healthy Swedish women. *Journal of clinical microbiology* 40:2746–2749.

Voravuthikunchai, S. P., Bilasoi, S., and Supamala, O. 2006. Antagonistic activity against pathogenic bacteria by human vaginal lactobacilli. *Anaerobe* 12:221–226.

Wächtler, B., Citiulo, F., Jablonowski, N., Förster, S., Dalle, F., Schaller, M., Wilson, D., and Hube, B. 2012. Candida albicans-epithelial interactions: dissecting the roles of active penetration, induced endocytosis and host factors on the infection process. *PloS one* 7:e36952.

Wang, F.-J., Zhang, D., Liu, Z.-H., Wu, W.-X., Bai, H.-H., and Dong, H.-Y. 2016. Species Distribution and In Vitro Antifungal Susceptibility of Vulvovaginal Candida Isolates in China. *Chinese medical journal* 129:1161–1165.

Warington, K. 1923. The Effect of Boric Acid and Borax on the Broad Bean and certain other Plants. *Annals of botany* 37:629–672.

Wayne, P. A. 2004. Methods for antifungal disk diffusion susceptibility testing of yeasts: approved standard M44-A.

Wayne, P. A. 2002. Reference method for broth dilution antifungal susceptibility testing of yeasts, approved standard. *CLSI document M27-A2*. Available at: https://ci.nii.ac.jp/naid/10026406912/.

Weerasekera, M. M., Wijesinghe, G. K., Jayarathna, T. A., Gunasekara, C. P., Fernando, N., Kottegoda, N., and Samaranayake, L. P. 2016. Culture media profoundly affect Candida albicans and Candida tropicalis growth, adhesion and biofilm development. *Memorias do Instituto Oswaldo Cruz* 111:697–702.

Wickham, H., Averick, M., Bryan, J., Chang, W., McGowan, L., François, R., Grolemund, G., Hayes, A., Henry, L., Hester, J., et al. 2019. Welcome to the tidyverse. *Journal of open source software* 4:1686.

Willems, H. M. E., Ahmed, S. S., Liu, J., Xu, Z., and Peters, B. M. 2020. Vulvovaginal Candidiasis: A Current Understanding and Burning Questions. *Journal of fungi (Basel, Switzerland)* 6. Available at: http://dx.doi.org/10.3390/jof6010027.

Wilson, D., Naglik, J. R., and Hube, B. 2016. The Missing Link between Candida albicans Hyphal Morphogenesis and Host Cell Damage. *PLoS pathogens* 12:e1005867.

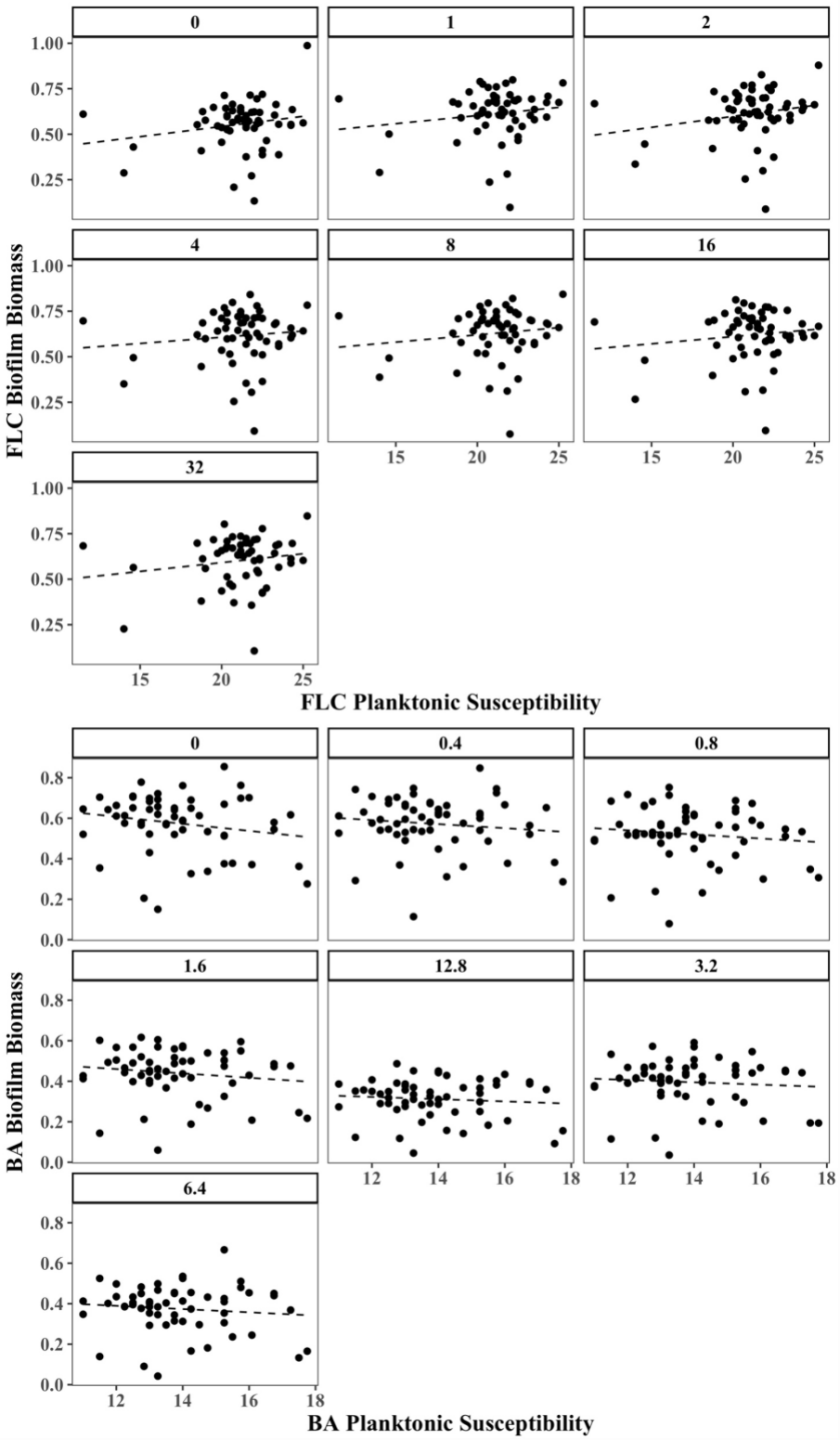
Wu, W., Lockhart, S. R., Pujol, C., Srikantha, T., and Soll, D. R. 2007. Heterozygosity of genes on the sex chromosome regulates Candida albicans virulence. *Molecular microbiology* 64:1587–1604.

Wu, X., Zhang, S., Li, H., Shen, L., Dong, C., Sun, Y., Chen, H., Xu, B., Zhuang, W., Deighton, M., et al. 2020. Biofilm Formation of Candida albicans Facilitates Fungal Infiltration and Persister Cell Formation in Vaginal Candidiasis. *Frontiers in microbiology* 11:1117.

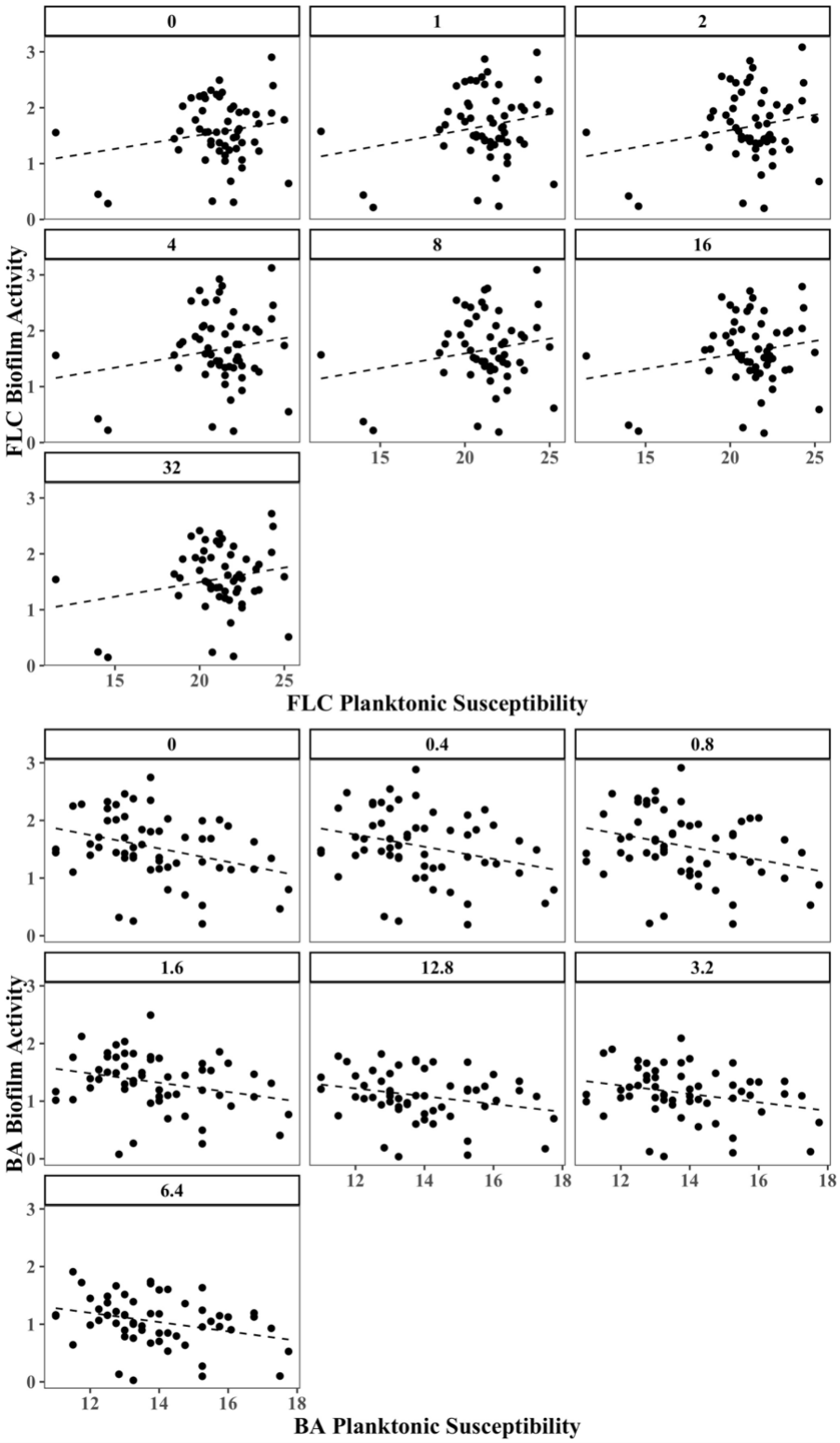
Zhang, J.-Y., Liu, J.-H., Liu, F.-D., Xia, Y.-H., Wang, J., Liu, X., Zhang, Z.-Q., Zhu, N., Yan-Yan, Ying, Y., et al. 2014. Vulvovaginal candidiasis: species distribution, fluconazole resistance and drug efflux pump gene overexpression. *Mycoses* 57:584–591.

Zhao, S., Huang, J.-J., Sun, X., Huang, X., Fu, S., Yang, L., Liu, X.-W., He, F., and Deng, Y. 2018. (1-aryloxy-2-hydroxypropyl)-phenylpiperazine derivatives suppress Candida albicans virulence by interfering with morphological transition. *Microbial biotechnology* 11:1080–1089.

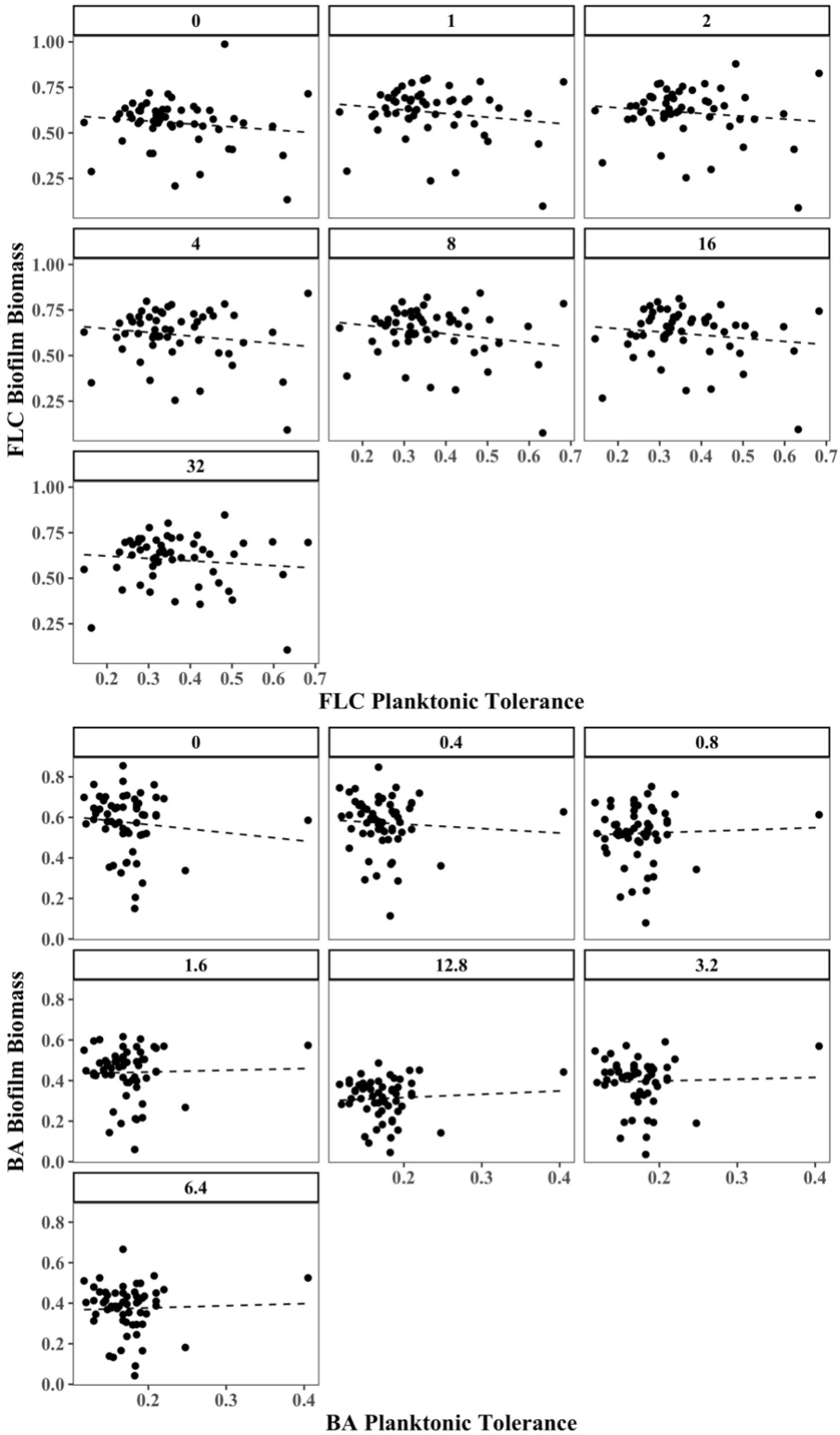
Supplementary Material for Chapter 3



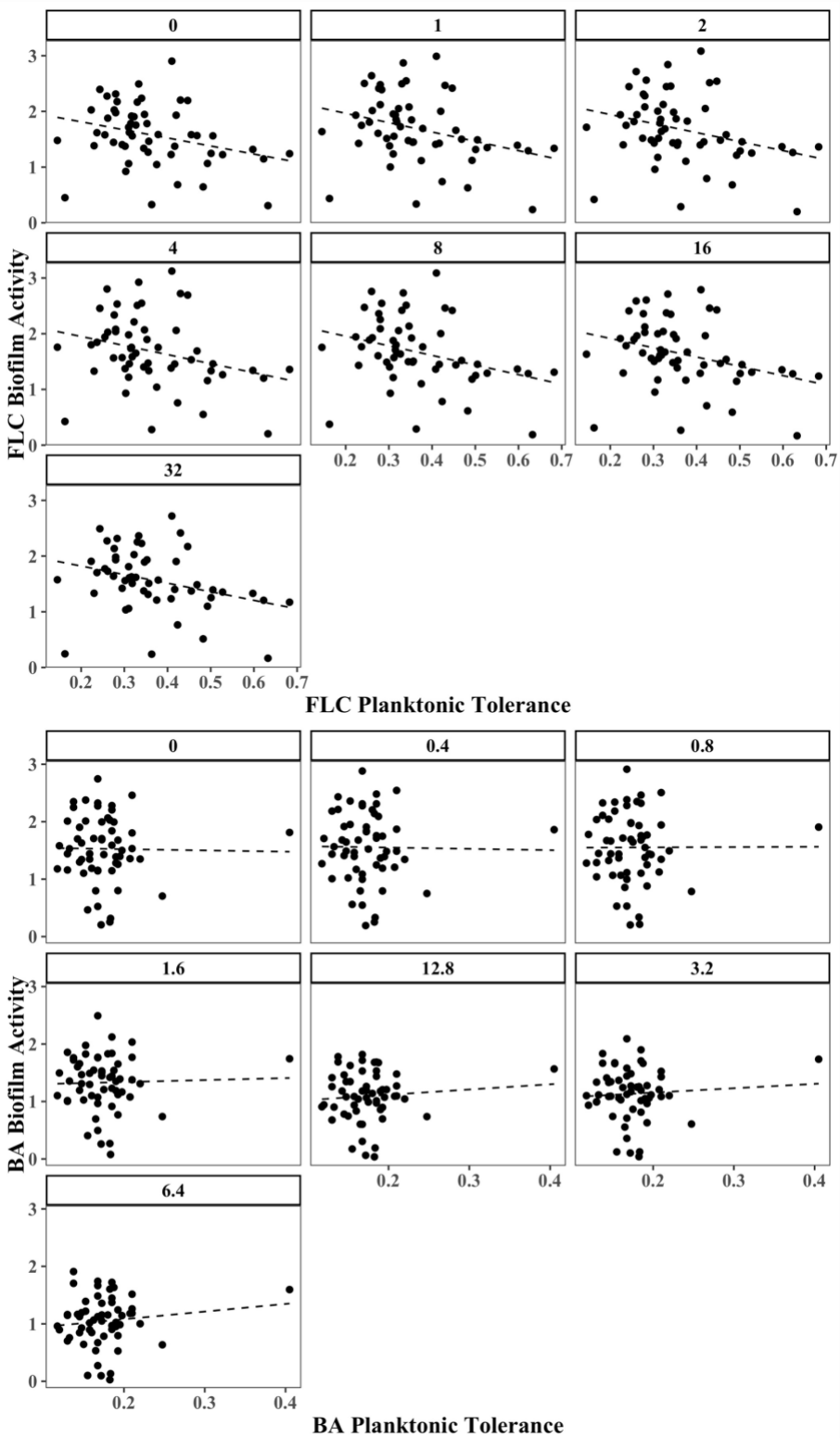
Supplementary Figure 3. 1 Association of planktonic susceptibility and biofilm biomass of *C. albicans* isolates. There is no association between planktonic susceptibility and biomass of the biofilms for both FLC and BA (linear mixed-effect model).



Supplementary Figure 3. 2 Association of planktonic susceptibility and biofilm activity of *C. albicans* isolates. There is an association between BA planktonic susceptibility and biomass of the biofilms; however, this association absent in FLC (linear mixed-effect model).

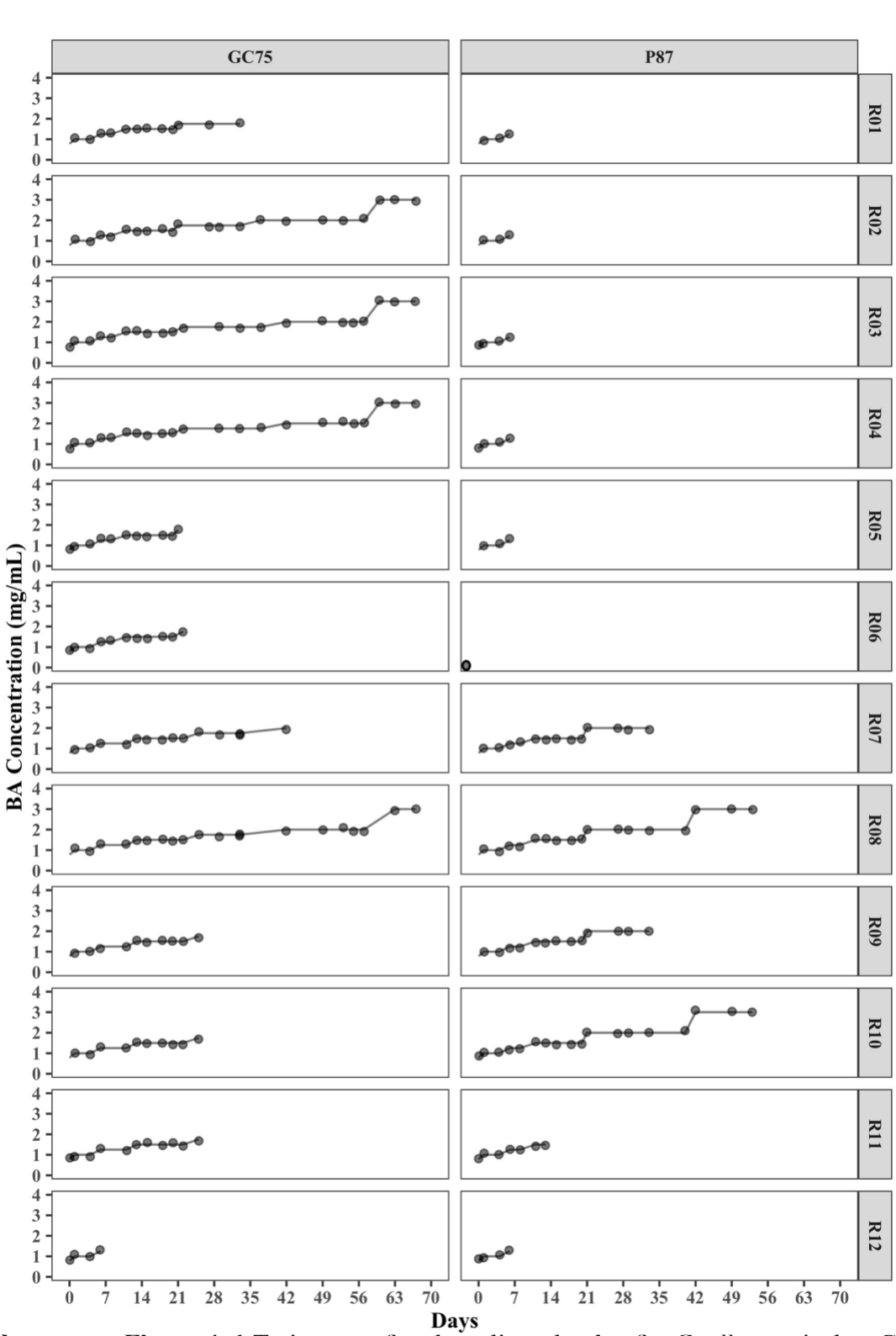


Supplementary Figure 3. 3 Association of planktonic tolerance and biofilm biomass of *C. albicans* isolates. There is no association between planktonic tolerance and biomass of the biofilms for both FLC and BA (linear mixed-effect model).

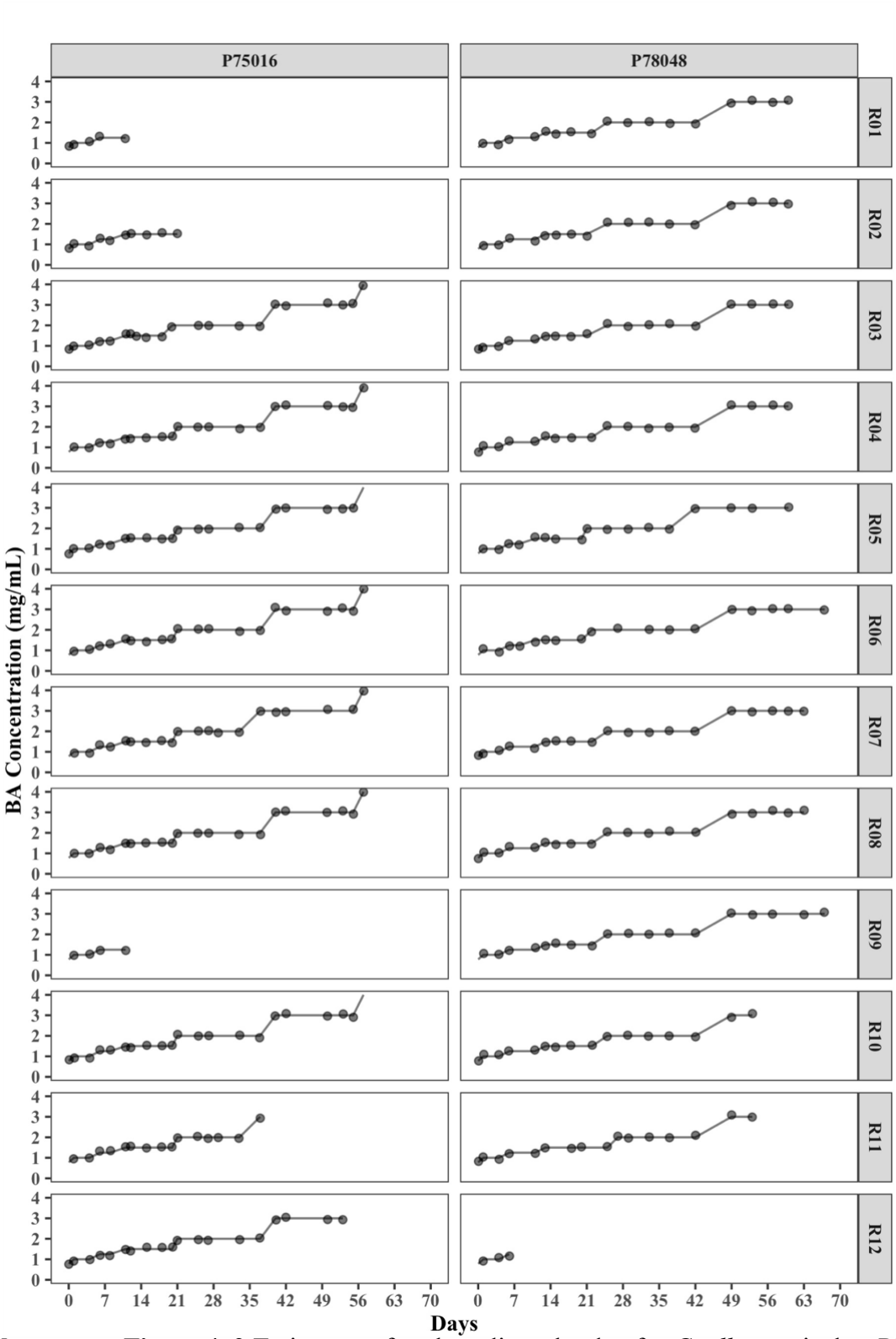


Supplementary Figure 3. 4 Association of planktonic tolerance and biofilm activity of *C. albicans* isolates. There is an association between FLC planktonic tolerance and activity of the biofilms (linear mixed-effect model); however, this association is absent in BA.

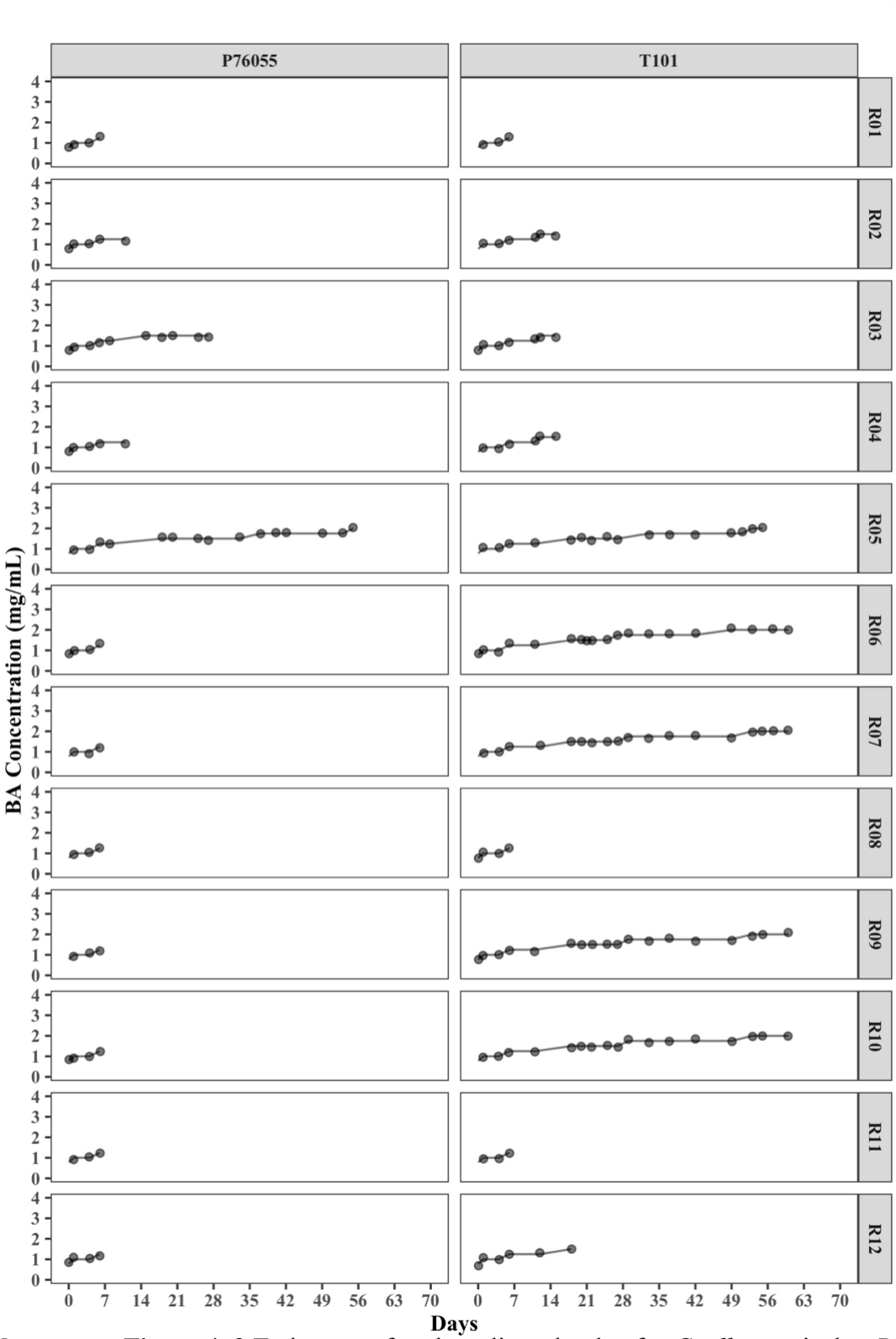
Supplementary Material for Chapter 4



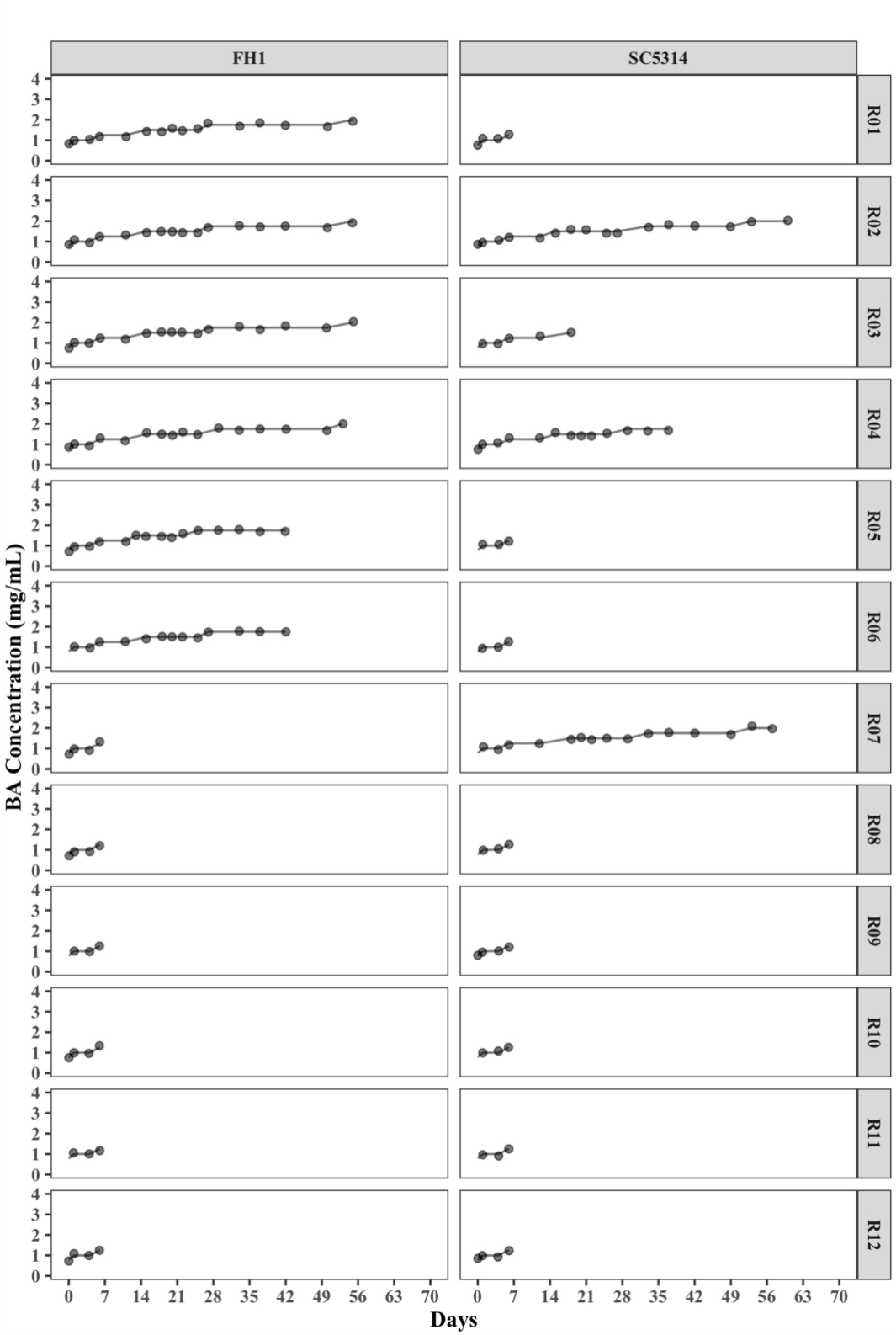
Supplementary Figure 4. 1 Trajectory of each replicate by day for *C. albicans* isolate GC75 and P87.



Supplementary Figure 4. 2 Trajectory of each replicate by day for *C. albicans* isolate P75016 and P78048.



Supplementary Figure 4. 3 Trajectory of each replicate by day for *C. albicans* isolate P76055 and T101.



Supplementary Figure 4.4 Trajectory of each replicate by day for *C. albicans* isolate FH1 and SC5314.